International Journal of Extreme Manufacturing

TOPICAL REVIEW • OPEN ACCESS

Advanced biofabrication techniques of muscle cell-powered biohybrid robots

To cite this article: Niyou Wang *et al* 2026 *Int. J. Extrem. Manuf.* **8** 012007

View the article online for updates and enhancements.

You may also like

- Ethics of biohybrid robotics and invertebrate research: biohybrid robotic jellyfish as a case study
Nicole W Xu, Olga Lenczewska, Sarah E Wieten et al.
- Organisms as sensors in biohybrid entities as a novel tool for in-field aquatic monitoring
Wiktoria Rajewicz, Chao Wu, Donato Romano et al.
- Quantifying the biomimicry gap in biohybrid robot-fish pairs
Vaios Papaspyros, Guy Theraulaz, Clément Sire et al.

This content was downloaded from IP address 42.60.63.185 on 18/10/2025 at 14:13

OPEN ACCESS
IMMT | IOP Publishing
International Journal of Extreme Manufacturing
Int. J. Extrem. Manuf. **8** (2026) 012007 (48pp)
https://doi.org/10.1088/2631-7990/ae0bc7

Topical Review

Advanced biofabrication techniques of muscle cell-powered biohybrid robots

Niyou Wang[1,2,§], Yipei Yang[1,3,§], Zahra Rezaei[1], María José Veana Hernández[1,4], Kannan Govindaraj[1,5], Carolina Vazquez Garzon[1,6], Marina Colin[1,7], Alan de Jesus Alarcon Rodríguez[1,6], Alvaro Dario Martinez Blanco[1,8], Jose Joaquin Velasco[1,6], Jihyun Lee[1], Jeong-Woo Choi[9] and Su Ryon Shin[1,*]

[1] Division of Engineering in Medicine, Department of Medicine, Brigham and Women's Hospital, Harvard Medical School, 65 Landsdowne Street, Cambridge, Massachusetts 02139, United States of America
[2] Institute of Materials Research and Engineering (IMRE), Agency for Science, Technology and Research (A*STAR), 2 Fusionopolis Way, Innovis #08-03, Singapore 138634, Singapore
[3] Department of Orthopedic Surgery, The Second Affiliated Hospital of Guangzhou University of Chinese Medicine, Guangzhou 510120, People's Republic of China
[4] Monterrey Institute of Technology, School of Engineering and Science, Atlixcayotl 5718, Atlixcayotl Territorial Reserve, Heroica Puebla de Zaragoza, Puebla 72453, Mexico
[5] Department of Developmental Bioengineering, Faculty of Science and Technology, Technical Medical Centre, University of Twente, Drienerlolaan 5, Enschede 7522NB, The Netherlands
[6] Monterrey Institute of Technology, School of Engineering and Science, Eugenio Garza Sada Avenue 2501 South, Monterrey, Nuevo Leon 64849, Mexico
[7] ESPCI Paris, PSL Research University, 10 rue Vauquelin, Paris 75005, France
[8] Monterrey Institute of Technology, School of Science and Engineering, Epigmenio González 500, Fraccionamiento San Pablo, Santiago de Querétaro, Querétaro 76130, Mexico
[9] Department of Chemical & Biomolecular Engineering, Sogang University, 35 Baekbeom-ro, Mapo-gu, Seoul 04107, Republic of Korea

E-mail: sshin4@bwh.harvard.edu

Received 25 March 2025, revised 30 June 2025
Accepted for publication 25 September 2025
Published 17 October 2025

Abstract

Muscle cell-powered biohybrid robots represent a transformative fusion of biological tissue engineering and robotics, offering unprecedented potential for biomedical applications targeted at drug delivery, regenerative medicine, bioengineered heart patches, lab-on-a-chip devices, biosensors, and soft surgical tools. This review categorizes the currently available examples and further explores advanced biofabrication techniques that drive the development of biohybrid systems, with a focus on 3D bioprinting, electrospinning, micro/nano patterning, self-assembly,

§ These authors contributed equally to this work and should be considered co-first-author.
* Author to whom any correspondence should be addressed.

Original content from this work may be used under the terms of the Creative Commons Attribution 4.0 licence. Any further distribution of this work must maintain attribution to the author(s) and the title of the work, journal citation and DOI.

© 2025 The Author(s). Published by IOP Publishing Ltd on behalf of the IMMT

and microfluidic devices. These fabrication strategies facilitate precise cell alignment, enhance electrical and mechanical properties, and enable the seamless integration of biological components with engineered structures. By incorporating both cardiomyocytes and skeletal muscle cells, biohybrid robots achieve controlled actuation, autonomous movement, and adaptability to environmental stimuli. Furthermore, we discuss the latest optimization strategies in biofabrication, addressing key challenges such as scalability, biocompatibility, and functional integration. Biohybrid robots, including swimmers, actuators, and pumps, enable targeted drug delivery, assistive devices, and fluid transport in engineered tissues. Their integration with biological systems advances regenerative medicine, disease modeling, drug screening, and soft robotics. This review provides a comprehensive perspective on the state-of-the-art advancements and potential optimization in the fabrication techniques, paving the way for the next generation of biohybrid robotic systems.

Keywords: biohybrid robots, biofabrication, skeletal muscle cell, cardiomyocyte, bioactuators, tissue engineering

1. Introduction

Biohybrid robotics, the convergence of biology and engineering, is revolutionizing biomedical research by enabling the development of muscle cell-powered robotic systems[1–3]. Unlike traditional robotic actuators, biohybrid robots leverage the contractile properties of skeletal muscle cells or cardiomyocytes to achieve dynamic and adaptive movement[4]. Skeletal muscle cells facilitate precise, externally controlled actuation, while cardiomyocytes generate autonomous rhythmic contractions, making them ideal for continuous motion[5]. By integrating these biological components with engineered scaffolds and stimuli-responsive materials, biohybrid robots have shown promising applications in functional tissue engineering, regenerative medicine, drug screening, and soft robotics[6–8]. The success of biohybrid robots largely depends on advancements in biofabrication techniques, which play a critical role in constructing structurally organized, functionally active, and scalable muscle tissue constructs[9,10]. 3D bioprinting has emerged as a key fabrication method, allowing for high-precision deposition of cells and biomaterials into anatomically relevant architectures[11–14]. Electrospinning and rotary jet spinning generate aligned nanofiber scaffolds that promote cellular organization and mimic native extracellular matrix (ECM) environments[15–19]. Micro/nano patterning techniques provide microscale patterning that enhances muscle tissue integration with engineered platforms[20–25]. Additionally, self-assembly approaches leverage the intrinsic biological behaviors of cells to form functional muscle structures without the need for predefined scaffolds[26–30]. Lastly, microfluidic systems enable dynamic control of the cell culture microenvironment, improving nutrient exchange, mechanical stimulation, and real-time monitoring of engineered muscle constructs[31–38].

Optimizing these fabrication techniques is essential for achieving greater cell alignment, functional integration, and mechanical-electrical stability in biohybrid robots. Strategies such as biochemical modifications of scaffolds, electroconductive nanomaterials, and external stimulation have been employed to enhance muscle contractility and longevity[5,39]. Additionally, hybrid fabrication approaches that combine 3D bioprinting with micro/nano patterning or electrospinning with conductive biomaterials offer promising solutions to improve structural reliability and force output in biohybrid systems[40].

This review aims to address the key challenges in developing muscle cell-powered biohybrid robots by exploring advanced fabrication techniques and their applications in biomedical research and clinical settings (Figure 1). We begin by examining recent breakthroughs in cell-laden printing, bioactive scaffolding, micro-engineered muscle architectures, and adaptive stimulation systems, which together define the evolving landscape of biofabrication for these systems. Particular attention is given to strategies that target structural and functional limitations, such as cell alignment, neuromuscular connectivity, mechanical adaptability, and long-term tissue viability. By analyzing how these approaches overcome specific bottlenecks in biohybrid robot development, we offer a structured framework for understanding the critical design principles driving this field forward. Through a comprehensive discussion of optimization techniques, this review aims to bridge the gap between biological actuation and engineered functionality, supporting the advancement of next-generation biohybrid robotic systems.

2. Biohybrid robots based on the type of muscle cells

2.1. Cardiomyocytes

Cardiomyocytes, known for their rhythmic and spontaneous contractions, play a crucial role in the development of biohybrid robots. Their inherent ability to generate continuous and autonomous beating has been primarily leveraged in the creation of biohybrid actuators, swimmers, and pumps, where rhythmic motion is essential for fluid transport and locomotion. These distinct characteristics have enabled the design of robots that closely mimic natural movements, accelerating progress in soft robotics and biomedical applications while

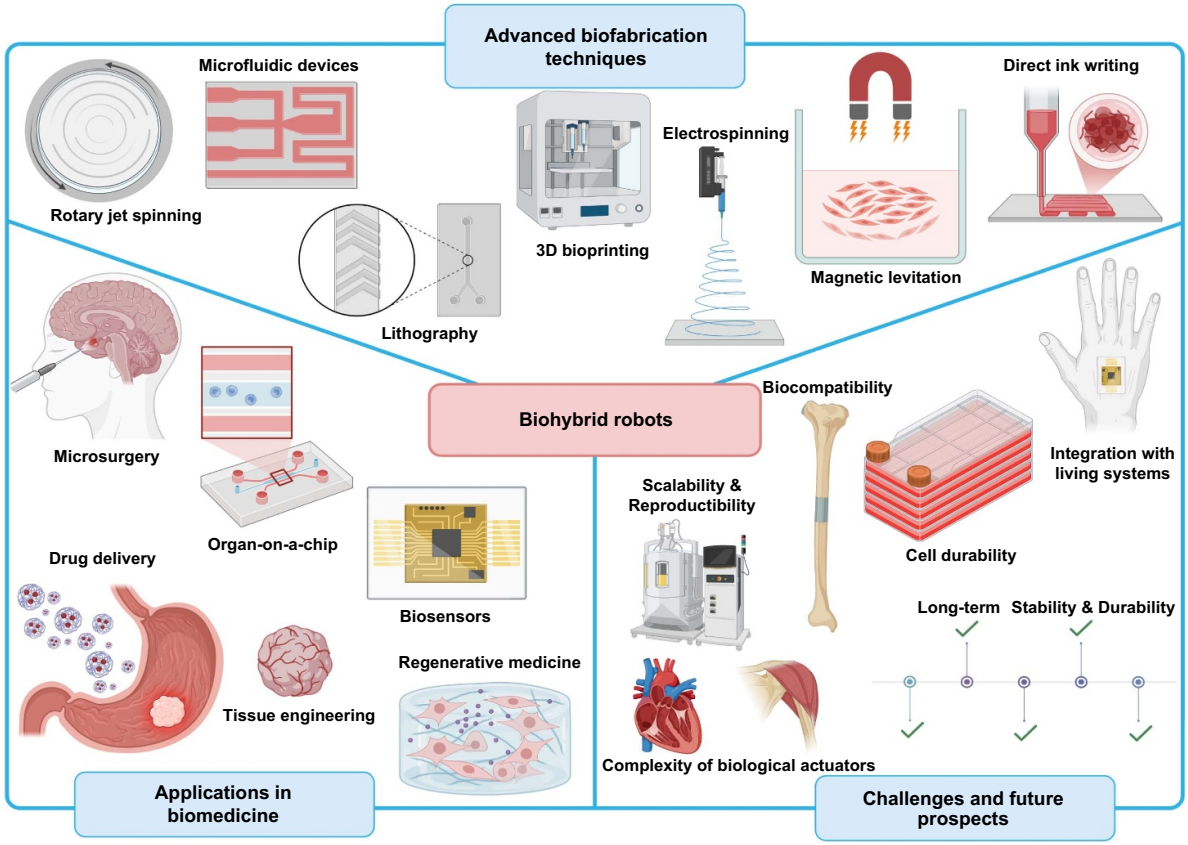

Figure 1. Schematic illustrations of the topics related to biohybrid robots covered in this review, including fabrication techniques, applications, challenges, and future prospects. Each component highlights a critical aspect of the field: fabrication techniques enable precise integration of biological and synthetic elements; applications demonstrate real-world relevance in drug delivery and soft robotics; challenges underscore the current limitations in scalability and control; and prospects point to emerging opportunities for clinical translation and next-generation designs. Created in BioRender with permission.

promoting seamless integration between biological and artificial systems[3,5].

2.1.1. Actuators. Actuators powered by cardiomyocytes harness the cells' intrinsic contractile behavior to generate motion without the need for external control inputs[41]. Chen et al. used the wings of Morpho butterflies as an elastic substrate to create a biohybrid system driven by cardiomyocyte contractions[42]. The rhythmic contractions of the cardiomyocytes produced deformation-induced color changes, demonstrating potential applications for biohybrid sensors that visually report biomechanical activity[42]. Precise control over cardiomyocyte activity is essential for the development of functional biohybrid systems. Optogenetic control is one of the methods used to achieve precise spatiotemporal control of cardiac contractions[5]. Chan et al. fabricated multi-strip cardiac muscle constructs that incorporated optogenetically modified cardiomyocytes[43]. By applying pulses of light to these constructs, cardiomyocyte contractions were spatially and temporally controlled, enabling the fine regulation of contraction timing and synchronization[43]. Dipalo et al. advanced the control of cardiomyocyte-driven devices by using fuzzy graphene microelectrodes to record and modulate intracellular action potentials[44]. Their method allowed precise control of the electrophysiological behavior of cardiomyocytes, which is essential for controlling contractions in biohybrid systems. A study conducted by Vurro et al. demonstrated light-triggered control of cardiomyocyte activity using organic phototransistors[45]. By illuminating specific regions of cardiac tissues, precise and localized contractions were achieved, supporting the development of light-controlled biohybrid devices[45]. Biohybrid robots, designed based on biomimetic structures, have been developed using cardiomyocytes to achieve autonomous contraction and controlled movement[46–49]. Batalov et al. used fibronectin micropatterns to align cardiomyocytes into functional tissues, significantly improving their contractile performance[50]. This alignment approach allows for the creation of tissues that more closely resemble the natural myocardium, improving the viability and efficiency of cardiomyocyte-powered devices[50].

2.1.2. Swimmers. Cardiomyocytes have also been widely employed in swimmer-type biohybrid robots, where their spontaneous and rhythmic contractions generate propulsion in fluid environments. One well-known example of a cardiomyocyte-driven biohybrid project is the development

of fish-inspired robots that swim autonomously using cardiomyocyte layers[51]. Lee et al. created a biohybrid fish model powered by human cardiomyocyte bilayers, which uses mechanoelectrical signaling and automaticity to accomplish synchronized antagonistic muscle contractions and continuous propulsion like natural swimming[51]. The biohybrid fish exhibited swimming speeds of more than one body length per second (15 mm·s^{-1}) while being efficient[51]. This novel system incorporates cardiac biophysical principles into synthetic designs, acting as both a functioning fluid transport model and a platform for investigating biological feedback processes and enhancing biohybrid technology[51]. Similarly, Zhang et al. developed a biohybrid micro-swimmer system that uses cardiomyocytes cultivated on polydimethylsiloxane (PDMS) structures to achieve propulsion, drawing inspiration from aquatic propulsion principles[52]. These microswimmers have dolphin-shaped features to improve stability and swimming efficiency, which is powered by the contraction of cardiomyocytes seeded on the tail-mimicked scaffolds[52]. The study focuses on a mathematical model that links swimming velocity to cardiomyocyte concentration, allowing for precise regulation of motion[52].

2.1.3. Pumps. Cardiomyocyte-powered micropumps represent a unique application in the field of biohybrid robotics. Tanaka et al. used a PDMS-made micropump system produced by micro-patterning to seed cardiomyocytes on a tent-like scaffold[53]. The repetitive contractions of the cardiomyocytes caused fluid oscillations, resulting in a flow rate of 6.9 nL·min^{-1}. This technology demonstrated the utility of cardiomyocyte-powered pumps in microfluidic systems, such as organ-on-a-chip devices[53]. This highlights the feasibility of integrating living cardiac tissues into engineered platforms for microscale fluid control. Building on this concept, Bliley et al. demonstrated a contractile micropump model of the embryonic human heart using 3D bioprinting with human embryonic stem cell-derived cardiomyocytes and cardiac fibroblasts[54]. The team employed the FRESH (Freeform Reversible Embedding of Suspended Hydrogels) bioprinting technique to fabricate collagen-based heart tubes, which supported spontaneous contractions within 3–4 days and remained functional for up to 30 days[54]. These heart tubes exhibited unidirectional calcium wave propagation, anisotropic conduction ($\sim$5 cm·s^{-1}), and were capable of pumping fluid at 1.1 mm·s^{-1}, as evidenced by fluorescent bead displacement within the lumen[54]. This study represents a significant advance in the creation of stem-cell-based, functional cardiac micropumps for developmental modeling and potentially scalable therapeutic applications[54].

Cardiomyocyte-powered biohybrid robots have made significant progress and have proven effective as actuators in various biohybrid applications, including swimming robots and micropumps, yet they still face challenges, particularly in maintaining the structural integrity and long-term performance of cardiomyocytes[51]. Table 1 presents an overview of recent examples of actuators, swimmers, and pumps driven by cardiomyocytes.

2.2. Skeletal muscle cells

Skeletal muscle cells play a pivotal role in biohybrid robotics, offering precise actuation and modularity that surpass other biological actuators[64]. The human body contains over 600 skeletal muscles, which are attached to bones and controlled by motor neurons, enabling a wide range of dynamic and highly coordinated movements[65]. These muscles exhibit a modular structure, consisting of parallel bundles of muscle fibers formed by the fusion of myoblast precursor cells into multinucleated myotubes[5]. Their ability to generate voluntary, forceful contractions under external control makes them suitable for diverse biohybrid applications, including actuators, swimmers, pumps, and grasping systems.

2.2.1. Actuators. Skeletal muscle cells offer a modular architecture and precise controllability that make them particularly advantageous for biohybrid robotics. These cells are organized into parallel bundles of multinucleated myotubes formed from the fusion of myoblast precursors, enabling efficient contractile force generation[5]. Unlike cardiomyocytes, which exhibit spontaneous rhythmic contractions due to intrinsic pacemaker activity, skeletal muscle cells require external stimuli such as electrical, chemical, or optogenetic cues to contract[66,67]. This characteristic enables tight temporal control of actuation, essential for tasks requiring precision, such as grasping, locomotion, or directional pumping[68–70]. Upon stimulation, skeletal muscle cells initiate contraction via neural-like pathways where motor neuron signals trigger voltage-gated ion channels, leading to calcium influx and activation of the actin-myosin machinery[5].

Compared to cardiomyocytes, skeletal muscle cells can produce higher peak contractile forces and possess an energy-efficient ATP consumption profile, making them suitable for powering intricate robotic tasks[64]. Their "on-off" control enables programmable, adaptive movement critical for robotics applications. In one landmark study, Kim et al. developed a wireless skeletal muscle-powered robot by embedding optogenetic C2C12 myoblasts into hydrogels integrated with micro-light-emitting diodes[71]. These devices allowed for non-tethered muscle activation through resonant magnetic induction, enabling precise control of movement and steering with a top speed of 800 μm·s^{-1} and turning accuracy within $\pm 10°$[71].

Recent advancements in tissue engineering have further enhanced the alignment, maturation, and scalability of skeletal muscle constructs. Deshmukh et al. introduced an acoustic patterning technique that precisely aligns murine muscle progenitor cells within GelMA-based hydrogels using bulk-assisted wave devices[72]. The resulting high-density, anisotropic muscle tissues show significantly improved differentiation and mechanical integrity, making them promising for use in robotics and disease modeling[72].

Nevertheless, challenges remain in achieving reproducible long-term function. Functional skeletal muscle bioactuators require optimized biochemical, topographical, and mechanical cues to promote sustained contractility, robust myotube alignment, and resilience to mechanical stress[34,73]. Despite

Table 1. A summary of the recent actuators, swimmers, and pumps powered by cardiomyocytes. Reproduced with permission from[4]. CC BY-NC 3.0. Reprinted (adapted) with permission from[55]. Copyright (2022) American Chemical Socie. Adapted from[43] with permission from the Royal Society of Chemistry. Reproduced from[45]. CC BY 4.0. Reproduced with permission from[56]. CC BY-NC-ND 3.0. [42] John Wiley & Sons. © 2018 WILEY-VCH Verlag GmbH & Co. KGaA, Weinheim. [57] John Wiley & Sons. © 2019 WILEY-VCH Verlag GmbH & Co. KGaA, Weinheim. From[58]. Reprinted with permission from AAAS. From[51]. Reprinted with permission from AAAS. Adapted from[59], with permission from Springer Nature. Adapted from[60], with permission from Springer Nature. From[61]. Reprinted with permission from AAAS. From[62]. Reprinted with permission from AAAS. Reproduced from[52]. © IOP Publishing Ltd. All rights reserved. [63] John Wiley & Sons. © 2015 WILEY-VCH Verlag GmbH & Co. KGaA, Weinheim. Reprinted from[53], Copyright (2015), with permission from Elsevier.

Biohybrid Type	Structure	Performance	Schematic	References
Actuator	200–500 μm thick antagonistic pair of cardiac muscle rings in a centimeter-sized biohybrid self-beating actuator	Maximum contraction force ~850 μN	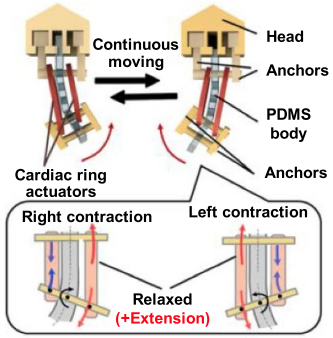	[4]
	Autonomous cardiomyocyte-based beating actuator of 4 mm diameter (low frequencies) to 6 mm (high frequencies), adjustable with acoustic frequency	Average motion of 0.7 mm·s^{-1} at 5 Hz; contraction and relaxation controlled by electrical stimulation	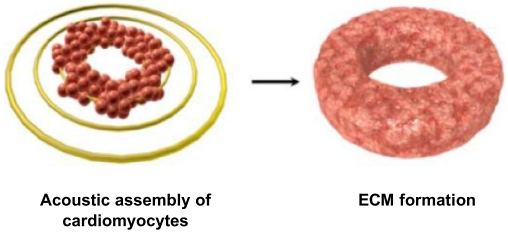	[55]

(Continued.)

Table 1. (Continued.)

Biohybrid Type	Structure	Performance	Schematic	References
	Mimic structure and function of native myocardium with a multi-strip cardiac muscle. Initial diameter of 356 μm (final ≈ (138 ± 62) μm); adjustable length	Maximum force per multi-strips ~5.50 μN; maximum stress ~368 Pa	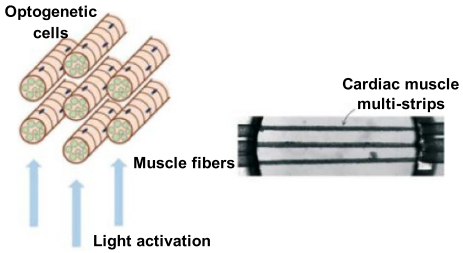	[43]
	The biohybrid cardiac model is a millimeter-scale muscular thin film cantilever with an elastic substrate and cardiomyocyte layer, enabling light-triggered contractions	Increasing in contraction frequency from (0.31 ± 0.10) Hz to (0.78 ± 0.11) Hz under light stimulation	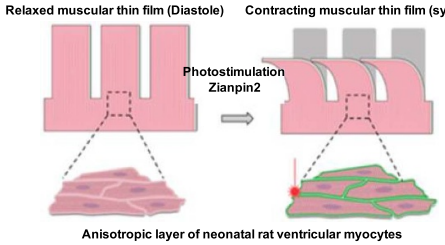	[45]
	Controlled locomotion by leveraging asymmetric design and friction modulation. Cantilever longitude of 732 μm	Maximum speed of 236 μm·s^{-1} with an average contraction frequency of 1.5 Hz	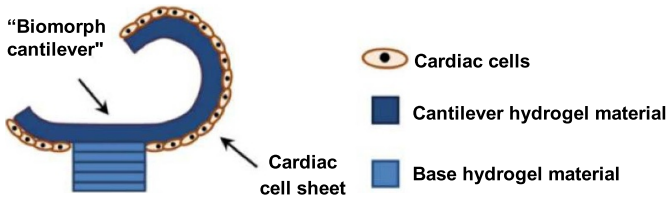	[56]

(Continued.)

Table 1. (Continued.)

Biohybrid Type	Structure	Performance	Schematic	References
	The biohybrid, resembling Morpho butterfly wings, has a flexible rectangular shape with nanoridges and dimensions around 150 μm × 90 μm, deforming dynamically with cardiomyocyte contractions to produce synchronized color shifts	Structural color shifts with reflection peak changes from 558 nm to 470 nm	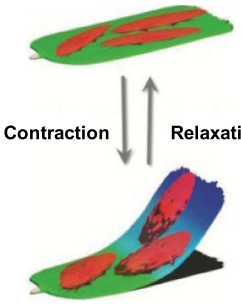	[42]
Swimmers	Floating-plane design with a flexible elastic body of 6 mm × 15 mm × 30 μm	Average speed ~0.8 mm·s^{-1}; Acceleration ~9 mm·s^{-2}	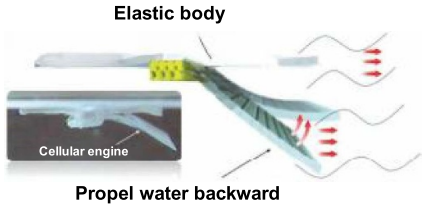	[57]
	Butterfly wing-shaped fin structure with a thickness of ~150 μm, integrated with a wireless frequency multiplexing bioelectronic device	Average locomotion speed of (0.52 ± 0.22) m·s^{-1} with a flapping frequency up to 2.0 Hz	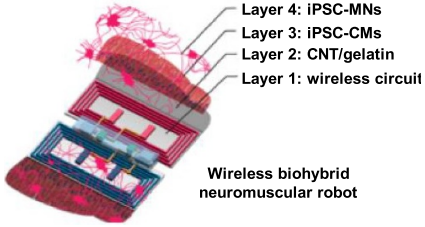	[58]

(Continued.)

Table 1. (Continued.)

Biohybrid Type	Structure	Performance	Schematic	References
	Muscular bilayer with human stem cell-derived cardiomyocytes, and a geometrically insulated cardiac tissue node all with a total length of 14 mm	Maximum swimming speed: 15 mm·s^{-1}	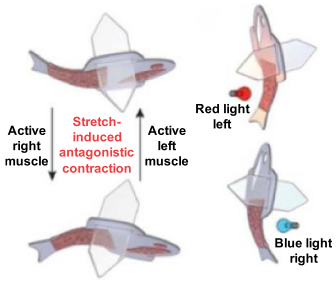	[51]
	Total diameter of 1 cm with eight lobes (2 mm). A 22 μm PDMS film	Swimming efficiency of 0.4–0.7 body lengths per stroke	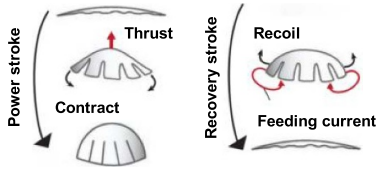	[59]
	Legs are 138 μm long and 40 μm wide. Film thickness of 20 nm/300 nm	Average speed of 38 m·s^{-1}, with a step frequency of 1.8 Hz and step size of 25 μm	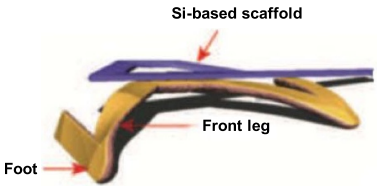	[60]

(Continued.)

Table 1. (Continued.)

Biohybrid Type	Structure	Performance	Schematic	References
	Various 3D shapes, including coiled, helical, and triangular forms, adapting dynamically for biomimetic motion. Films range from 14 μm to 60 μm thick.	Forces up to 1–4 mN·mm^{-2}. MFT swimmers reach 24 mm·min^{-1} at a frequency of 1 Hz	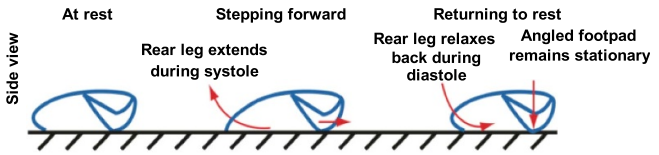	[61]
	16. 3 mm in length and weighs 10.18 mg	Maximum speed of 3.2 mm·s^{-1} at a 1.5 Hz pacing	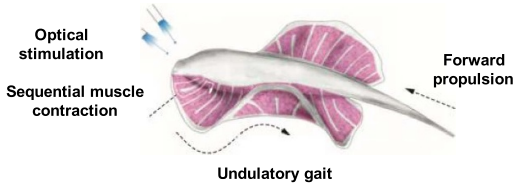	[62]
	Dolphin-shaped PDMS microstructure with 2 mm in length and 500 μm in width, with two elongated, flexible tails each 800 μm long and 200 μm wide, and a total thickness of 50 μm	Maximum velocity of 236 μm·s^{-1} at a frequency of 1.5 Hz	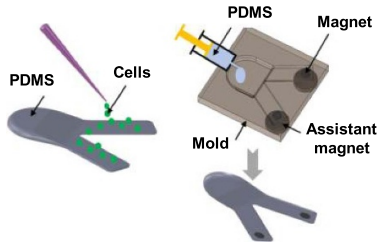	[52]
	2.11 cm diameter microelectronic swim, embedded in jellyfish of 13 cm to 19 cm diameter, maintaining a compact, neutrally buoyant, and streamlined shape to enhance natural propulsion.	Maximum swimming speed of 3.8 cm·s^{-1} when externally stimulated at 0.50 Hz to 0.62 Hz	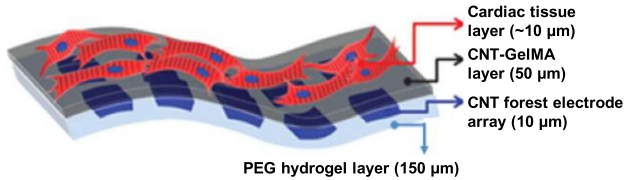	[63]
Pump	Micropump by differentiating iPS cells into beating cardiomyocytes. 2 cm × 2 cm microchip with microchannels 200 μm wide and deep	Theoretical flow rate: 6.9 nL·min^{-1}	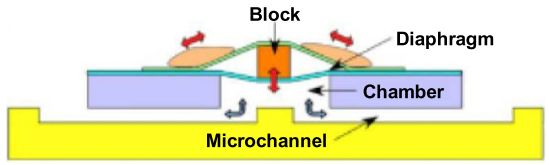	[53]

these complexities, skeletal muscle cells have been successfully applied in a wide range of biohybrid constructs, including actuators, swimmers, pumps, and grippers, underscoring their versatility and value in robotic systems[74,75].

2.2.2. Walkers. Several notable studies have advanced the field of muscle cell-powered biohybrid walkers by addressing the core challenges of locomotion control, mechanical performance, and structural design. These robots demonstrate how specific architectural and actuation strategies can be combined to generate walking behavior in untethered soft systems, powered solely by engineered muscle tissues. One of the earliest and most recognized works in this area was conducted by Pagan-Diaz et al., who developed a series of biohybrid walking robots with progressively larger and stronger skeletal muscle actuators[76]. Their work introduced a modular polyethylene glycol diacrylate (PEGDA) skeleton and a refined muscle ring-based actuation strategy that mimicked tendon-muscle interactions. By altering the dimensions of the skeleton and increasing the muscle mass, they demonstrated enhanced walking performance, including greater force generation and improved displacement[76]. Their findings underscored the importance of tuning both scaffold geometry and muscle maturation to optimize locomotion. This foundational approach provided a baseline design that others would later build upon to enhance control and complexity[76]. Kinjo et al. developed a biohybrid bipedal robot powered by engineered skeletal muscle tissues cultured from murine myoblasts[77]. The robot consists of two artificial legs made of a 3D-printed PEGDA skeleton, each actuated by an independently controlled muscle tissue anchored at the hip and knee joints. To fabricate the actuators, myoblasts were embedded in fibrin/matrigel hydrogels and molded around flexible PDMS pillars, promoting alignment and maturation of the muscle fibers under static tension[77]. Following a 14-day differentiation period, the matured muscle tissues exhibited striated morphology and robust contractile function, enabling leg actuation through alternating electrical pulse stimulation. The robot achieved symmetrical and repeatable bipedal walking, with a step size of approximately 400 μm and gait cycles synchronized to a 1 Hz stimulation frequency[77]. This work represents one of the first demonstrations of muscle-driven bipedal locomotion in a biohybrid platform, showcasing the potential for increasingly complex gait coordination in engineered robotic systems[77].

Building on this framework, Cvetkovic et al. developed a biohybrid bipedal walker with two distinct skeletal muscle actuators placed on each leg of a printed PEGDA scaffold[78]. This configuration enabled alternating leg motion, which more closely mimicked natural walking gaits. The muscle constructs were engineered from fibrin-based tissue, and the robot could produce rhythmic, directionally stable motion under electrical stimulation[78]. This study highlighted the value of coordinated actuation from independent muscle tissues and showed how structural symmetry and muscle placement can be exploited to emulate more lifelike locomotion[78]. Compared to the previous unidirectional ring-based designs, this model introduced the possibility of controlled, symmetric bipedal gait. Expanding further, Wang et al.[79] introduced a dual-ring walking biobot featuring two independent muscle actuators on a four-legged asymmetric scaffold. This design not only preserved forward locomotion but also introduced the capacity for turning, an essential step toward maneuverable biohybrid systems[79]. They implemented a computationally guided design and selection process to evaluate candidate geometries and muscle configurations before fabrication. Through simulations and experimental validation, they demonstrated that differential electrical stimulation of each muscle ring could direct the robot's turning behavior. This level of control marked a substantial leap toward more sophisticated, steerable biohybrid walkers capable of adaptive movement in complex environments[79].

Together, these studies illustrate the evolving complexity in biohybrid walking robots. From unidirectional motion using a single muscle ring to coordinated bipedal gaits and eventually to turnable, computationally optimized designs, they showcase how biofabrication strategies, muscle arrangement, and stimulation schemes can be systematically refined. These advancements not only improve locomotion fidelity but also pave the way for intelligent, responsive biohybrid systems in biomedical and soft robotics applications.

2.2.3. Swimmers. Another advancement in skeletal muscle-powered systems is the development of biohybrid swimmers[31,51,80]. Guix et al. engineered a swimming biobot by integrating C2C12 muscle tissue into a 3D-printed serpentine spring skeleton that provided both mechanical integrity and self-stimulation during maturation[81]. The compliant design enabled cyclic stretching after spontaneous contractions, enhancing myotube alignment and contractile force. Asymmetric stiffness in the skeleton induced directional motion, achieving speeds up to 800 $\mu m \cdot s^{-1}$, outperforming previous skeletal muscle swimmers. In parallel, Xu et al. developed a biohybrid jellyfish robot by embedding low-power microelectronics into live Aurelia aurita to externally drive muscle contractions[82]. Controlled stimulation increased swimming speed nearly threefold, reaching up to 3.8 $cm \cdot s^{-1}$, with only 10 mW of power input. This system highlights the potential of using living organisms as energy-efficient, controllable actuators for marine biohybrid robotics. Biohybrid robotics leverage the unique properties of both cardiomyocytes and skeletal muscle cells to enable lifelike movements and biocompatibility. These characteristics allow biohybrid robots to perform complex tasks such as crawling, swimming, and manipulating objects[53,74].

2.2.4. Pumps. Recent developments in biohybrid systems have demonstrated the potential of skeletal muscle cells not only as actuators but also as efficient components in fluidic devices. In particular, muscle-based pumps have emerged as promising platforms for applications requiring controlled microscale fluid transport. Li et al. engineered a valveless pump powered by a contractile skeletal muscle ring made with C2C12 mouse skeletal myoblasts[31]. The pump achieved flow rates up to 22.5 $\mu L \cdot min^{-1}$, which is three times higher than the

pumps of similar size powered with cardiomyocytes, demonstrating thus potential applications in microfluidics and drug delivery[31]. More recently, Li et al. developed an adaptive biohybrid pumping machine with flow-loop feedback[83]. This system utilized tissue engineered from C2C12 skeletal muscle cells embedded in a collagen I/matrigel matrix, achieving flow rates of up to 13.62 $\mu L \cdot min^{-1}$. While lower than the earlier-mentioned pump, these flow rates remain significantly higher than the typical nanoliter to sub-microliter per minute range achieved by cardiomyocyte-powered pumps[83]. These findings demonstrate the functional advantages of skeletal muscle actuators in generating higher mechanical output, which is critical for scalable and controllable perfusion in biomedical applications[84]. Nevertheless, challenges remain, including the need for long-term contractile stability, integration with sensing or regulatory circuits, and responsiveness to dynamic in vivo conditions. Despite these limitations, the modular structure and tunable output of skeletal muscle–driven pumps suggest strong potential for use in personalized therapeutic systems, soft robotic perfusion devices, and implantable drug delivery platforms[85,86].

2.2.5. Grippers. A key development in biohybrid functional grasping systems is the design of an engineered skeletal muscle-driven microhand controlled by surface electromyographic (EMG) signals[29]. Prosthetic and assistive technology particularly needs grasping functionality, where restoring voluntary grip and object manipulation by fine motor control is essential in order to improve user autonomy and quality of life. In this context, Kabumoto et al. created an aligned skeletal muscle tissue-driven gripper-type microhand using primary rat myoblasts embedded in a collagen-Matrigel matrix[87]. Neuromimetic electrical signals derived from human EMG recordings were used to induce muscle contraction, enabling voluntary and precise control of grip movement[87]. The device exhibited frequency-dependent contractile performance and was capable of mimicking natural tetanic contractions when integrated into a PDMS-based gripper structure[87]. This work demonstrates the potential of combining bioactuated muscle tissue with human-inspired neural control interfaces to create soft robotic systems capable of performing complex, intentional tasks. Moreover, by linking external bioelectric signals to engineered biological motion, the system bridges the gap between user intent and mechanical execution, offering a promising pathway toward more responsive and personalized prosthetic devices. Furthermore, Hoshino and Morishima developed a muscle-powered microtweezer system using rat primary skeletal myotubes cultured on an artificial microskeleton fabricated from dog hair, demonstrating a unique biohybrid actuator designed for grasping tasks[88]. The microscale cantilevers were shaped using focused ion beam (FIB) milling, allowing precise anisotropic stiffness to guide movement. Skeletal myotubes, aligned along the hair axis and activated via electrical stimulation, generated contraction forces around 1–2 μN, sufficient to produce measurable tip displacement (∼0.6 μm)[88]. Although the displacement was small, this proof-of-concept shows the potential of skeletal muscle cells for microscale mechanical grasping applications. The system also highlights the role of fiber geometry and stiffness gradients in enhancing directional force transmission, a critical design consideration for functional biohybrid grippers[88].

Although previous work had shown the promise of muscle-powered microgrippers, Morimoto et al. designed a significant actuation control constraints through the introduction of an antagonistic skeletal muscle configuration[74]. This biohybrid gripper mimicked natural musculoskeletal structures and enabled bidirectional rotation up to 90° through alternating electrical stimulation. Engineered from three layers of myoblast-laden hydrogel with ∼100 μm striped microstructures, the tissues showed ∼20% contractile strain, strong alignment, and stable actuation after 10 days of differentiation[74]. The gripper exhibited tunable, frequency-dependent motion and generated forces up to 0.3 $mN \cdot \mu m^{-2}$. It successfully performed functional pick-and-place tasks, including lifelike object manipulation[74].

Building on earlier advances, Ren et al. developed a fully functional, multi-jointed biohybrid hand that represents a major leap in scale and complexity for muscle-actuated robotics[89]. Unlike previous millimeter-scale systems limited to single-joint movement, this centimeter-scale hand features five independent fingers, each powered by a MuMuTA (Multiple Muscle Tissue Actuator) composed of eight parallel-aligned engineered human muscle bundles[89]. These bundles are fabricated as aligned hydrogel sheets, rolled into cylindrical "sushi-roll" actuators, and anchored to tendon-like parylene structures. Upon electrical stimulation, each MuMuTA contracts linearly (∼4 mm displacement, ∼8 mN force), enabling up to 130° of finger flexion through a cable-driven mechanism. The actuators exhibited high force density ($\sim 0.7\ mN \cdot mm^{-2}$) and angular velocities up to $500° \cdot s^{-1}$, closely matching human finger physiology[89]. A key innovation was the selective stimulation of individual fingers, achieved by inserting insulating glass walls to prevent electrical crosstalk, allowing for coordinated gestures like a scissors sign. The hand also demonstrated object manipulation capabilities, including pipette repositioning. Importantly, the MuMuTAs showed excellent maturation and long-term stability, maintaining contractility for up to 178 days in vitro, with consistent force output during 30 minutes of continuous operation. This work marks a significant step toward anatomically scaled, human-like biohybrid soft robots[89]. Table 2 provides an overview of recent examples of actuators, walkers, swimmers, and pumps driven by skeletal muscle cells.

3. Advanced biofabrication techniques and their promising potential in biohybrid robots

3.1. 3D printing

3D printing is utilized in sectors such as tissue engineering and regenerative medicine, offering a flexible approach to creating intricate objects using various materials, including metals, ceramics, and polymers[92–94]. Among the many

Table 2. A summary of the recent actuators, swimmers, and pumps powered by skeletal muscle cells. From[71]. Reprinted with permission from AAAS. Reproduced from[90]. CC BY 4.0. Adapted from[91], with permission from Springer Nature. Reprinted from[77], Copyright (2024), with permission from Elsevier. Reproduced from[79]. CC BY 4.0. [76] John Wiley & Sons. © 2018 WILEY-VCH Verlag GmbH & Co. KGaA, Weinheim. Reproduced with permission from[78]. Reproduced with permission from[69]. From[81]. Reprinted with permission from AAAS. Reproduced with permission from[82]. Copyright © 2020 The Authors, some rights reserved; exclusive licensee American Association for the Advancement of Science. No claim to original U.S. Government Works. Distributed under a Creative Commons Attribution NonCommercial License 4.0 (CC BY-NC). Reproduced with permission from[2]. Copyright © 2019 the Author(s). Published by PNAS. This open access article is distributed under Creative Commons Attribution-NonCommercial-NoDerivatives License 4.0 (CC BY-NC-ND). Reproduced with permission from[31]. Copyright © 2019 the Author(s). Published by PNAS. This open access article is distributed under Creative Commons Attribution-NonCommercial-NoDerivatives License 4.0 (CC BY-NC-ND). Reproduced from[83]. © IOP Publishing Ltd. All rights reserved. Reproduced with permission from[88].© 2010 by The Japan Society of Mechanical Engineers. From[74]. Reprinted with permission from AAAS. From[89]. Reprinted with permission from AAAS.

Biohybrid type	Structure	Performance	Schematic	References
Actuator	1.4 cm in length and 0.7 cm in width and an optogenetic control system of 5 mm in diameter. Optogenetic C2C12 cells and wireless optoelectronics	Muscle forces up to 1 403 μN using 5 μ-LEDs; with a maximum walking speed of 0.83 mm·s^{-1} when the robot was stimulated at 4 Hz	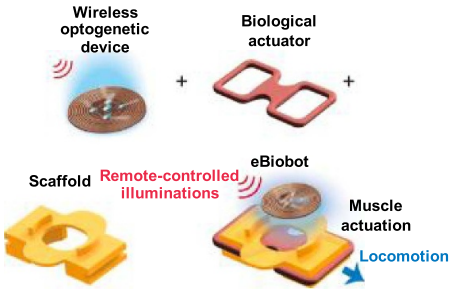	[71]
	The biohybrid robot-on-a-chip, over 3 mm in diameter, mimics the human motor system with a multilayered structure of cerebral organoid, motor neuron spheroids, and muscle bundle for drug evaluation	Demonstrated muscle bundle movement increasing from (4.5 ± 0.99) μm to (18.67 ± 2.25) μm in response to levodopa	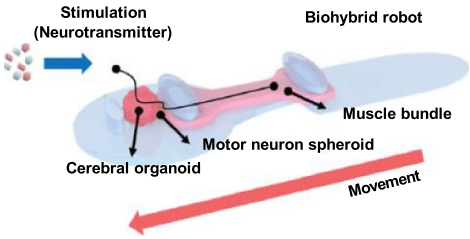	[90]
	Centimeter-scale biohybrid robot with a modular muscle-powered structure, with a flexible beam and anchor pillars for controlled locomotion	1.7 mN (3.2 kPa) of passive tension force and 300 mN (0.56 kPa) of active tension force in response to external stimulation	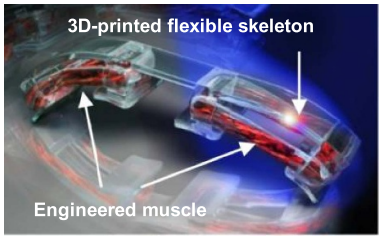	[91]

(Continued.)

Table 2. (Continued.)

Biohybrid type	Structure	Performance	Schematic	References
Walker	A bipedal biohybrid robot with two independently actuated muscle legs, enabling symmetric walking motion via fibrin-based muscle tissue	The average walking speed was calculated to be 5.4 mm·min^{-1}. The amount of forward movement induced by a single electrical stimulus was 0.47 mm	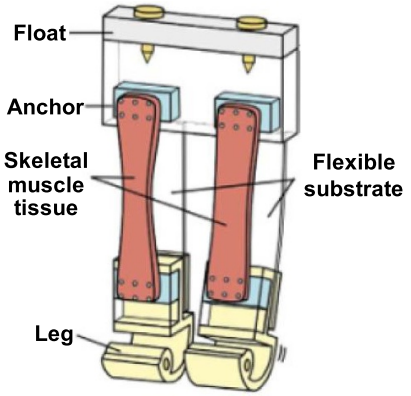	[77]
	A dual-ring biohybrid walker with an asymmetrical scaffold, designed through computational modeling to enhance maneuverability using two independently actuated muscle rings	Walking speed of 5.9 mm·min^{-1}	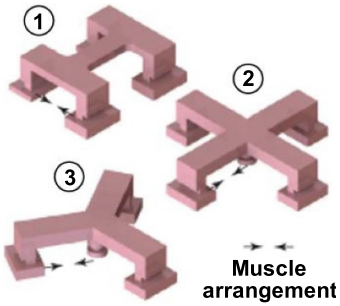	[79]
	Muscle-pillar-beam design mimics the muscle-tendon-bone relationship with a scaffold thickness of ∼400 μm	Walking speed of 0.5 mm·s^{-1}	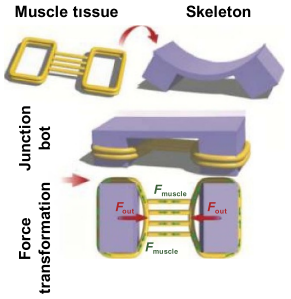	[76]

(Continued.)

Table 2. (Continued.)

Biohybrid type	Structure	Performance	Schematic	References
	Untethered bipedal biorobot with a total length of 7 mm and a muscle strip thickness of ∼500 μm	Locomotion at 156 μm·s^{-1} under electrical stimulation (1.5 body lengths per min); active tension force of (394.7 ± 56.6) μN	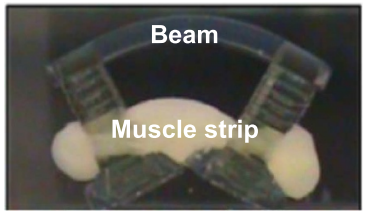	[78]
	Quadruped robot with optogenetically modified muscle rings with a thickness of 700 μm.	Directional movement at 310 μm·s^{-1} (1.3 body lengths·min^{-1}); rotational movement (2°·s^{-1}); forces of 300 μN per muscle ring	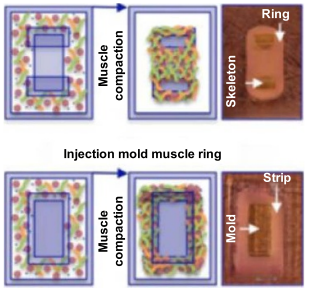	[69]
Swimmer	3D-printed skeletons and muscle cells, featuring dual swimming modes. Total length 12 mm	Swimming speed of 0.554 mm·s^{-1}	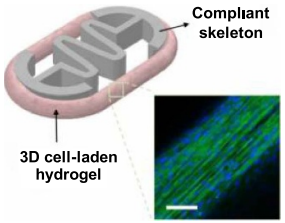	[81]

(Continued.)

Table 2. (Continued.)

Biohybrid type	Structure	Performance	Schematic	References
	The biohybrid jellyfish robot, approximately 8–10 cm in diameter, integrates low-power microelectronics within a flexible bell structure, using embedded electrodes to enhance natural propulsion	The jellyfish robot increased swimming speed by up to 2.8 times with only a twofold rise in metabolic cost and 10 mW of external power input	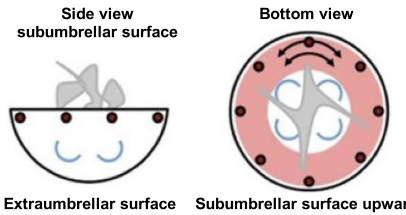	[82]
	Tail length is between 0.5 and 0.3 mm with a total length of 3.2 mm. Powered by C2C12 muscle cells paired with optogenetic neurons	Propulsion around 0.7 $\mu m \cdot s^{-1}$	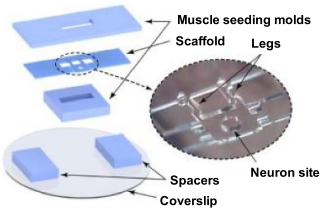	[2]
Pump	Valveless pump powered by contractile skeletal muscle ring with 12 mm outer diameter, 5 mm inner diameter, and 3 mm thickness	Flow rates up to 22.5 $\mu L \cdot min^{-1}$ at 4 Hz electrical stimulation	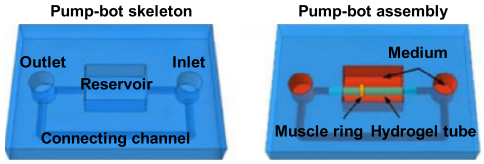	[31]

(Continued.)

Table 2. (Continued.)

Biohybrid type	Structure	Performance	Schematic	References
	Adaptive pumping machine with flow-loop feedback, using C2C12 cells and collagen I/Matrigel matrix., 12 mm outer diameter, 6 mm inner diameter and 3 mm thick muscle ring	Flow rates up to 13.62 μL·min^{-1}.	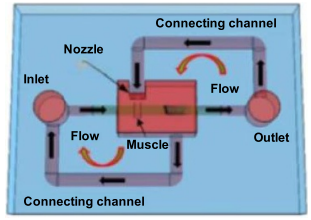	[83]
Gripper	Microcantilever-based microtweezer structure fabricated from a strand of dog hair, serving as an artificial skeleton, on which aligned rat primary myotubes are cultured to generate contraction-driven motion.	1 μN for maximum griping force of the tips	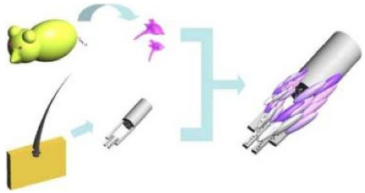	[88]
	3D printed jointed biohybrid gripper powered by an antagonistic pair of skeletal muscle tissues cultured on micropatterned hydrogels, enabling bidirectional gripping motion.	20% strain under tetanic stimulation and electrically induced actuation using 1.5 V·mm^{-1}, 2 ms pulse duration, 50 Hz	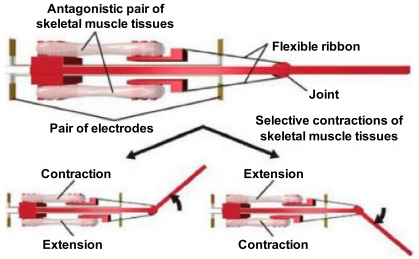	[74]
	Multi joined hand skeleton actuated by rolled bundles of aligned human skeletal muscle tissue, producing tendon driven finger flexion via linear contraction.	Maximum contractile force per MuMuTa is 8 mN	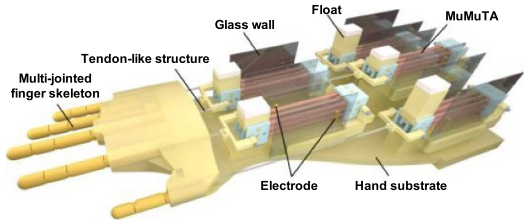	[89]

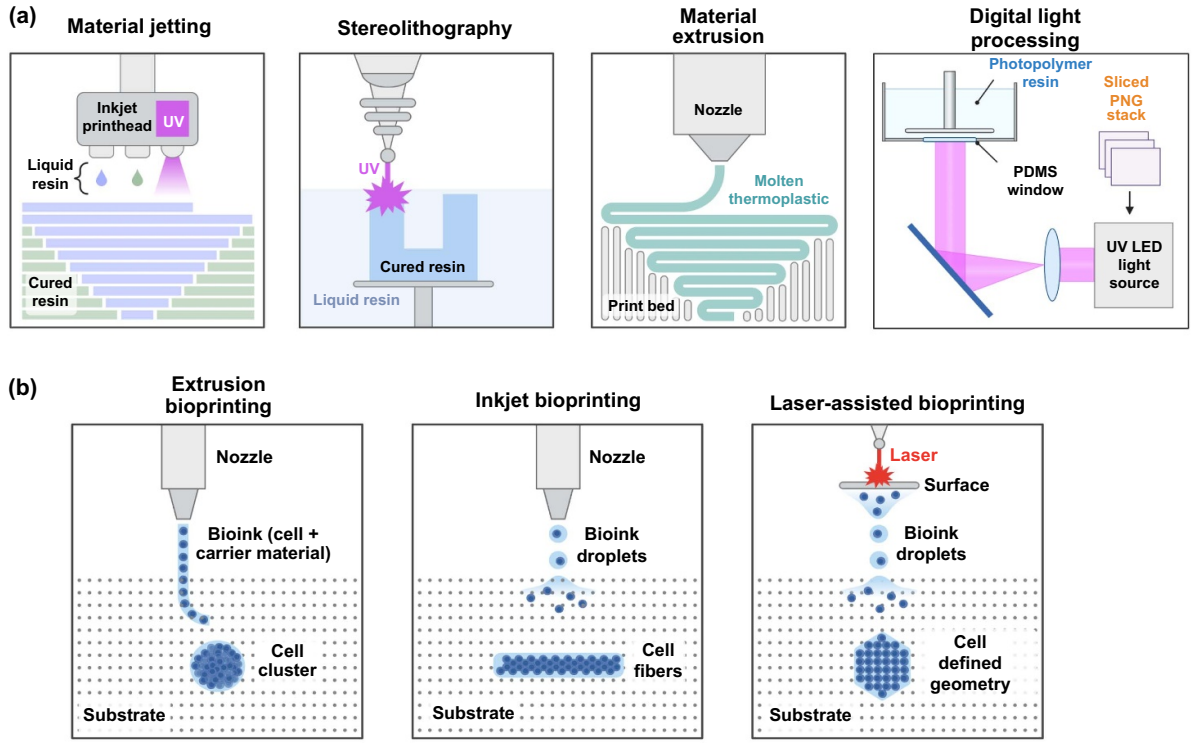

Figure 2. Commonly used 3D printing techniques in biohybrid robot fabrication (a) Schematic shows the commonly used 3D printing techniques in fabricating biohybrid robots, with material jetting deposits liquid photopolymer droplets layer by layer, curing them with UV light to create high-resolution, multi-material structures with smooth surfaces. Stereolithography (SLA) uses a laser to selectively cure photopolymer resin point by point, producing highly detailed structures with excellent surface finish. Material extrusion extrudes thermoplastic or hydrogel filaments through a heated nozzle, building structures layer by layer for biofabrication and structural components. Digital light processing (DLP) cures entire layers of photopolymer resin simultaneously using a digital light projector, enabling fast and precise fabrication of intricate designs. (b) Schematic shows the commonly used 3D bioprinting techniques, with extrusion bioprinting deposits bioinks through a controlled dispensing system, enabling the fabrication of cell-laden scaffolds with tunable porosity and mechanical properties. Inkjet bioprinting uses drop-on-demand technology to precisely place bioinks, allowing for high-resolution patterning of cells and biomaterials. Laser-assisted bioprinting (LAB) utilizes laser pulses to transfer bioinks onto a substrate, achieving precise cell placement without nozzle clogging, making it ideal for high-resolution tissue engineering applications. Created in BioRender with permission.

advancements driven by 3D printing, its role in the biomedical field has been particularly transformative[95–100]. One emerging area that leverages this technology is biofabrication, which focuses on organizing cellular structures in a way that mimics or is inspired by natural biological processes. This field has gained significant attention for its potential to create engineered tissue constructs that integrate living cells with extracellular or biochemical components[101–105]. These constructs are designed to form specific architectures, making them highly valuable in applications such as regenerative medicine and drug testing[106]. By combining principles of 3D printing with biological materials, bioprinting opens new possibilities for developing functional tissues and complex biological systems[107,108]. Figure 2(a) shows an overall procedure of 3D printing that can be used in producing biohybrid robots, while Figure 2(b) shows the commonly used 3D bioprinting techniques in biohybrid robot fabrication.

A typical example is that Raman et al. developed an optogenetic skeletal muscle-powered biohybrid robot (bio-bot) using a fabrication approach that integrates genetic modification with SLA 3D printing (Figure 3)[69]. The process begins with the SLA 3D printing of injection molds and bio-bot skeletons, designed to accommodate muscle constructs with precise geometries (Figure 3(a))[69]. These molds facilitate the formation of muscle strips and rings through compaction, ensuring optimal attachment to the bio-bot skeleton (Figures 3(b) and (c))[69]. The assembled biohybrid robots exhibit controlled contraction and directional movement in response to blue light stimulation, demonstrating their adaptability to environmental signals. Functional testing confirmed their ability to execute linear motion and directional adjustments while maintaining performance over repeated stimulation cycles[69]. This fabrication approach highlights the potential of integrating 3D printed scaffolds, engineered muscle tissues, and optogenetic control to advance biohybrid robotics for biomedical and soft robotics applications. Another example also utilized SLA 3D printing, Cvetkovic et al. presented a bio-bot powered by engineered skeletal muscle tissues[78]. The hydrogel structures with flexible beams and stiff pillars were optimized to support muscle contraction. Skeletal muscle strips were cultured in fibrin- or collagen-based ECM, supplemented with insulin-like growth factor 1 to enhance myotube formation and contractility. Electrical stimulation triggered synchronized muscle contractions, enabling controlled locomotion in bio-bot, with asymmetric designs achieving directional crawling movement at speeds up to

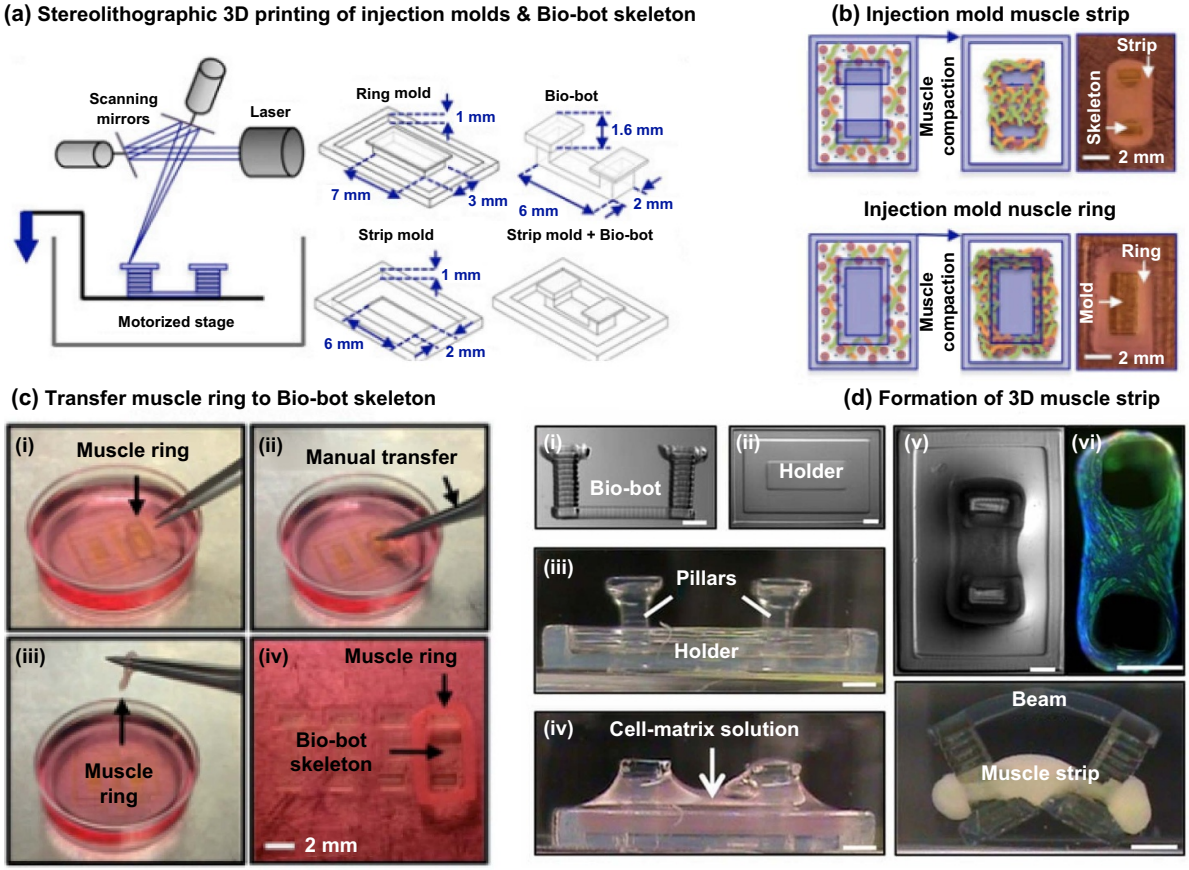

Figure 3. Design and fabrication process for optogenetic muscle ring-powered bio-bots. This figure demonstrates a modular biofabrication approach that combines stereolithographic 3D printing and engineered muscle rings to enable light-responsive actuation in soft robotic systems. (a) SLA 3D printing is utilized to create injection molds for muscle rings and strips, as well as bio-bot skeletons, using a PEGDA photosensitive resin. (b) The cell-laden hydrogel solution is injected into molds to form muscle strips and rings. (c) Muscle rings are manually transferred from the molds to the bio-bot skeletons. (a)–(c) Reproduced with permission from[69]. (d) The assembled bio-bot ((i) side view) and its corresponding holder ((ii), top view) were set up. A cell-matrix solution was slowly dispensed into a polymerized holder containing the bio-bot framework ((iii) and (iv), side view). The cells and matrix gradually aggregated around the pillars, forming a stable muscle strip ((v) and (vi), top view; stained for MF-20 in green and DAPI in blue). Finally, the device was released from the holder ((vii), side view). Scale bars, 1 mm. Reproduced with permission from[78].

156 μm·s^{-1}[78]. Computational modeling and experimental testing further optimized their performance, with fibrin-based muscle strips demonstrating significantly enhanced force output and sustained functionality under prolonged stimulation (Figure 3(d))[78].

Besides SLA, DLP 3D printing, which offers high-resolution, rapid fabrication of intricate structures, making it ideal for biohybrid robot fabrication[109–111]. Its ability to precisely pattern complex microarchitectures with biocompatible materials enables the integration of biological and synthetic components with seamless structural alignment[112,113]. This study used DLP to fabricate flexible substrates with gold electrodes and anchoring structures, providing a stable and conductive framework for engineered skeletal muscle tissue[114] (Figure 4(a)). Figure 4(b) illustrates the actuation mechanism, where electrical stimulation triggers muscle contraction, generating a controlled bending motion. The biofabrication process involves layer-by-layer deposition of myoblast-laden hydrogel sheets, followed by encapsulation using a sacrificial alginate gel, which is later dissolved to form a hollow collagen chamber that preserves humidity and cell viability for sustained actuation (Figures 4(c)–(g))[114]. The integration of precisely engineered perfusable tubes further enhances the long-term contractile function, demonstrating how DLP enables scalable, high-precision biofabrication for biohybrid robots[114]. Figures 4(h) and (i) show the actual images of the assembled biohybrid actuator.

While SLA and DLP have demonstrated high-resolution fabrication of biohybrid scaffolds, 3D bioprinting introduces the capability to directly print cell-laden structures, enabling the creation of complex, functional tissues[115]. An interesting project conducted by Esser et al. showcases the potential of hiPSC-derived cardiomyocytes (hiPSC-CMs) in bioprinted cardiac constructs[116]. By utilizing a collagen-hyaluronic acid bioink, this approach eliminates the need for pre-cast molds, allowing direct deposition of functional cardiac tissues (Figure 5(a)). The printed constructs exhibited precise, well-defined edges and closely replicated the intended 3D models, as confirmed by overlap maps, without (Figure 5(b)) and with hiPSC-CMs (Figure 5(c))[116]. The printed constructs

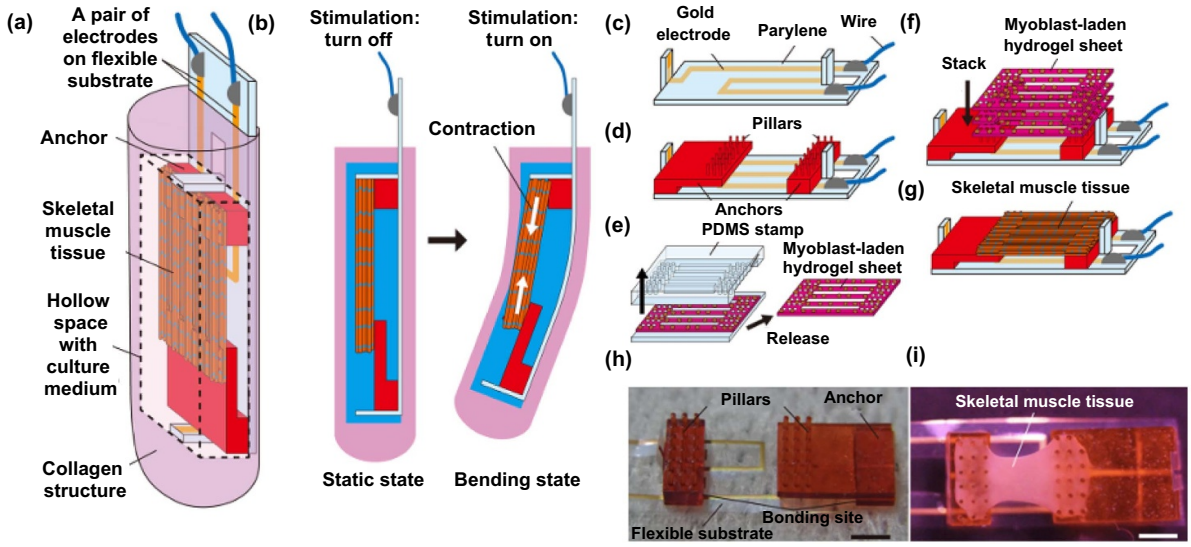

Figure 4. Illustration of the biofabrication and functional design of a biohybrid actuator powered by skeletal muscle tissue, integrating engineered muscle, flexible substrates, and electrical stimulation for controlled motion. The combination of flexible substrates and electrical stimulation is critical for achieving both biomechanical adaptability and reliable signal transduction. (a) Schematic shows the overall schematic, where the actuator is encased in a collagen structure with a hollow space containing culture medium to maintain muscle viability. (b) Demonstration of the actuation mechanism, where electrical stimulation induces muscle contraction, resulting in a bending motion. (c)-(g) Details of the fabrication process, starting with a flexible substrate with gold electrodes (c), followed by micro-pillars for anchoring (d), and PDMS stamp-assisted transfer of myoblast-laden hydrogel sheets (e). The hydrogel sheets are stacked (f) to form a multi-layer muscle tissue (g), ensuring proper alignment and contractility. (h) and (i) Photographs of the assembled biohybrid actuator, highlighting the anchoring system, flexible substrate, and integrated skeletal muscle tissue. Scale bars, (h) and (i) 2 mm. Reproduced from[114]. CC BY 4.0.

demonstrated well-organized sarcomeres, exhibited spontaneous contractions for over 30 days, and responded to adrenergic stimulation, highlighting their suitability for drug screening applications[116]. Figures 5(d) and (e) show printed tissues after 30 days of culture, including maximum intensity projections of confocal z-stacks from whole-mount staining (Figure 5(d)) and stained cryosections (Figure 5(e))[116]. Moreover, the ability to fabricate geometrically complex structures, such as ventricle-like constructs, highlights the scalability of 3D bioprinting in tissue engineering. This work underscores how 3D bioprinting enhances tissue functionality and structural complexity, bridging the gap between engineered cardiac models and clinically relevant heart tissue[116].

An illustrative example of muscle-cell-based biohybrid robotics is provided by Mestre et al., who developed fully functional skeletal muscle actuators using a one-step 3D bioprinting strategy (Figure 6)[117]. In this approach, C2C12 mouse myoblasts were encapsulated in a bioink composed of fibrinogen, gelatin, and hyaluronic acid, forming a supportive matrix for cell viability and myotube formation (Figure 6(a))[117]. Following bioprinting, myoblasts underwent myogenic differentiation through a well-defined timeline involving the sequential expression of MyoD, Myogenin, and MyHC in growth and differentiation media (Figure 6(b)), resulting in aligned, mature myotubes within the hydrogel constructs[117]. The printing process enabled the formation of complex and customizable tissue geometries, including rings and patterned structures (Figure 6(c)), demonstrating excellent shape fidelity and versatility[117]. Additionally, the technique supported the scalable fabrication of structured tissues such as rectangular and dumbbell-shaped muscle constructs (Figure 6(d)), which incorporated integrated PDMS posts for real-time force measurement[117]. The printed muscle actuators displayed tunable force output and adaptability under various mechanical and electrical stimulation conditions. This study highlights the potential of 3D bioprinting not only for scaffold fabrication but as a direct and scalable platform for engineering contractile muscle units tailored for soft robotics applications[117].

There is no doubt that 3D printing is a powerful tool in the fabrication of biohybrid robots, offering precise and complex structural control, material versatility, and seamless cellular integration[118–120]. Various additive manufacturing techniques contribute uniquely to biohybrid system development, each with distinct advantages and limitations. SLA and DLP provide high-resolution fabrication of biocompatible scaffolds and flexible substrates, crucial for supporting engineered muscle tissues and bioelectronic components. While SLA offers superior detail, it is slower due to its point-by-point laser curing process, whereas DLP enables faster fabrication by curing entire layers simultaneously, though it is limited by pixel resolution[69]. Material jetting and extrusion bioprinting further enhance fabrication capabilities by enabling multi-material deposition[121–123]. Material jetting, with its UV-curable photopolymers, allows for smooth, high-precision structures, but its limited bioink compatibility restricts its use in living tissue applications. Extrusion bioprinting, on the other hand, enables hydrogel-based scaffold fabrication, making it well-suited for cell-laden constructs. However, it suffers from lower resolution compared

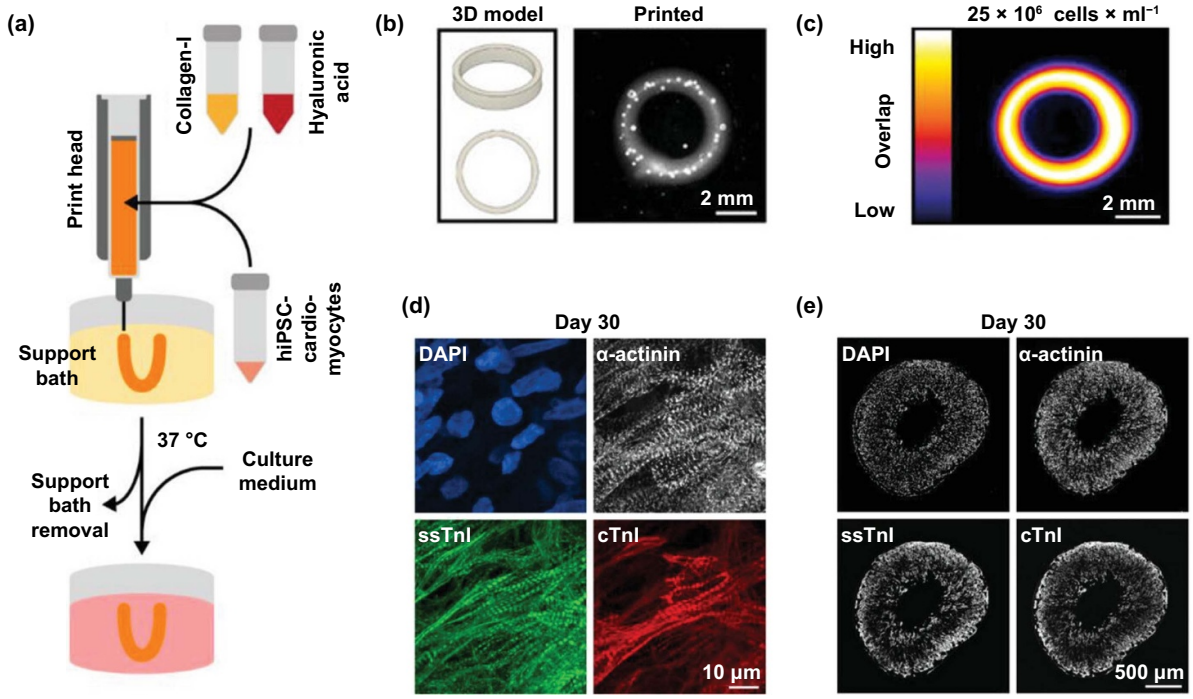

Figure 5. Bioprinting of hiPSC-derived cardiomyocytes with direct encapsulation and deposition of cells within the gel. (a) Schematic representation of the in-gel bioprinting method, utilizing collagen-based bioinks within a thermo-responsive microparticle support bath. It allows bioinks to be deposited with high precision while maintaining embedded cells in a 3D structure. (b) 3D models of ring-shaped constructs, accompanied by dark-field images of printed structures using a bioink containing 3.0 mg·mL^{-1} collagen-I and 3.0 mg·mL^{-1} hyaluronic acid (CollHA3-3), with corresponding overlap maps (n = 22–24). (c) Overlap map of rings printed with CollHA3-3 incorporating 25 million hiPSC-CMs per mL (n = 119), constructs maintain precise geometry and uniform cell distribution. (d) and (e) Representative images of bioprinted tissues after 30 days of culture, showing maximum intensity projections of whole-mount-stained confocal z-stacks (d) and stained cryosections (e). Sarcomeric proteins detected include α-actinin, slow skeletal troponin I (ssTnI), and cardiac troponin I (cTnI), with cell nuclei stained by DAPI, scale bar, (d) 10 µm, (e) 500 µm. This figure highlights the benefits of printing cells directly into scaffolds, enabling physiological 3D architecture, and functional contractility. Reproduced with permission from[116]. (CC BY-NC-ND 4.0).

to SLA and DLP[124]. Inkjet bioprinting and LAB refine cell placement and biomaterial patterning. Inkjet bioprinting, utilizing drop-on-demand deposition, achieves high-precision cell placement with minimal shear stress, making it ideal for layered tissue engineering[125]. However, its low viscosity bioink requirement limits material options[126,127]. LAB, relying on laser-induced forward transfer, enables nozzle-free, high-resolution bioink deposition, preventing clogging and allowing for precise printing and fast speed[128]. Table 3 below summarizes the advantages, disadvantages, and applications of the commonly used 3D printing methods.

Despite this, it requires complex laser calibration and expensive setups, and results in less cell viability[145,146]. By leveraging these complementary fabrication techniques, biohybrid robots can be tailored for specific functions, ranging from muscle-actuated bio-bots and neuromuscular interfaces to soft robotic systems with responsive and adaptable motion[147–149]. The combination of high-resolution structuring, multi-material integration, and advanced bioprinting strategies ensures scalable, functional bioactuation systems, driving advancements in soft robotics, bioengineering, and regenerative medicine[84,150]. 3D printing enables the design of precise structures, but current systems struggle to balance high resolution with high throughput, and scalability is limited[151]. Additionally, prolonged exposure to UV or pressure-based extrusion can reduce cell viability, especially in dense tissues. To address these limitations, novel strategies utilizing visible-light photoinitiators and low-shear bioprinting are being actively explored[152].

3.2. *Micro/nano patterning*

One of the main goals of micro/nano patterning in tissue engineering is to control the anisotropic organization of cells, particularly in muscle constructs[153]. Surface features such as microgrooves and nanopillars provide topographical cues that influence cytoskeletal organization, leading to guided cell orientation. This controlled alignment is critical in promoting the fusion of myoblasts into functional myotubes or enhancing synchronous contraction in cardiomyocytes[154]. The advancement of biohybrid robots has been driven by key micro/nano patterning techniques such as photolithography, soft lithography, nanoimprint lithography (NIL), and dielectrophoresis (DEP). These approaches enable the precise manufacture of structures required for biohybrid actuators, microswimmers, and microfluidic devices[32,155,156]. These patterning processes have improved the usefulness and versatility of biohybrid robots

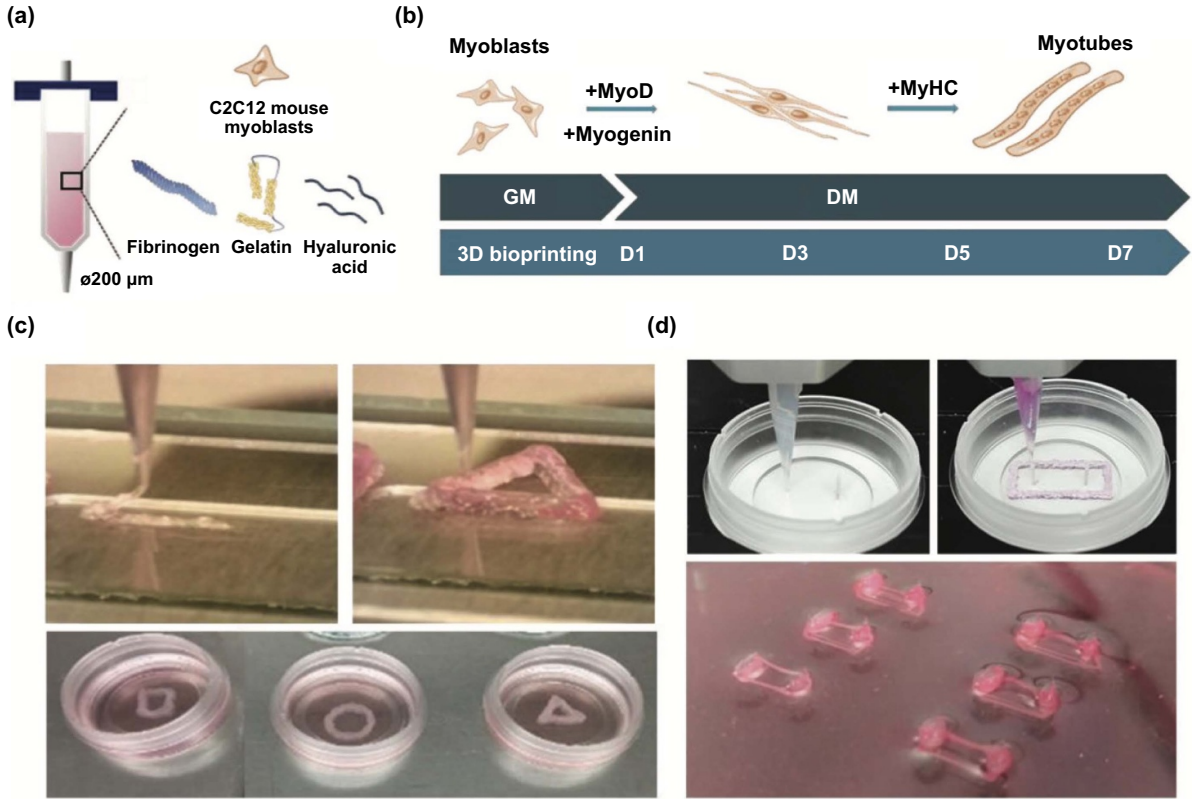

Figure 6. Overview of the fabrication and characterization of 3D-bioprinted skeletal muscle-based bioactuators using C2C12 myoblasts. The process integrates cell-laden hydrogels, geometric control, multi-material bioprinting, and functional evaluation to generate viable, contractile tissue constructs. (a) Diagram illustrating the 3D bioprinting strategy, where C2C12 mouse myoblasts are encapsulated in a hydrogel blend of fibrinogen, gelatin, and hyaluronic acid. (b) Overview of the differentiation timeline and expression of key myogenic markers. (c) Sequential images and outcomes of bioprinted muscle constructs with simple geometries. (d) Representative results of multi-material bioprinting used to fabricate muscle-based actuators with integrated PDMS posts for force sensing. [117] John Wiley & Sons. © 2018 WILEY-VCH Verlag GmbH & Co. KGaA, Weinheim.

for applications, such as robotics, healthcare, and biomedical applications[157]. The following schematic compares these four key techniques, each offering unique advantages for patterning and structuring materials at micro/nanoscale levels (Figure 7).

In polymer-based photoresists, photolithography is a patterning technique used to achieve surface relief structures down to the nanoscale, such as grooves, ridges, or nanopillars. This technique enables precise patterning of microstructures that guide cell alignment and promote anisotropic tissue formation[23]. For instance, Choi et al. used photolithography to create microgrooves on PDMS substrates with dimensions of 20 μm in width and 2 μm in height, which directed the alignment of skeletal muscle cells, leading to the development of anisotropic muscle tissues for biohybrid actuators (Figure 8(b))[154]. These cells, cultured on the surfaces of both nano-sized graphene oxide-modified nanopillars and microgroove hybrid polymer array (NMPA), were able to express higher levels of myosin heavy chain and hence differentiate into skeletal muscle cells (Figure 8(a))[154]. Similarly, Tognato et al. utilize photolithography to make anisotropic nanocomposite hydrogels in 3D microfluidic channels that act as molds for flexible biohybrid robotics devices[159]. With the aid of external stimuli like light and magnetic fields, this technique guarantees excellent precision in the formation of aligned iron oxide nanoparticle filaments within a GelMA matrix[159]. The anisotropic nanocomposite hydrogels efficiently aligned cells in both 2D and 3D, encouraging C2C12 myoblasts to differentiate into myotubes even in the absence of differentiation medium. Furthermore, these techniques have demonstrated potential uses in soft robotics and biomedical domains by successfully creating a soft robot in the shape of a star that responds to magnetic fields due to the presence of iron oxide nanoparticles, which align into filamentous structures when exposed to a low-intensity magnetic field. These different techniques enable researchers to carefully manage the flow of essential nutrients, oxygen, or growth factors with mechanical and electrical stimulation to the cells[10,160]. However, these techniques are mainly limited to surface level or 2D structures and struggle to integrate into thick or vascularized tissues[161]. For functional biohybrid applications that require volumetric structures, current micro/nano patterning methods need to be combined with 3D printing or self-assembly strategies to achieve scalable and clinically relevant tissue

Table 3. Advantages, disadvantages and applications of different 3D printing methods.

Biofabrication method	Advantages	Disadvantages	Applications	References
Material jetting	High resolution, multi-material printing, smooth surface finish	Limited material choices, requires post-processing, slow speed	Prototyping, multi-material biohybrid structures, detailed scaffolds	[95,129,130]
SLA	High precision, excellent surface quality, suitable for complex structures	Requires photopolymer resins, limited to certain materials, slow speed	Biohybrid scaffolds, precise microstructures, bone and dental implants	[131–133]
Material extrusion	Cost-effective, compatible with a wide range of materials, scalable	Lower resolution, rougher surface, limited to thermoplastic/hydrogel materials	Soft robotics, muscle-tissue constructs, personalized implants	[134,135]
DLP	Fast printing speed, high-resolution, layer-by-layer curing	Material constraints, requires photopolymer, can have oxygen inhibition	Biohybrid robots, high-resolution scaffolds, vascularized tissues	[136–138]
Extrusion bioprinting	Allows cell-laden bioink deposition, supports complex tissue structures	Lower resolution, shear stress can damage cells, slow fabrication speed	3D tissue engineering, organoids, biohybrid muscle constructs	[139,140]
Inkjet bioprinting	High-resolution cell patterning, minimal shear stress, good for delicate cells	Limited material options, lower cell density, requires optimized bioink viscosity	High-precision bioprinting, tissue engineering, controlled cell patterning	[126,141]
LAB	Nozzle-free, precise cell placement, ideal for high-density cell constructs	Expensive, complex setup, requires precise control over laser parameters	Engineered tissues, high-density cell constructs, organ-on-a-chip systems	[142–144]

structures. This extent of regulation is essential in achieving the best culture conditions as well as the required cell growth and differentiation[160].

Soft lithography, which is a group of methods that use an elastomeric stamp for printing and molding, enhances photolithography by enabling the duplication of soft, flexible, and stretchable components[24]. This technology uses elastomeric molds to manufacture highly precise micro/nano patterning[24]. Zhang et al. developed a novel soft lithographic technique to fabricate liquid metal-based soft microfluidic sensors with integrated conductive pathways[164]. Using curable elastomers and liquid metal stamps, the process combined channel fabrication and liquid metal patterning into a single step, eliminating complex photolithographic methods[164]. This method highlights significant potential for applications in wearable electronics and biosensing technologies[164]. Similarly, Shin et al. constructed 3D biohybrid actuators composed of cardiac tissues on the surface of a multilayered hydrogel sheet, incorporating aligned carbon nanotubes (CNTs) microelectrodes embedded within it using soft lithography techniques[63]. To promote the proper conditions for cardiac tissue formation, a 50-μm-thick CNT-GelMA hydrogel layer was applied to the poly (ethylene glycol) (PEG)/CNT microelectrodes matrix and cross-linked using UV light[63]. The CNT microelectrodes that were aligned improved signal propagation and decreased excitation limits for tissue stimulation by facilitating anisotropic electrical conductivity. External electrical fields (Figures 8(c) and (d)) were used to control the actuation of cardiac tissues grown on the construct, which showed synchronous beating, improved intercellular connectivity, and homogenous alignment[63].

While soft lithography provides a versatile approach for fabricating flexible and biohybrid structures, another emerging technique, NIL, offers a highly scalable method for creating nanoscale features with exceptional precision[165]. NIL is the process of creating nanoscale resist deformation by using a mold, followed by curing it with heat or UV light[158]. This technique enables the production of patterns that influence cell attachment, alignment, and growth. A study utilizes NIL to fabricate anisotropic structural color graphene films, enhancing cardiomyocyte alignment and force sensing[162]. Using a sandwich NIL technique, the films feature microgrooves (Figure 8(e)) for cell alignment and a 2D photonic crystal array (made from PDMS) enabling color shifts in response to contraction[162]. Figure 8(f) highlights the effectiveness of microgrooves in guiding cardiomyocyte orientation, mimicking native tissue structure[162]. The integration of rGO enhances electrical conductivity, enabling synchronized contractions. This graphene-based biointerface supports real-time contractility monitoring, with applications in drug screening, disease modeling, and biohybrid robotics[162]. In biohybrid robots, incorporating these nanostructures into scaffolds or substrates can lead to more efficient force transmission and improved robotic performance[40].

DEP utilizes the movement of polarizable particles in a non-uniform electric field. Living cells, acting as dipoles, migrate within these fields, making DEP an effective tool for cell manipulation and assembly[18]. Yang et al. demonstrated the use of a non-uniform electric field to align

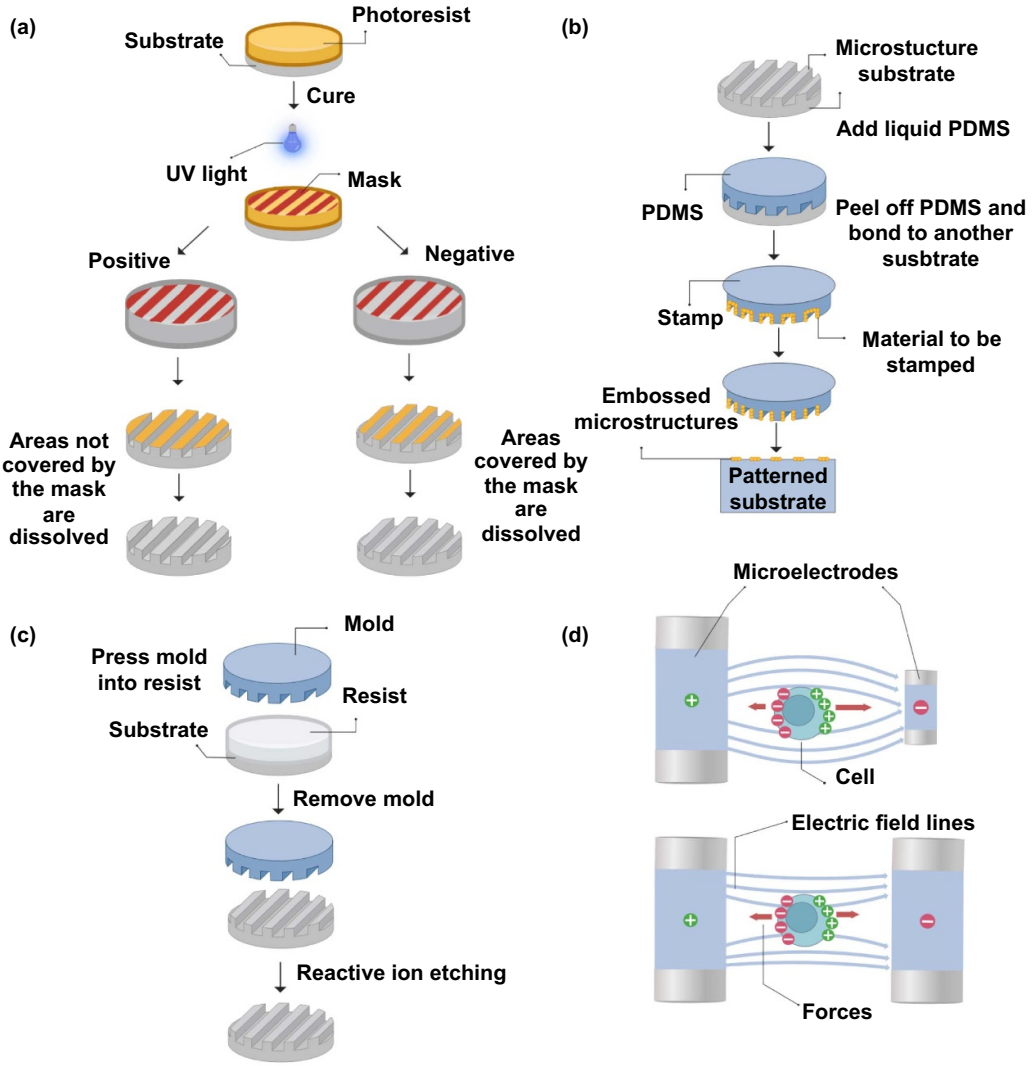

Figure 7. Schematic summary of micro- and nano-patterning techniques and their relevance to biohybrid devices. (a) Photolithography—a light-based patterning method using photoresists that enables precise microgrooves and surface features[23]. (b) Soft lithography—a flexible molding technique for micro/nanoscale pattern transfer, ideal for making stretchable substrates that support functional integration[24]. (c) Nanoimprint lithography (NIL)—a high-resolution imprinting method for structuring surfaces, enhancing cellular adhesion and contractile uniformity[158]. (d) Dielectrophoresis (DEP)—an electric field-driven technique for manipulating particles or patterning materials, facilitating the alignment of cells to improve actuation efficiency[19]. Created in BioRender. Shin (2025) https://BioRender.com/k78c428.

and assemble CNTs between parallel microelectrodes, forming ordered CNT structures (Figure 8(g))[163]. As previously deposited nanotubes altered the electric field distribution, CNTs formed interconnected networks at 10 μm gaps (Figure 8(h))[163]. These findings highlight DEP's ability to create flexible conductive networks that facilitate seamless integration of synthetic materials with biological components, a critical aspect of biohybrid robotics. Additionally, precise CNT alignment via DEP enables the development of smart materials responsive to external stimuli and ultrasensitive biosensors for detecting chemical or electrical signals. This technique enhances biohybrid robot fabrication by enabling the precise manipulation and assembly of cells and synthetic components under non-uniform electric fields, as well as the positioning and control of micro/nanorobots in fluid environments, supporting autonomous biohybrid devices for biomedical applications[166]. The advantages, along with the limitations of these micro/nano patterning techniques in manual assembly, pattern replication, and resolution constraints, are summarized in Table 4. Addressing these issues will enable biohybrid robots to revolutionize medical applications, from regenerative tissue engineering to minimally invasive precision surgery, bridging biology and engineering in transformative ways[166].

3.3. *Electrospinning and rotary jet spinning*

Electrospinning and rotary jet spinning are two important techniques for producing fibrous scaffolds, widely used in tissue engineering[171,172] (Figure 9). Electrospinning and rotary jet spinning enable the fabrication of fibrous scaffolds that mimic the native extracellular matrix. When the fibers are

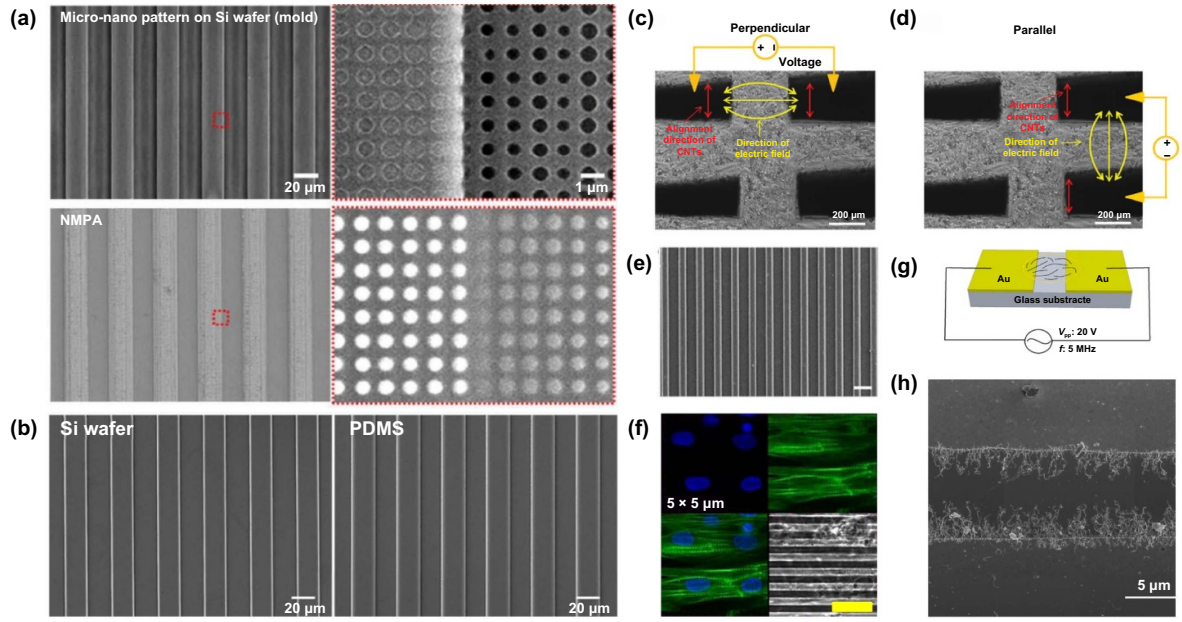

Figure 8. Overview of Micro/Nano Patterning and Alignment Strategies in Bioelectronics. (a) Micro/nano pattern on silicon wafer and NMPA (field emission scanning electron microscope (FESEM) photos). (b) Micropatterned silicon wafer and PDMS (FESEM photos, side view), both fabricated using photolithography. Reprinted from[53], Copyright (2015), with permission from Elsevier. (c) and (d) Phase contrast that indicates the applied field's direction, which is parallel and perpendicular to the CNT forests' alignment. [63] John Wiley & Sons. © 2015 WILEY-VCH Verlag GmbH & Co. KGaA, Weinheim. (e) SEM images of microgroove structure made by NIL, scale bar, 20 μm. (f) Shows how the effect of the alignment of the cardiomyocytes of the microgroove structure, scale bar, 20 μm. From[162]. Reprinted with permission from AAAS. (g) Schematic of DEP experimental system. (h) SEM pictures of CNT networks deposited for 60 seconds on parallel electrodes from a DEP system with a 10 μm spacing. Reprinted from[163], Copyright (2014), with permission from Elsevier.

Table 4. Advantages and disadvantages of different micro/nano patterning techniques.

Technique	Advantages	Disadvantages	Produced material	Precision	References
Soft lithography	Fast and economical for manufacturing multilayer devices	Manual assembly of layers	PDMS laminates, Polyethylene terephthalate (PET) membranes	Resolution up to 200 μm	[167]
Photolithography	Pattern replication using a film	Limited resolution for nano patterning.	Thin films of metals, photoresist polymers	Dependent on the wavelength and the film resolution	[168]
NIL	High resolution and ease of processing Nanoscale patterns.	2D manufacturing strategy Nominal resolution.	Gold, polymers, alkanethiols, dendrimers, antibodies, organic dyes, DNA	Resolution up to 100 nm	[169]
DEP	Selective manipulation of bioparticles	Precise design requirements for electrodes and channels.	Nanoparticles, DNA, cells, proteins	Almost 100% capture of nanoparticles	[170]

aligned, they provide directional cues that guide cell elongation, alignment, and fusion, essential for the formation of contractile muscle tissue. These anisotropic scaffolds are particularly effective for promoting uniaxial myotube formation and improving the mechanical functionality of biohybrid actuators[171,172].

Electrospinning utilizes electrostatic forces to produce fibers[173–180]. In this process, high voltage (typically 10–30 kV) is applied between a needle containing polymer solution and a grounded collector[18,171,172]. The electrostatic force overcomes the solution's surface tension, forming a Taylor cone (a Taylor cone is a conical fluid shape that forms

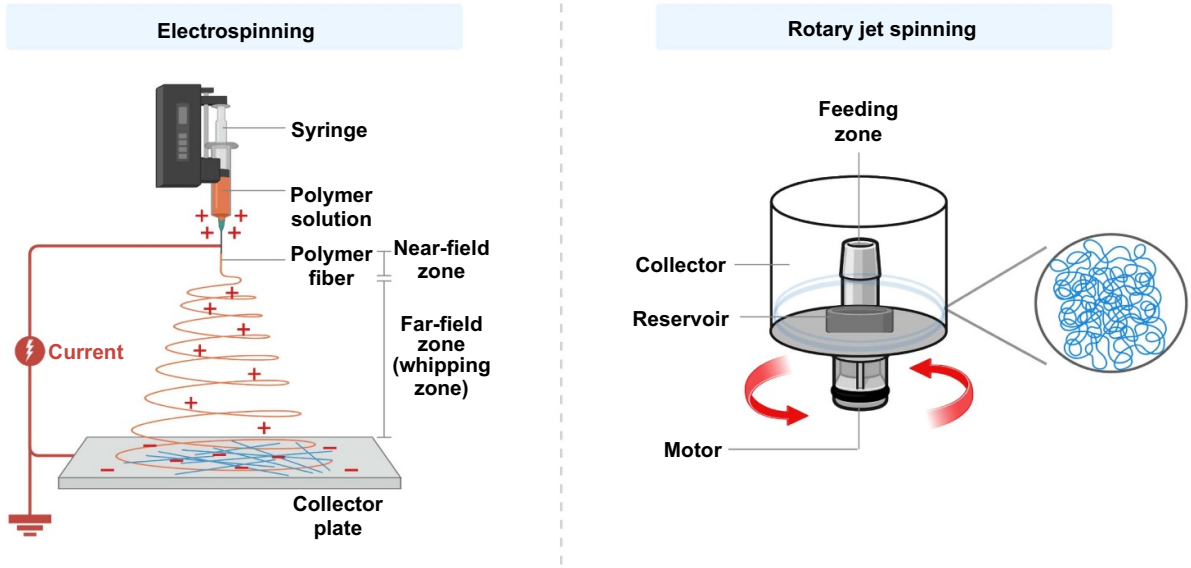

Figure 9. A schematic of the synthesize process of electrospinning and rotary jet spinning. Created in BioRender. Shin (2025) https://BioRender.com/g12u955.

during electrospinning, where a jet of charged particles is emitted once the applied voltage exceeds a critical threshold) and ejecting a thin polymer jet. The jet is stretched and whipped during flight, with solvent evaporating to form solid fibers on the collector. In muscle tissue engineering, electrospinning has been widely used to create aligned fibrous scaffolds that guide myoblast orientation and fusion into aligned myotubes, which is critical for proper muscle function and force generation[181]. For instance, electrospun polycaprolactone (PCL) meshes with microgroove patterns have been shown to promote myotube formation, with 200 μm spacing found optimal for this purpose[182]. Additionally, electrospun scaffolds can be functionalized with conductive materials like gold nanoparticles to enhance electrical stimulation of muscle cells, further mimicking the physiological environment of natural muscle[182–184]. Rotary jet spinning, on the other hand, employs centrifugal forces to generate fibers without the need for high voltage[185]. In this process, polymer solution is loaded into a perforated reservoir connected to a high-speed rotating motor (typically 3 000–12 000 rpm)[185]. As the reservoir spins, polymer solution is ejected through small orifices. Centrifugal forces stretch the polymer jets, and rapid solvent evaporation forms solid fibers on a stationary collector[15]. Compared to electrospinning, rotary jet spinning offers higher production rates, easier fiber alignment, and the ability to form more complex 3D structures[18]. This technique has been used to produce fibrous anisotropic gelatin scaffolds for muscle tissue engineering, demonstrating the potential to create structures that closely resemble the hierarchical organization of native muscle tissue[186]. A typical example is done by Chang et al.[187], who recreated the heart's helical structure. Figure 10(a) shows the focused rotary jet spinning (FRJS) schematic for recreating the heart's helical structure-function relationship[187]. This method fabricates aligned micro/nanofiber scaffolds that mimic the natural helical orientation of myocardial fibers by utilizing centrifugal jet spinning with an airstream to control fiber deposition (Figure 10(b))[187]. To construct a dual-chamber ventricle model, PCL fibers were spun onto a rotating mandrel, with parameters such as airflow, rotation speed, and solution viscosity adjusted to achieve controlled fiber alignment (Figures 10(c) and (d))[187]. The resulting scaffold was seeded with neonatal rat ventricular cardiomyocytes (NRVMs), which aligned along the fibers and exhibited synchronized contractions[187]. Functional assessments, including force generation, calcium transient imaging, and ejection fraction measurements, demonstrated that the helical constructs facilitated more uniform deformations and higher ejection fractions than circumferentially aligned models. Furthermore, the team used FRJS to produce a dual-chambered ventricle (DCV) with multiple helical angles (Figure 10(e)) and a full-scale human heart model (Figure 10(f))[187]. This approach underscores the importance of fiber architecture in cardiac biomechanics and provides a scalable strategy for engineering biomimetic cardiac tissues[187]. The same technique could be applied to biohybrid robots, where fiber-aligned scaffolds can enhance contractility and directional movement, improving the efficiency and performance of muscle-powered robotic systems.

Both electrospinning and rotary jet spinning enable control over fiber diameter, morphology, and scaffold porosity by adjusting process parameters and solution properties[16]. These fibrous scaffolds mimic the ECM, supporting tissue engineering applications in bone, cartilage, cardiac, vascular, neural, and skin regeneration[16]. In muscle tissue engineering, they promote cell adhesion, proliferation, and differentiation while ensuring efficient nutrient diffusion, waste removal, and cell migration[188]. Their tunable mechanical

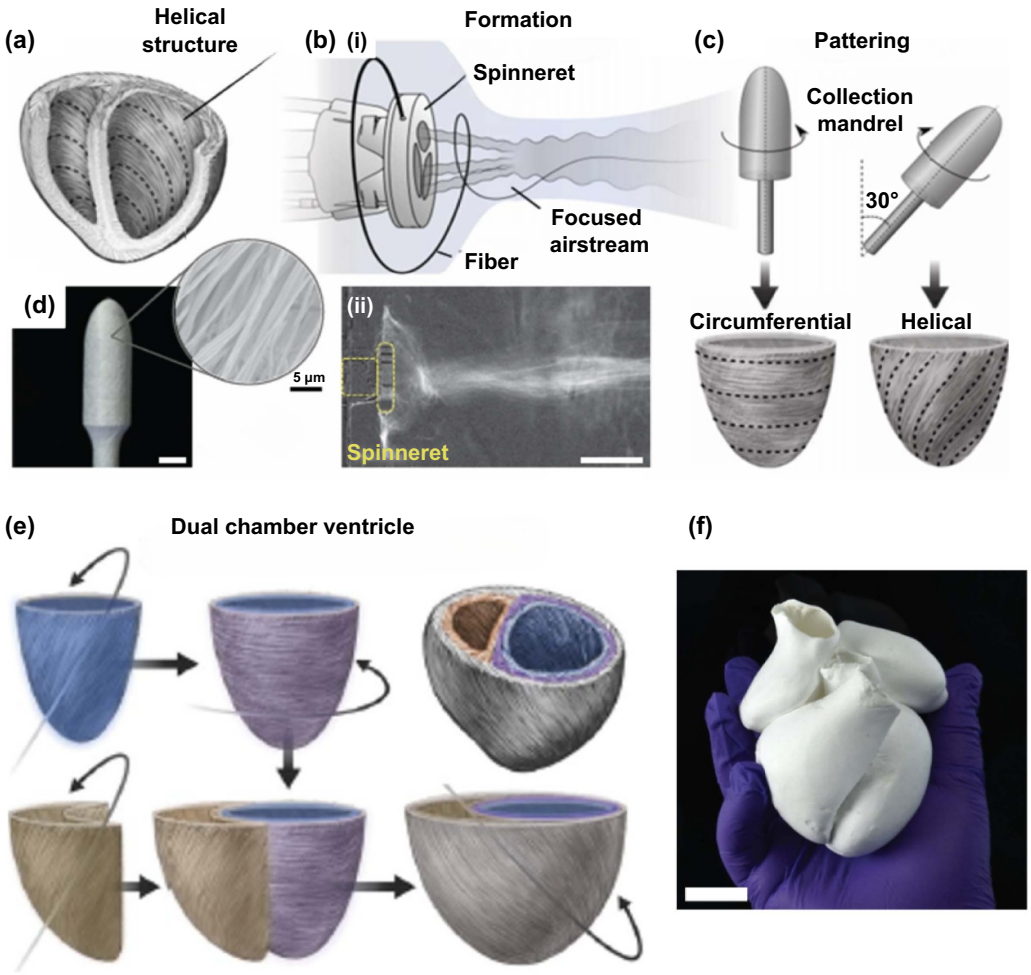

Figure 10. FRJS for engineering cardiac structure with helical fiber structures. (a) Schematic representation of the helical alignment in the human heart, which is crucial for coordinated contraction. (b) and (c) FRJS utilizes focused airflow to separate fiber production into two distinct phases: (b-i) formation and (c) patterning, facilitating controlled fiber orientation during the deposition process. (b-ii) Differential contrast imaging of the fiber stream, shown as a maximum projection (scale bar, 5 cm). (d) Polycaprolactone fibers deposited onto a rotating mandrel (scale bar, 5 mm), accompanied by an SEM image demonstrating the formation of aligned fibers with an average diameter of approximately 900 nm (scale bar, 5 mm). (e) Multiscale cardiac models featuring a simplified tri-layered DCV structure, designed to replicate the native ECM alignment of the heart, outlining the four-step fabrication approach. (f) A full-scale four-chambered human heart model constructed from single-micrometer fibers (scale bar, 2 cm). This technique enables the fabrication of geometrically biomimetic cardiac scaffolds with tunable mechanical anisotropy, critical for designing muscle-powered biohybrid robots with efficient force transmission and actuation. From[187]. Reprinted with permission from AAAS.

properties, typically within a few MPa elastic modulus, match native muscle tissue and support mechanotransduction for cell maturation[175,189–191].

3.4. Self-assembly/externally guided assembly

Self-assembly has emerged as an interesting and promising approach in advanced biofabrication, leveraging natural cellular behaviors and external stimuli to construct 3D structures[26]. This process takes advantage of the intrinsic tendency of cells to aggregate and organize into functional tissues, often supplemented by biophysical forces such as magnetic fields to guide and enhance assembly, thus constituting an approach better described as externally guided assembly[27]. Figure 11(a) outlines the process, which involves the application of external (e.g., heat, light, ultrasound, magnetic fields) or internal stimuli (e.g., pH, redox activity, enzymatic activity, and cellular interactions) to drive the externally guided assembly process. Unlike traditional scaffold-based methods, self-assembly and assisted-assembly still need to overcome challenges, such as material selection, mechanical property mismatches, and degradation inconsistencies[28]. By enabling the formation of tissue constructs directly from cells and ECM components, it provides a scaffold-free alternative that aligns closely with natural tissue architecture. Recent innovations, particularly in magnetic levitation and biohybrid systems, have further refined externally guided assembly, enabling precise control over structure, size, and complexity while maintaining biological functionality[26,192,193]. Vannozzi et al. introduced a method leveraging stress-induced rolling of PDMS bilayers to create 3D tubular structures[30]. This innovative

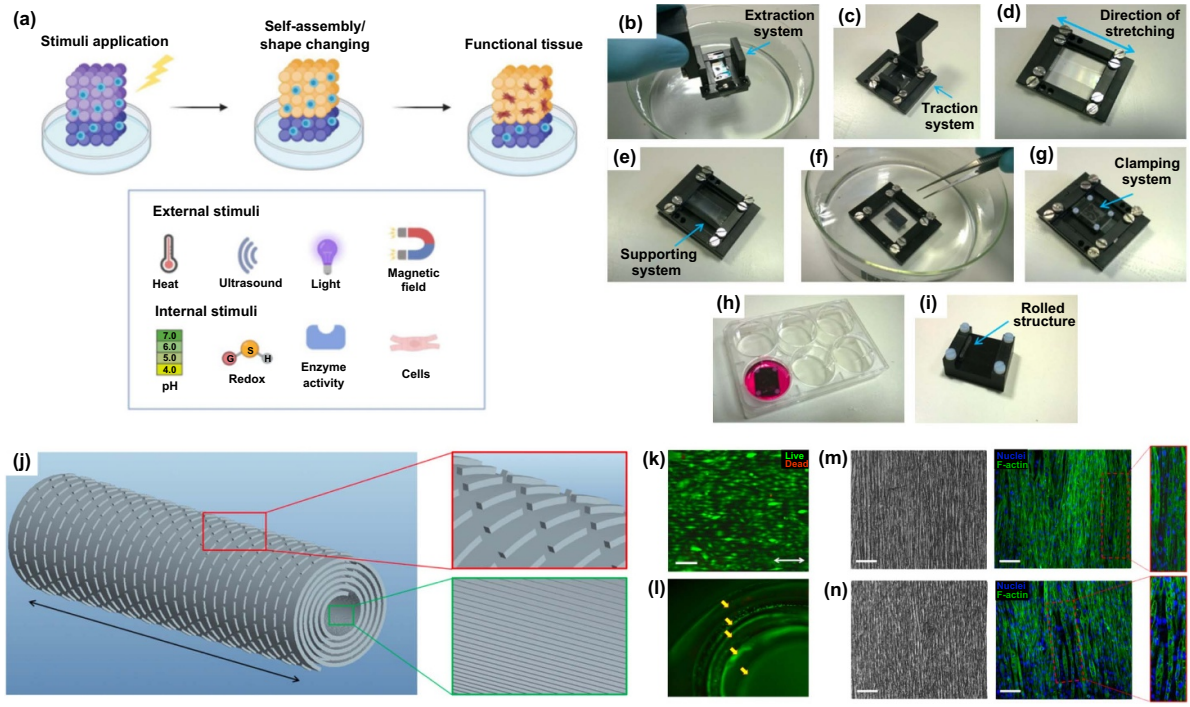

Figure 11. Fabrication and cellular integration of a rolled microgrooved PDMS biohybrid construct (a) Schematic illustration of assisted-assembly-based biofabrication driven by external and internal stimuli. Created in BioRender with permission. (b)–(j) Photographs show key stages of the fabrication process facilitated by a custom-built assembly system. (b) An extraction mechanism enabled the retrieval of the PDMS membrane from water. (c) A traction setup was employed to stretch the membrane along the longitudinal axis (d). (e) A support system was used to align and bond it with the semi-cured bottom layer. Following thermal treatment, the PDMS bilayer was immersed in water to separate the silicon-support from the bottom layer (f), which was then locked in a stressed state using a clamping system (g) before being prepared for cell culture (h). When required, one end of the structure was severed to produce a rolled configuration (i). A computer-aided design (CAD) model (j) of the rolled PDMS structure showcases the integration of pillars (red box, bottom layer) and grooves (green box, top layer). A black arrow denotes the alignment direction of the micro-grooves, emphasizing their structural orientation (j). (k) Fluorescence image of C2C12 cultured on a microgrooved PDMS surface, scale bar, 50 μm. (l) Fluorescence image of a rolled PDMS structure, green-labeled live cells with yellow arrows show the cell-provided concentric layers of the structure, scale bar, 100 μm. Bright field image and fluorescence (confocal) images of different cells on a PDMS substrate with microgroove, C2C12 of differentiation on day 7 (m), and C2C12 & normal human dermal fibroblast of differentiation on day 7 (n), scale bar, 50 μm. This system demonstrates how mechanical programming and topographic cues can be combined to produce scaffold-free, biohybrid actuators that mimic cylindrical muscle bundles. (b)–(n) Reproduced from[30]. © IOP Publishing Ltd. All rights reserved.

externally guided assembly process transforms 2D precursors into 3D scaffolds, enabling the seamless integration of C2C12. As illustrated in Figures 11(b)–(i), the method involves distinct fabrication stages, supported by a custom-designed assembly system to ensure precision and reproducibility. Figure 11(j) shows the CAD design of the rolled PDMS substrate with grooves on the top side (green), and pillars on the bottom side (red). C2C12 align and adhere to the PDMS substrate at day 7 of differentiation (Figures 11(k)–(n)), forming biohybrid actuators that exhibit contractile behavior in response to electrical stimulation. Figure 11(l) shows the whole structure after being rolled up with cells on it. Various surface topographies in this project facilitated muscle cell alignment on the top layer, directing their contraction along the longitudinal axis while simultaneously preserving gaps between concentric layers to ensure cell viability. This study underscores the synergy between externally guided assembly synthetic frameworks and biological tissues, providing a scalable and efficient approach to developing biohybrid systems for applications in soft robotics[30]. To achieve better integration of the structure, Guix et al. developed a skeletal muscle-powered biohybrid swimmer incorporating a 3D-printed serpentine spring skeleton with asymmetric stiffness, combined with a muscle cell-laden hydrogel bioactuator[81]. The flexible skeleton facilitated mechanical self-stimulation during muscle development, reinforcing contractile strength through cyclic feedback mechanisms. This innovative design enabled the swimmer to exhibit two distinct motion modes: inertial propulsion along an interface and coasting near a surface, reaching speeds of up to 33.24 mm·min^{-1}, comparable to biohybrid robots powered by cardiomyocytes. The study highlights how externally guided assembly muscle tissues and engineered components can be integrated for efficient biohybrid actuation[81].

Morita et al. extended the concept of self-assembly to cardiac systems by fabricating 3D scaffold-free cardiac muscle rings from induced pluripotent stem cells (iPSCs) (Figure 12(a))[4]. When incorporated into biohybrid actuators, the rings were configured into an antagonistic pair structure, with two rings sandwiching a PDMS body. This design enabled synchronized mutual contraction of the rings to drive a

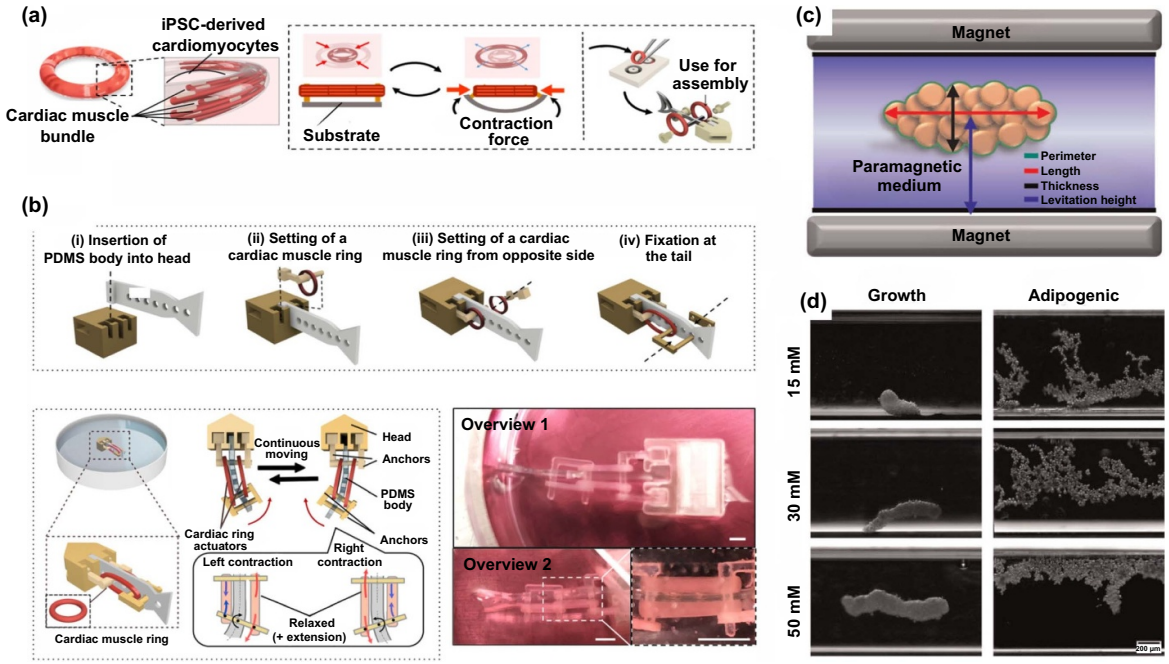

Figure 12. Scaffold-free cardiac tissue-based actuator using self-assembled iPSC-derived muscle rings. (a) Conceptual images of the cardiac muscle ring and its spontaneous contraction. (b) Development of a centimeter-scale biohybrid actuator featuring self-sustaining rhythmic contractions driven by an antagonistic arrangement of cardiac muscle rings. (a) and (b) Reproduced with permission from[4]. CC BY-NC 3.0. (c) Diagram depicting a scaffold-free levitation culture system, enabling suspended cell growth and tissue formation without physical support structures. (green line: perimeter of 3D cluster, red arrow: length, black arrow: thickness, blue arrow: levitation height). (d) Microscopic images showing the proliferation and adipogenic differentiation of 7F2 cells cultured under 15, 30, and 50 mM Gd concentrations over time. This figure highlights two scaffold-free strategies for generating biohybrid actuation: ring-shaped cardiac tissues enabling coordinated contraction, and magnetically levitated tissues supporting spheroid formation and 3D patterning. Both techniques eliminate the need for external scaffolds and open new directions in autonomous biohybrid device development. (c) and (d) Reproduced from[194]. John Wiley & Sons. © 2020 Wiley Periodicals LLC.

beating motion at the tail portion of the actuator. As illustrated in Figure 12(b), the study provided detailed schematics and views of the centimeter-sized biohybrid self-beating actuator, showcasing its functionality and scalability. This work highlights the potential of self-assembled cardiac tissues to power advanced biohybrid robotic systems. Transitioning to scaffold-free techniques, Sarigil et al. demonstrated the utility of magnetic levitation for enabling cell self-assembly, particularly through the suspension of cells in a paramagnetic medium[194]. Magnetic levitation facilitated the 3D organization of cells without external scaffolds, underscoring the value of external forces in promoting natural cell aggregation and alignment for biohybrid actuators. As illustrated in Figure 12(c), the levitation-based culture process is detailed, with a schematic showing the perimeter, thickness, and levitation height of 3D clusters (green, red, and black arrows, respectively). Culture images further highlight the growth and adipogenic differentiation of 7F2 cells under varying gadolinium (Gd) concentrations (15, 30, and 50 mM), demonstrating the adaptability of this technique for advanced biofabrication (Figure 12(d)).

In another externally guided assembly example, Wang et al. demonstrated that the in situ integration of microrobots using biomolecular motor-based artificial muscles[195]. Inspired by natural self-assembly, the team used a microfluidic chip to fabricate hydrogel components and integrate them with actuators in a single step[195]. While the focus was on engineered systems, the assembly mimicked biological processes and showed potential for scaling up muscle-based biohybrid actuators. This work highlights the versatility of externally guided assembly concepts for creating functional microrobots[195]. Complementing these advancements, Xie et al. introduced a magnet-assisted fabrication strategy that utilized 2D-to-3D transformation driven by magnetic and gravitational forces to create freestanding bio-scaffolds (Figure 13(a))[119]. This innovative approach incorporated sacrificial magnetic inks and thermo-responsive gels, enabling precise hydrogel shaping into structures that mimic vascular topologies. The scaffolds were further employed to support biohybrid soft actuators powered by cardiomyocytes, which exhibited dynamic movement capabilities. Figure 13(b) illustrates the fabrication strategy, where materials are deposited into flat hydrogel precursors and transformed into 3D morphologies under magnetic, buoyancy, and gravitational forces. It also demonstrates 4D printing of vascular geometries, with AutoCAD-designed flat hydrogels shaping into complex structures. This study highlights the versatility of magnetically driven transformations in creating functional scaffolds for biohybrid systems. It serves as a platform for future 3D/4D bioprinting with soft biomaterials.

Furthermore, Lin et al. developed a bio-inspired, magnetic-driven folded diaphragm for biomimetic robotics, drawing inspiration from earthworm locomotion (Figure 14)[196]. The diaphragm, fabricated using a simple one-piece mold and radial magnetization, achieves large 3D and bi-directional

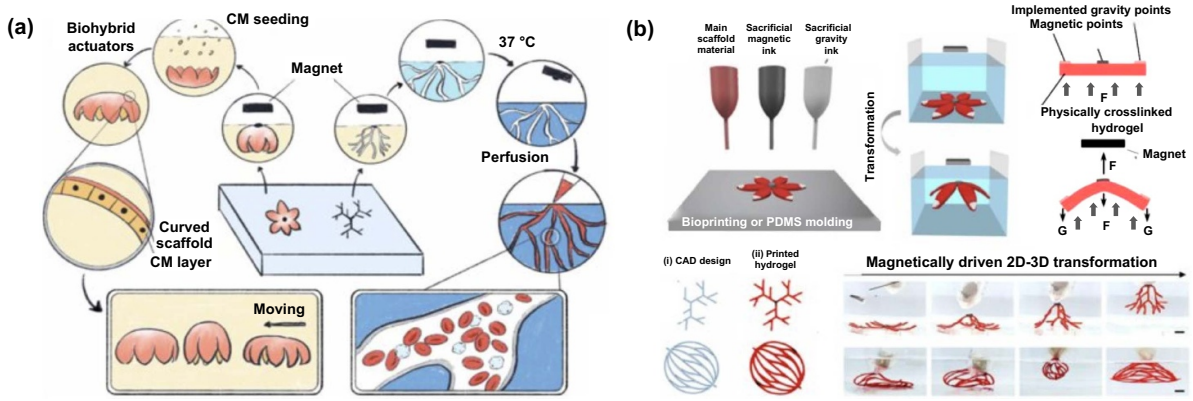

Figure 13. Magnetically triggered shape-morphing hydrogel actuators for biohybrid locomotion. (a) Schematic representation of magnetically induced shape transformation and its applications in engineering 3D perfusable vascular networks and a biohybrid actuator capable of walking. (b) Overview of the fabrication approach utilizing magnetic-driven deformation. This approach provides large deformation and multifunctionality, demonstrating the potential of magneto-responsive 4D structures for untethered soft robotic systems. Reproduced from[119]. CC BY 4.0.

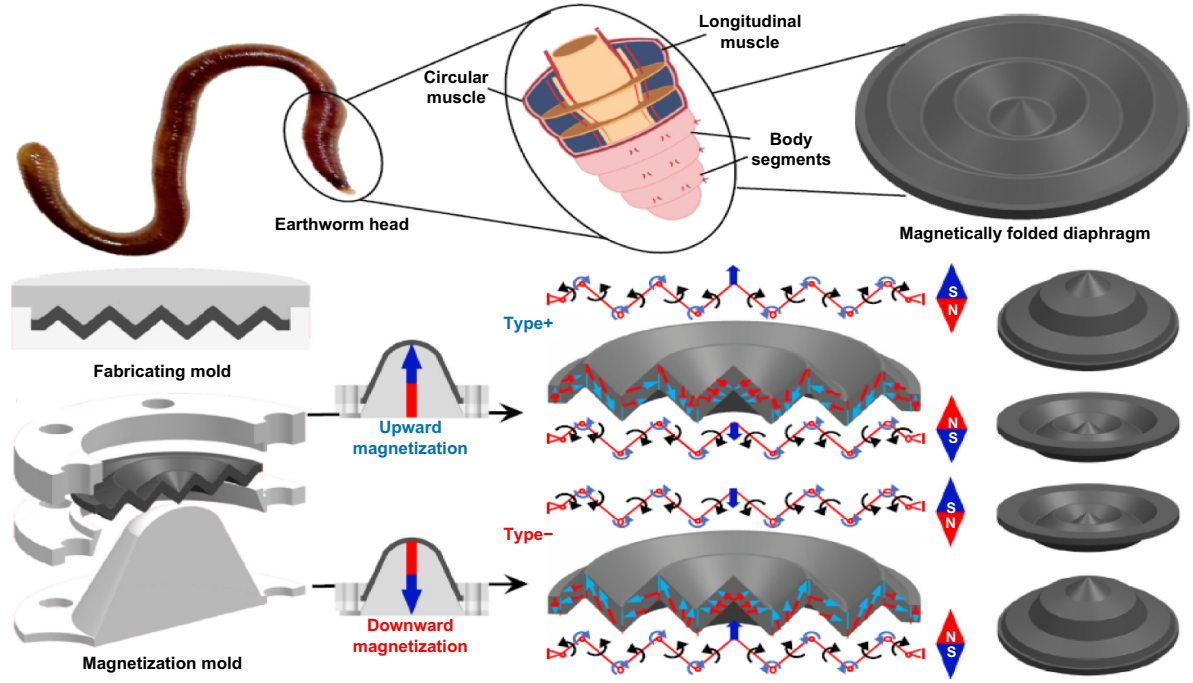

Figure 14. A biomimetic folded diaphragm designed based on the segmented structure of an earthworm, enabling adaptable movement and flexibility. The integrated structure demonstrates high efficiency and adaptability in biomimetic soft robotic devices. Reproduced from[196]. CC BY 4.0.

deformations with minimal elastic resistance under low magnetic fields (40 mT). This system was tested in various applications, including a diaphragm pump and two biomimetic robots. The pump demonstrated exceptional efficiency, with high specific pressure and flow rates superior to conventional systems[196]. Meanwhile, the crawling robot mimicked earthworm movements, achieving climbing, turning, and slope navigation under a homogenous magnetic field. Lastly, the swimming robot, inspired by squid jet propulsion, achieved controlled snorkeling and diving. These versatile systems underscore the potential of magnetic soft actuators for lightweight, efficient, and adaptive robotics in diverse applications[196].

These studies mentioned above demonstrate how assisted fabrication methods can yield complex, functional robotic systems by precisely controlling material placement and external actuation. Transitioning from externally guided assembly to autonomous organization, self-assembly offers a fundamentally different strategy for building biohybrid systems. As a representative example of self-assembled biohybrid robots, Kriegman et al. (Figure 15) developed reconfigurable living organisms, later termed xenobots, using Xenopus laevis embryonic epidermal and cardiac progenitor cells[197]. Designed computationally through evolutionary algorithms and manually assembled, these constructs

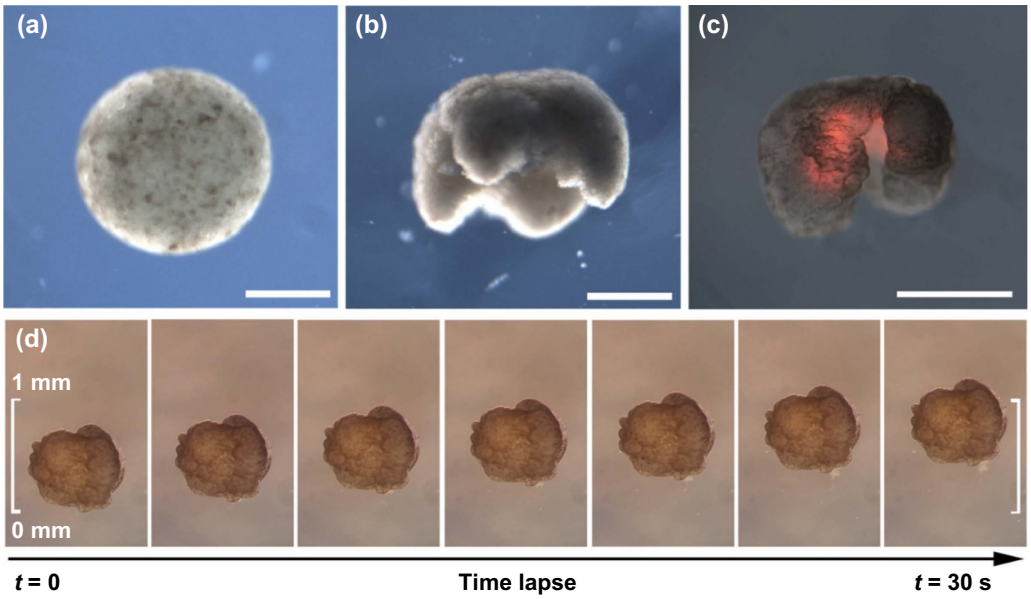

Figure 15. Creating reconfigurable biological constructs. (a) Clusters of pluripotent blastula cells are collected from Xenopus laevis embryos. (b) The cells are sculpted into three-dimensional forms based on digitally evolved designs. (c) Cardiac progenitor cells are strategically layered to generate contractile cardiomyocyte regions, marked by a red fluorescent lineage tracer. (d) Sequential imaging captures the spontaneous movement of the construct in a water-based environment. Reproduced from[197]. CC BY 4.0.

exhibited spontaneous contraction-driven locomotion, enabled by the rhythmic beating of cardiac muscle tissue. Remarkably, they also demonstrated self-healing capabilities, such as functional recovery after bisection, highlighting their resilience and adaptability[197]. Although derived from amphibian rather than human cells, this work exemplifies how cardiomyocyte-based actuation can be integrated into self-assembling biohybrid systems and underscores the potential of bottom-up design strategies in building functional, autonomous living machines[197].

3.5. *Microfluidic devices*

Microfluidic devices have emerged as essential tools for the precise manipulation, culture, and spatial arrangement of muscle cells, driving significant advancements in the development of biohybrid robots and tissue engineering strategies[31]. These devices, consisting of micro-scale channels and chambers, provide unparalleled control over cellular microenvironments, allowing researchers to replicate physiological conditions with high precision. By integrating 3D scaffolds into microfluidic systems, these platforms enable the cultivation of complex tissue architectures that closely mimic in vivo counterparts, fostering new opportunities for studying muscle biology and engineering[32]. Figure 16(a) illustrates the progression from traditional 2D and 3D static cultures to advanced microfluidic systems, which integrate scaffolds and channels to precisely control the cellular environment[160]. This transition enables optimized nutrient flow, tissue organization, and functionality, making it critical for biohybrid robotics development. These systems provide precise regulation of fluid dynamics, ensuring uniform cell distribution and promoting the formation of highly organized muscle tissues essential for integration into biohybrid systems (Figure 16(b))[160]. Microcylinder actuators are fabricated by partially coating microstructures with PEG and seeding them with cardiomyocytes, enabling contractile motion upon cellular actuation. Sheet actuators consist of thin elastomeric films or multilayer hydrogel sheets seeded with cardiomyocytes or myoblasts, allowing for untethered movement or bimorph cantilever actuation. Additionally, rolled polymeric structures cultured with myoblasts function as linear bio-actuators, while 3D modular muscle tissue rings provide adaptable components for integrating bio-actuators into 3D-printed skeletal frameworks. These different actuator designs demonstrate the versatility of biohybrid robots, where controlled contraction and relaxation facilitate locomotion, force generation, and soft robotic functionalities. The use of spatially confined microfluidic hydrogels enhances tissue alignment and functional properties, which are particularly crucial for muscle-based biohybrid applications. Furthermore, the continuous perfusion of nutrients and gases supports long-term muscle tissue development, maintaining cell viability and functionality over extended periods[198,199].

Microfluidic systems excel in enhancing tissue alignment, differentiation, and functionality through spatially confined cell environments and controlled stimuli. Figure 17(a) illustrates the fabrication of a muscular thin film (MTF) on a chip substrate, showcasing its ability to support functional tissue formation[200]. Fluorescent images of vascular smooth muscle cells (VSMCs) highlight anisotropic actin organization, while a graph tracks the stress generated over time.

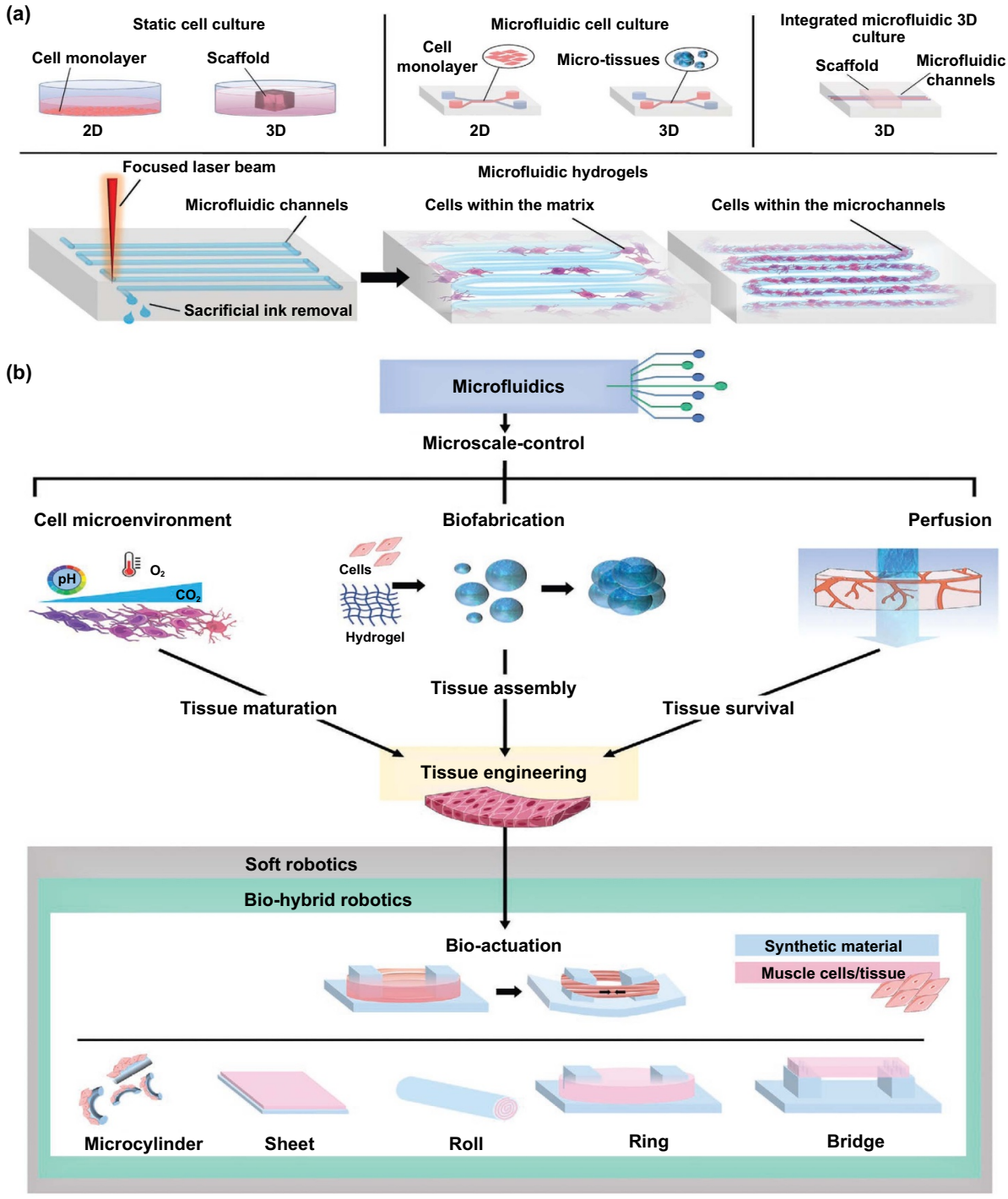

Figure 16. Transformative role of microfluidic control in enhancing the viability, organization, and function of engineered muscle tissues for bioactuator. (a) Overview of static and microfluidic cell culture approaches, illustrating the progression from traditional 2D and 3D static cultures to advanced microfluidic systems. These systems integrate scaffolds and channels, enabling precise control of cell environments, nutrient flow, and tissue organization. (b) Schematic representation of microfluidic-based tissue engineering, emphasizing its role in controlling the cell microenvironment, facilitating biofabrication and tissue assembly, and enabling bio-actuation in biohybrid robotics. Reproduced from[160]. CC BY 4.0.

The team utilized this MTF platform, integrated into microfluidic channels, to study the contractility of smooth and striated muscle cells[200]. The platform's dynamic fluid regulation enabled consistent nutrient supply and efficient waste removal, addressing the limitations of static cultures and promoting sustained cell viability over extended periods[200]. The authors highlight its ability to support functional tissue formation, with VSMCs displaying anisotropic actin organization.

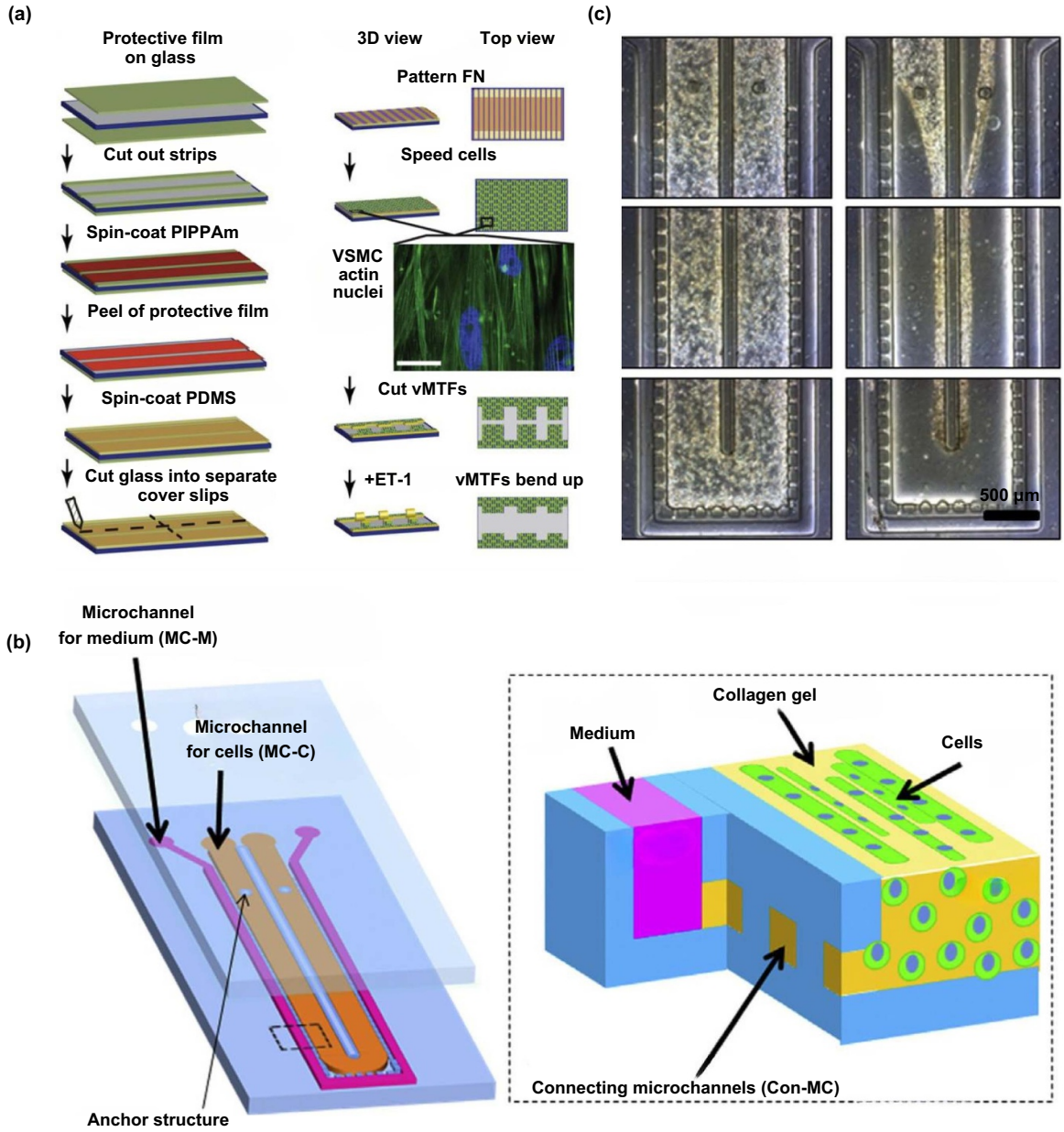

Figure 17. Integration of MTFs and microfluidic chips for high-throughput contractility assays and muscle tissue development. Schematic of the fabrication process and product of the MTF on a chip. (a) Schematic showing the fabrication of MTF on a chip substrate, with fibronectin microcontact printing used to create confluent tissues. VSMC fluorescent images highlight anisotropic actin organization within the monolayer (scale bar, 30 μm), while the stress generated by VSMCs is tracked over time. Reprinted from[200]. Copyright (2012), with permission from Elsevier. (b) A developed microfluidic device featuring skeletal muscle microtissues within microchannels, with bright field images. (c) Illustration of tissue growth after 1 and 6 days of cultivation. (b) and (c) Adapted from[35] with permission from the Royal Society of Chemistry.

The platform enables simultaneous contractility assays for multiple muscle types and allows for controlled drug testing applications. By leveraging engineered microenvironments and automated data acquisition, this system offers a high-throughput alternative to traditional muscle contractility assays. These innovations underscore the potential of microfluidic MTF systems in developing biohybrid robotic actuators and improving drug discovery platforms. Nevertheless, mechanical coupling between muscle tissue and microfluidic substrates remains fragile due to material mismatch and limited integration stability[201]. Moreover, most current platforms are limited by their reliance on benchtop instrumentation and lack system-level scalability or modularity for in vivo translation[202].

Building on this capability, the microfluidic muscle-on-a-chip platform by Shimizu et al. not only supports long-term muscle viability but also enhances myotube alignment and synchronized contractions via integrated electrical

stimulation, which are key features for functional biohybrid robots (Figure 17(b))[35]. Brightfield images showcase the growth and maturation of muscle microtissues over time, while both overall and microscopic views provide detailed insights into the platform's structure and functionality (Figure 17(c))[35]. The authors demonstrated that electrical stimulation within this microfluidic system significantly promoted the differentiation and alignment of myotubes, resulting in synchronized contractions critical for biohybrid actuators[35]. The combination of precise microfluidic control and dynamic electrical stimuli ensures optimal conditions for long-term tissue development and viability. Furthermore, they showed that continuous nutrient and oxygen perfusion within this platform supports the survival and functionality of vascularized muscle tissues, recreating dynamic in vivo environments and enabling improved structural and functional fidelity in engineered tissues[35]. Furthermore, the system has established itself as a promising platform for pharmacological screening by enabling real-time assessment of drug-induced contractile changes using muscle membrane bias[8]. The platform successfully quantified changes in contractile force following chemical stimulation, providing high-throughput compatibility and consistent performance across tissue samples[203]. However, the device's scalability to more complex organoid co-cultures or systemic drug delivery models is limited. On the other hand, its modularity and compatibility with standard lab-on-a-chip formats suggest potential utility for personalized drug screening or early toxicity screening, particularly for muscle-targeted therapeutics or neuromuscular diseases[35].

The integration of neuromuscular interactions within microfluidic systems further expands their utilities. Figure 18(a) highlights a microfluidic device designed to facilitate advanced biofabrication and tissue maturation processes, particularly for neuromuscular interaction studies[198]. The schematic illustrates the detailed design, including gel regions, vacuum channels, and layered structures, which provide a highly controlled environment for culturing muscle strips and neurospheres. Within these channels, dynamic mechanical and biochemical stimuli enhance tissue maturation, optimizing muscle cells for biohybrid applications[198]. Furthermore, these platforms allow researchers to monitor motor neuron differentiation and muscle co-culture timelines, including axon outgrowth and neuromuscular junction formation, as shown in Figure 18(b)[198].

Beyond alignment and maturation, microfluidic devices provide precise control over cell arrangement, critical for generating homogeneous populations of muscle cells. For example, Agrawal et al. demonstrated the creation of cylindrical muscle bundles with enhanced alignment and contractility using photo-patterned microfluidic systems, which are directly applicable as bioactuators (Figure 19(a))[34]. The schematic depicts the creation of cell-laden hydrogels with polyacrylamide (PAAm) pillars, which confine C2C12 and promote their alignment and long-term development. The team demonstrated that this method closely mimics native muscle tissue structures while enhancing contractility, showcasing the platform's utility for functional tissue engineering and biohybrid robotics[34].

In contrast to traditional studies focusing solely on skeletal muscle or cardiomyocyte contraction, which rely on direct external stimuli (e.g., electrical or optogenetic cues) to induce actuation, neuromuscular junctions (NMJs) enable signal transmission through biological pathways. Duc et al. highlight the use of a compartmentalized microfluidic platform for co-culturing motor neurons and skeletal muscle cells, effectively replicating in vivo neuromuscular interactions (Figure 19(b))[204]. Unlike direct muscle stimulation, NMJs facilitate the transmission of neural signals from motor neurons to muscle cells via chemical synapses, enabling physiologically relevant contractions. The schematic illustrates axonal invasion into muscle compartments and functional NMJ formation, with confocal imaging confirming the colocalization of pre- and post-synaptic markers (Figure 19(c)). This setup enhances synaptic connectivity and muscle contractility, offering insights into neuromuscular dynamics.

By enabling precise spatial control of cell alignment within microfluidic systems, this approach facilitates the development of functional muscle tissues while integrating biological neural control, distinguishing it from conventional muscle contraction studies. These advancements are essential for improving the performance and adaptability of biohybrid robotic systems, particularly those requiring biologically driven actuation[199,205].

As mentioned before, muscle cell-powered biohybrid robots also offer an important platform for drug testing by combining engineered muscle tissues with soft robotic structures to mimic physiological responses in a controlled environment[40]. These biohybrid systems enable precise monitoring of muscle contraction, fatigue, and recovery under various pharmacological interventions, providing a dynamic and realistic model for evaluating drug efficacy and toxicity[206]. Unlike traditional 2D cell culture models, muscle-powered biohybrid robots replicate the mechanical and functional properties of living tissues, allowing for more accurate predictions of drug behavior in vivo[6]. This innovative approach not only accelerates the drug development process but also reduces reliance on animal models, paving the way for personalized and ethical drug testing solutions[7]. As the field advances, researchers are integrating increasingly complex biological components into biohybrid systems to better mimic human physiology and disease states[207]. Shin et al. designed a human motor system-inspired biohybrid robot-on-a-chip to study the impact of drugs on neurodegenerative disorders. (Figure 20(c))[90]. The system integrates brain organoids, multi-motor neuron spheroids (MNS), and muscle bundles on a solid substrate, connected using vascularized networks and HA@Au-Ni-Au nanorods to enhance neural alignment and connectivity[90]. By combining iPSC-derived cerebral organoids with differentiated motor neurons and muscle tissues, the platform replicates the human motor

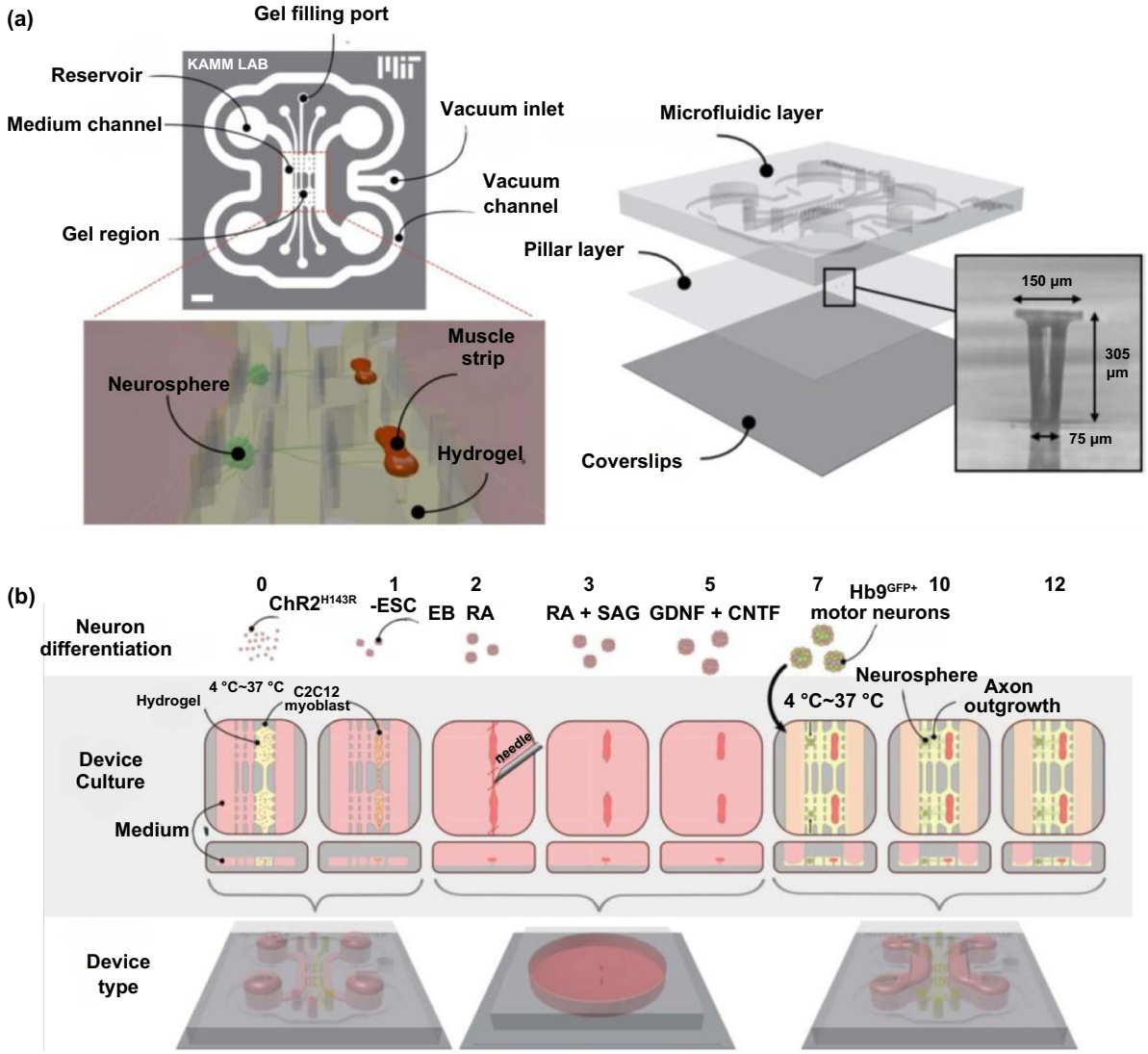

Figure 18. A case study of a microfluidic device for neuromuscular interaction studies. (a) Design of a microfluidic device for neuromuscular interaction studies, showcasing gel regions, vacuum channels, and multiple layers, including microfluidic and pillar layers, to culture muscle strips and neurospheres in controlled environments. (b) Timeline of neuron differentiation and muscle co-culture within a microfluidic device, detailing the stages of motor neuron development, axon outgrowth, and muscle-neuron interaction. This microfluidic system provides a controllable in vitro environment to study synaptic transmission and supports the development of biohybrid robots that can be driven by neuron-muscle signaling. Reproduced from[198]. CC BY 4.0.

system, transmitting electrophysiological signals from the brain organoid through motor neurons to induce muscle contraction (Figures 20(a) and (b)). Functional validation demonstrated that glutamate treatment increased muscle bundle displacement by 4.41 times, confirming the system's capability to transmit neural signals and evaluate drug effects[90]. Additionally, using a Parkinson's disease patient-derived midbrain organoid, the platform assessed the therapeutic effects of levodopa, with muscle bundle displacement increasing from 4.5 μm to 18.67 μm after treatment, showcasing its utility in studying disease-specific drug responses (Figure 20(d))[90]. The platform offers significant advantages over traditional organ-on-chip and animal models by accurately simulating human neuromuscular interactions and enabling precise drug evaluations[90]. Furthermore, its modular and scalable design paves the way for integrating additional capabilities, such as learning and sensory functionalities, to expand its applicability in biomedical research and personalized medicine. This innovative approach establishes a new standard for drug testing in neurodegenerative diseases and provides a foundation for future biohybrid robotic systems[90]. As such, this system represents a clear example of how muscle-powered biohybrid robots can be applied in translational biomedical contexts, providing both functional actuation and quantifiable drug response readouts.

4. Challenges and optimization strategies in biofabrication techniques

Designing muscle cell-powered biohybrid robots involves several multidisciplinary challenges that span cell biology,

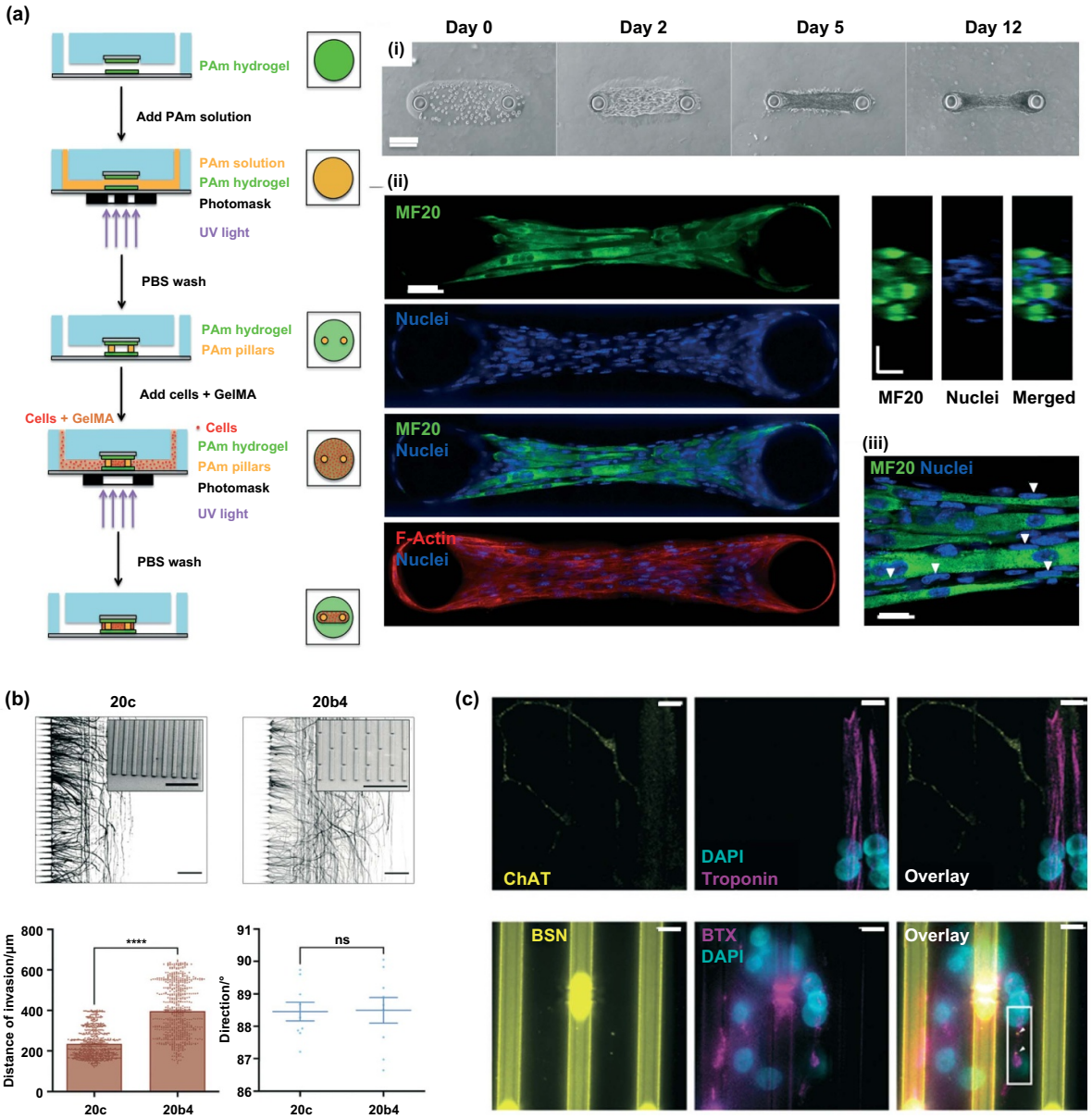

Figure 19. Microfluidic-assisted construction of aligned muscle bundles and neuromuscular junctions. By mimicking native muscle-nerve architecture, this system enhances physiological relevance for applications in soft robotics and disease modeling. (a) Schematic of the step-by-step process for creating cell-laden hydrogels using PAAm pillars. UV light and photomasks are used to pattern the hydrogels, encapsulating cells within a GelMA matrix. Time-lapse and immunofluorescence images illustrate muscle fiber alignment and maturation over 12 days, with myosin heavy chain (MF20), F-actin, and nuclei staining visualizing muscle development, scale bar, 150 μm for (i), 50 μm for (ii), 20 μm for (iii). Adapted from[34] with permission from the Royal Society of Chemistry. (b) Axonal invasion in muscle compartments is shown with both continuous and broken lines, highlighting greater invasion in the broken-line configuration and consistent fiber alignment in both cases, scale bar, 100 μm. (c) Confocal imaging of NMJs depicts the colocalization of pre- and post-synaptic markers (ChAT, Troponin, BTX, BSN), scale bar, 100 μm. (b) and (c) Reproduced with permission from[204]. CC BY-NC 3.0.

material science, and microengineering[208]. While numerous advanced biofabrication techniques have enabled progress in building these systems, the translation into robust, functional devices is often hindered by issues such as misaligned cells, limited actuation efficiency, poor integration of biological and synthetic materials, and insufficient long-term performance. These limitations not only affect the mechanical output and controllability of biohybrid robots but also constrain their clinical and translational potential.

The multidisciplinary challenges in designing biohybrid robots, which integrate biological and synthetic components, are huge[209,210]. Figure 21 is a schematic overview of key considerations in the development of biohybrid robots. Therefore, optimizing biofabrication techniques is critical for advancing muscle cell-powered biohybrid robots[40]. These robots depend on the precise engineering of cellular environments to enable the seamless integration of cells within engineered constructs. Key strategies include enhancing cell

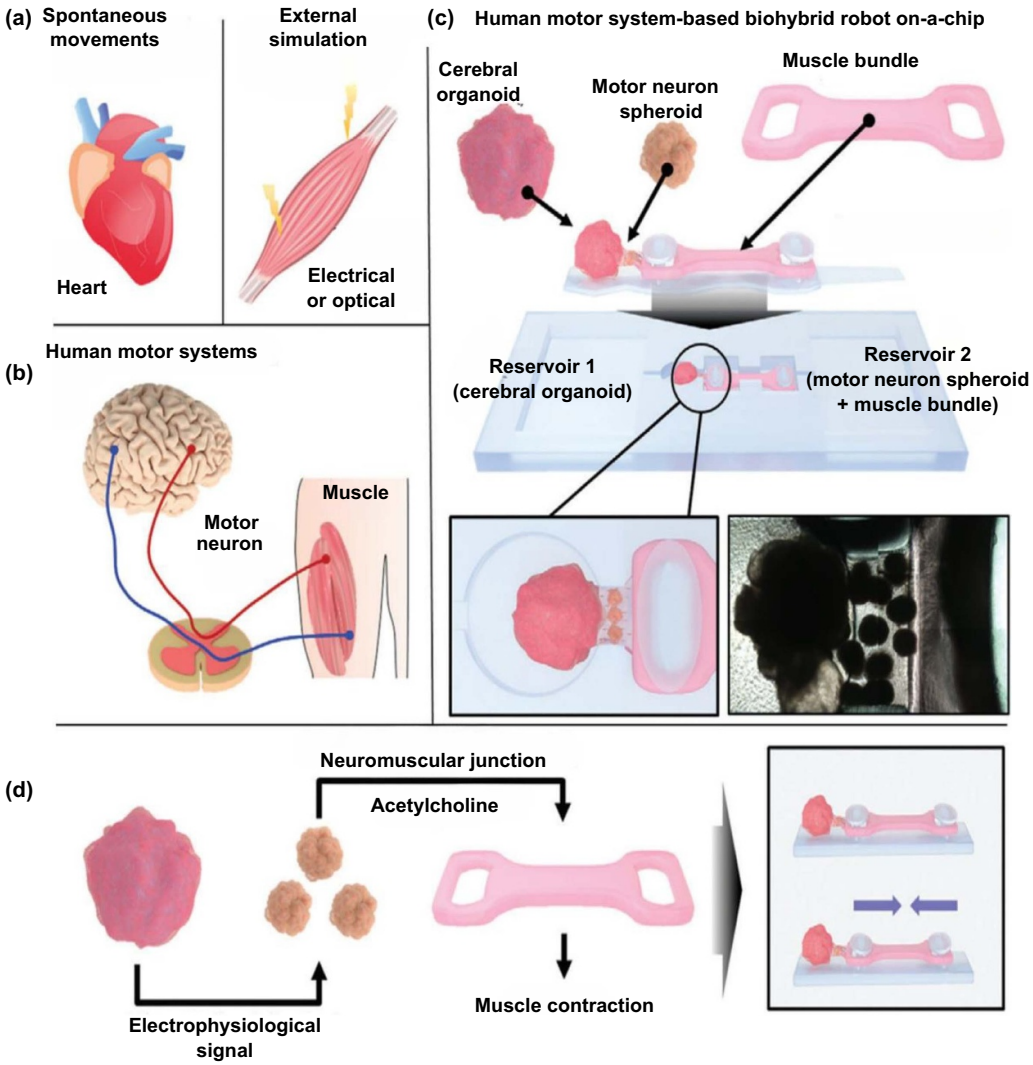

Figure 20. Neuromuscular robot-on-a-chip for drug testing and functional modeling. Illustration of a human motor system-inspired biohybrid robot-on-a-chip. (a) Representation of muscle movement, both spontaneous and externally induced. (b) Schematic depiction of the key components of the human motor system. (c) Illustration of the biohybrid robot-on-a-chip inspired by the human motor system, comprising a cerebral organoid, MNS, and a muscle bundle on a solid substrate. (d) Diagram showing muscle bundle movement facilitated by the connection between the cerebral organoid and multiple MNSs. This integrated platform bridges neuroscience, tissue engineering, and robotics, offering a powerful tool for neuromuscular disease research and therapeutic screening. Reproduced from[90]. CC BY 4.0.

alignment, improving the electrical and mechanical properties of biohybrid systems, achieving both functional and structural fidelity, and scaling up fabrication methods[153,211–213]. This section explores biofabrication approaches that optimize these essential aspects.

4.1. Strategies for improving cell alignment and integration

Cell alignment is fundamental for the proper contraction and functionality of muscle cell-powered constructs, as misaligned cells fail to generate coordinated movements essential for biohybrid robotics[153]. To mimic the native architecture of muscle tissue, several biofabrication techniques have been developed to guide muscle cell alignment. Among these, topographical cues embedded within biomaterials are particularly effective. These physical patterns guide cellular growth and organization, helping cells align along specific axes. For example, Mao et al. fabricated a microfibrous lattice using melt-based electrohydrodynamic printing[214]. This method created a three-dimensional scaffold with interconnected pores and a highly ordered microstructure[214]. The anisotropic design, formed by layering transverse and longitudinal fibers, enhances structural stability and supports the formation of densely organized tissues that closely replicate native cardiac function[214].

Biochemical cues also play a vital role in promoting alignment and contractility. Hydrogels composed of Matrigel, fibrinogen, and thrombin have been shown to support cell

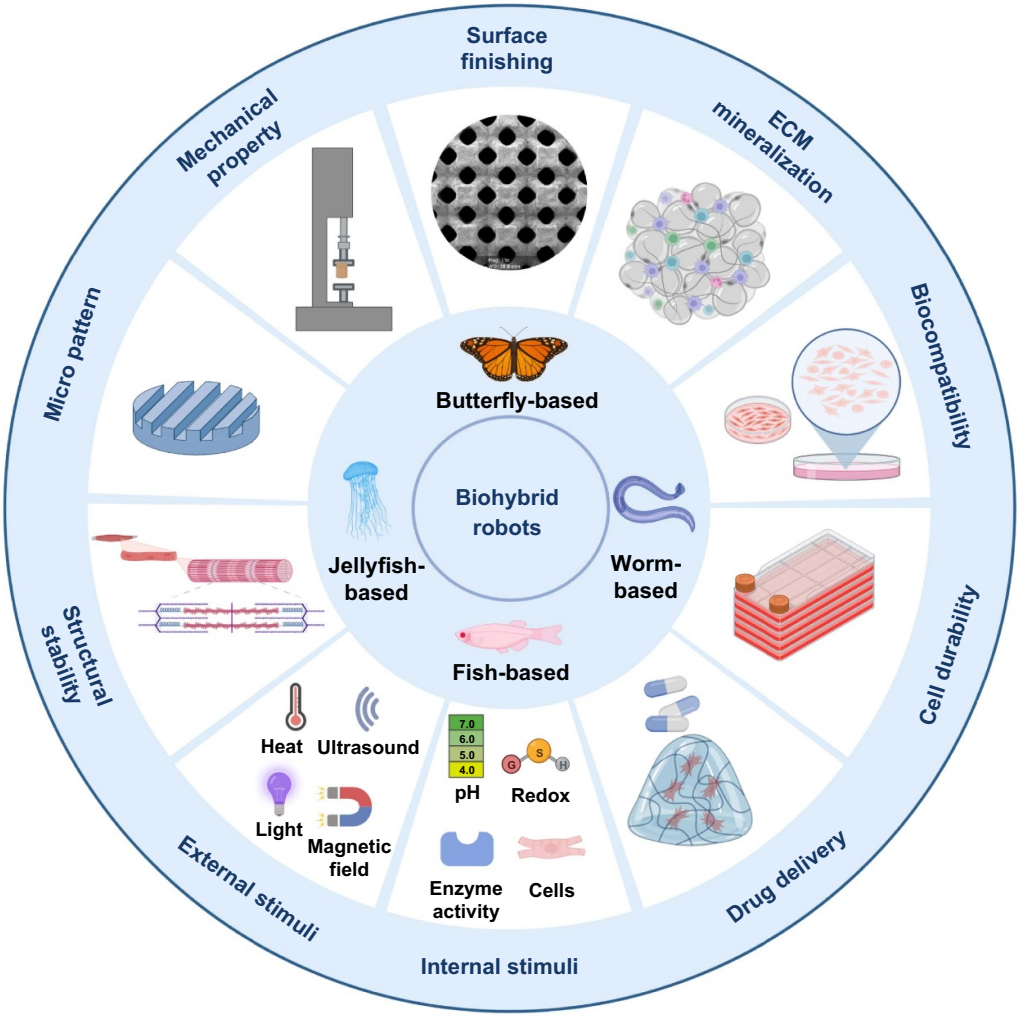

Figure 21. A schematic overview of key considerations in the development of biohybrid robots. The inner circle lists the common biohybrid robot models, such as jellyfish/worm/fish/butterfly-based systems. The outer circle highlights essential factors for improving biohybrid robot performance, each addressing specific technical challenges: mechanical strength enhances structural integrity during actuation cycles; surface finishing improving cell attachment and device-tissue interaction; ECM mineralization provides additional mechanical reinforcement and biomimicry; biocompatibility ensures minimal immune response for in vivo application; cell durability supports long-term functionality; and drug delivery introduces therapeutic relevance. Additionally, the figure emphasizes the importance of micro-patterning, structural stability, and responsiveness to external stimuli (heat, light, ultrasound, magnetic fields) and internal (pH, redox, enzyme activity, cells) stimuli for enabling dynamic, adaptive functionality in biomedical applications. Created in BioRender. Shin (2025) https://BioRender.com/s73v577.

adhesion and enable systolic-diastolic movements in engineered muscle tissues[215]. These matrices provide a bioactive environment that supports both cell integration and alignment, which are critical for functional biohybrid systems[215]. Similarly, topographical features such as micro/nano patterns mimic the natural ECM and encourage muscle cells to orient along predefined directions[48]. This approach has been demonstrated with aligned CNT substrates, which promote muscle cell alignment and improve functional integration in biohybrid constructs[82].

Electrospinning is another widely used method for fabricating aligned fiber scaffolds. The resulting fibers provide both physical support and directional cues for muscle cell orientation, leading to improved tissue organization and enhanced contractile properties[216,217]. Complementing these strategies, mechanical stretching during in vitro culture has also been shown to align cells along the axis of applied strain. Dynamic stretching promotes myotube formation and contributes to the development of more effective biohybrid actuators[82].

In addition to mechanical and topographical cues, electrical stimulation has proven valuable in promoting muscle cell alignment and synchronizing contraction. Applying electric fields during culture helps organize cells structurally and functionally, especially in systems that utilize optogenetic muscle cells[218]. These combined approaches like mechanical stretching, topographical patterning, biochemical signaling, and electrical stimulation, can synergistically enhance muscle cell alignment, differentiation, and integration into engineered constructs.

Importantly, the fabrication method for biohybrid robots must be adapted to the specific structural and functional characteristics of the muscle cell type used. Cardiomyocytes, for instance, are electrically coupled and contract spontaneously due to their intrinsic pacemaker activity[4]. These features necessitate fabrication strategies that preserve delicate cell–cell junctions and reduce mechanical tension[45]. Such an approach has been demonstrated in the development of a cardiomyocyte-powered swimming robot, where engineered platforms supported rhythmic and coordinated contractions for autonomous actuation[51]. Therefore, cardiomyocyte-based constructs benefit from gentle fabrication methods, such as microfluidic platforms and scaffold-free self-assembly, which maintain long-term cell viability and functional synchronization[4,46].

On the other hand, skeletal muscle cells require external stimulation, such as electrical or optogenetic activation to initiate contraction[71]. Their differentiation into functional myotubes depends heavily on a combination of mechanical, biochemical, and topographical cues[72]. Techniques such as electrospinning and micro/nano patterning have been particularly effective in guiding alignment and promoting contractile force generation in skeletal muscle constructs[159]. Furthermore, these constructs undergo repeated cycles of contraction, which places demands on scaffold mechanical stability. Studies have shown that the incorporation of collagen-based matrices and hybrid hydrogels can enhance long-term tissue support and improve contractile performance under sustained stimulation[114]. In addition, fine-tuning scaffold stiffness and matrix composition has been associated with improved myotube formation, force output, and overall cell viability[217].

Together, these strategies underscore the importance of aligning biofabrication methods with the unique biological requirements of different muscle cell types, ultimately enabling the construction of robust and functional muscle-powered biohybrid systems.

4.2. Techniques for enhancing electrical and mechanical properties of constructs

The functionality of biohybrid robots relies on the careful optimization of electrical and mechanical properties to ensure efficient actuation, durability, and adaptability. One key approach to enhancing electrical performance is the incorporation of conductive biomaterials into hydrogel matrices used for muscle cell cultures. Conductive materials, such as CNTs and boron nitride nanotubes, have been shown to improve both electrical conductivity and mechanical strength, facilitating efficient signal transmission across biohybrid constructs[159]. Additionally, electrical stimulation protocols play a crucial role in muscle cell maturation and improving contractile function, with controlled frequency and intensity adjustments enhancing synchronization in muscle-powered biohybrid robots[49,213]. By adjusting the frequency and intensity of electrical stimulation, it can promote muscle cell maturation and increase the electrical responsiveness of the tissues[17]. This approach not only enhances the contractile strength of the muscle tissue but also improves the coordination and control of biohybrid robots[10,49,58]. Electrical stimulation is particularly important for biohybrid systems that rely on synchronized contractions for locomotion or other complex movements[81]. In addition to internal electrical stimulation strategies, external field-responsive materials such as magnetic hydrogels are gaining attention for remote actuation and targeted navigation. These systems incorporate magnetic particles into hydrogel matrices to enable wireless control, spatial targeting, and enhanced integration with biological tissues. For example, a magnetically guided, blood-derived hydrogel robot demonstrated precise delivery to intracranial tumor sites, leveraging high biocompatibility and controllability for therapeutic applications[219]. Similarly, a vascular-deliverable biohybrid robot embedded with magnetic particles was used to restore neural connectivity, suggesting new possibilities for long-range delivery and functional interfacing with host tissues[220,221]. These examples highlight how magnetic materials can complement electrically stimulated systems to expand the scope of actuation and control in muscle-inspired biohybrid robots.

Beyond electrical optimization, mechanical properties must be carefully engineered to balance durability and actuation performance. Hydrogels composed of fibrinogen, thrombin, and matrigel have demonstrated favorable mechanical stiffness while supporting muscle contraction, making them promising candidates for biohybrid actuators[215,222,223]. By optimizing the composition of these hydrogels, researchers can tune the mechanical properties to better suit the functional demands of biohybrid robots. For example, stiffer hydrogels provide greater structural support, which is essential for maintaining the integrity of the construct during prolonged actuation. However, while increased stiffness enhances mechanical stability and durability, it can also hinder actuation behavior by restricting muscle contraction and reducing overall flexibility[29,111,224]. Therefore, achieving an optimal balance between structural support and actuation performance is crucial when designing biohybrid constructs[182,215,225,226]. Yuk et al. developed durable, stretchable hydrogels inspired by leptocephalus larvae, composed of alginate and acrylamide, which endured thousands of actuation cycles without rupture, emphasizing the critical role of elasticity and toughness in soft robotic applications[227].

To further optimize long-term performance, viscoelastic properties must be considered, as soft materials can exhibit creep and stress relaxation over time. Morimoto et al. addressed this issue by designing a biohybrid actuator with antagonistic muscle pairs, which prevented permanent shortening of muscle tissue and maintained consistent actuation for extended use[74]. Additionally, Cao et al. introduced a variable-stiffness actuator that remained flexible for movement initially but later reinforced itself via post-actuation stiffening[228]. This approach involved an electroactive polymer film that bent during actuation, bonded to a soft hydrogel layer infused with cell-derived vesicles, which subsequently mineralized into a bone-like structure in a calcium-rich solution. The resulting actuator transitioned from a compliant state to a durable, load-bearing structure, demonstrating how in situ

stiffening can enhance biohybrid robot longevity without sacrificing initial flexibility[228].

Even in purely hydrogel-based soft robots, selectively reinforcing specific regions with stiffer materials has been shown to improve structural integrity while preserving motion. For example, incorporating stiff elements in backbones or joints allows for enhanced support and controlled deformation, ensuring durability while retaining the necessary flexibility for actuation[229]. These advancements highlight the importance of strategic hydrogel design, where localized stiffness and adaptive material properties contribute to both functionality and longevity in biohybrid robots[230].

4.3. Achieving functional and structural fidelity in muscle cell-powered biohybrid robots

To achieve both functional and structural reliability in muscle cell-powered biohybrid robots, it is crucial to integrate strategies that ensure the constructs behave similarly to natural muscle tissue[96,212]. One of the primary challenges in biohybrid robotics is replicating the complex architecture and functionality of muscle systems in living organisms[231]. The use of bioactive hydrogels such as Matrigel and fibrinogen has proven effective in creating tissue-like environments that mimic the native ECM. These hydrogels support the development of muscle tissues with proper alignment and contractile properties[212]. For example, advanced 3D bioprinting techniques have been used to fabricate muscle tissues with aligned cells, which closely resemble the functional architecture of natural muscle[25]. Additionally, using acoustic patterning techniques has allowed researchers to create 3D printed tissues with highly aligned cellular arrays, significantly improving the structural fidelity of the constructs[232]. Achieving functional reliability also requires precise control over the mechanical properties of the constructs[233]. In large-scale systems, perfusable hollow fiber scaffolds have been proposed to improve oxygen and nutrient delivery throughout thick biohybrid muscle constructs, enhancing functional fidelity[234]. By adjusting the stiffness and elasticity of the biomaterials used, researchers can tailor the mechanical response of the biohybrid constructs to match that of native muscle tissues. In addition to optimizing the mechanical environment, the electrical properties of the constructs must be carefully tuned[210]. Biohybrid robots powered by muscle cells benefit greatly from materials that enhance electrical conductivity, enabling better signal transmission and coordination during contraction[70]. To ensure structural reliability, researchers have also explored the use of 3D or 4D bioprinting to fabricate muscle tissues with high spatial resolution[235]. A study by Lee et al. introduces a novel optic-fiber-assisted bioprinting (OAB) process, which significantly enhances high spatial resolution in muscle tissue fabrication by employing focused optical fibers for precise, localized crosslinking of methacrylated hydrogels, such as GelMA, collagen, and decellularized ECM[236]. This controlled crosslinking allows for the formation of well-defined, finely structured muscle tissues, closely replicating the aligned architecture of native muscle. Additionally, a functional nozzle with topographical cues directs uniaxial cell alignment, further refining cell organization and promoting myogenic differentiation[236]. Additionally, perfusable biohybrid architectures have recently enabled bioprinting of scalable, centimeter-scale skeletal muscle tissue with improved viability and alignment[237]. These advancements enable the fabrication of high-resolution muscle constructs that enhance muscle regeneration in volumetric muscle defect models, demonstrating the potential of OAB-based bioprinting for creating biomimetic, structurally stable muscle tissues[236]. By combining these strategies, researchers are making significant strides toward creating biohybrid robots that closely replicate the form and function of living muscle tissues. A comparative summary of these biofabrication techniques is provided in Table 5 to highlight their respective advantages, limitations, and application areas.

4.4. Scalable fabrication strategies for biohybrid robots

Traditional fabrication techniques like small-scale bioprinting have enabled groundbreaking biohybrid robots but are plagued by extreme scalability limitations. General bioprinting approaches could pattern at high resolution, but printed tissues were normally thin and small due to diffusion limits and the lack of perfusion, leading to cell death in larger samples. Lacking perfusable channels or vascularization, biological muscle actuators are not readily scalable to large sizes, as cells within large-scale tissue constructs will significantly decrease viability due to insufficient nutrient and oxygen supply[10]. Additionally, it may be challenging to induce uniform muscle cell alignment over large areas using traditional techniques[238]. These constraints inform the development of novel fabrication techniques that can maintain cell viability and orientation as biohybrid robots increase in size and functional sophistication.

To overcome these limitations, researchers are exploring a range of complementary strategies to build more sophisticated muscle-driven systems with increased sizes. Multimaterial DLP 3D printing is one such technique that uses projected light patterns to instantly cure resin layers and fabricate highly resolved 3D scaffolds[239]. Current developments provide the capability of printing multiple photopolymer resins in a single continuous structure, allowing for integrated soft and hard components or embedded conductors[240,241]. This provides the potential to create a robot's skeleton, joints, and wiring in a single step with enhanced precision and scalability. Recent developments fuse DLP with direct ink writing to simultaneously print composite hydrogel structures and conductive elements[112,113]. In muscle actuators, DLP printing has the capability to produce microfeatures that guide cell orientation across broad scaffolds[212]. Smooth integration of a variety of materials is particularly beneficial in scale-up, as it allows for incorporating perfusable channels and elastic supporting zones within one architecture[242].

Another approach involves modular assembly of pre-aligned muscle blocks. Rather than growing a large tissue, researchers grow small, oriented units of muscle, such as rings or strips, and then connect them to create larger systems. For example, one method of manufacture was to 3D-print a mold

Table 5. Comparison of major biofabrication techniques used in muscle cell-powered biohybrid robots.

Technique	Cell viability	Scalability	Functional integration	Typical applications	References
3D printing	Moderate to high	Moderate	High spatial control, suitable for complex geometry	Scaffold-based tissue fabrication	[96,108]
Micro/nano patterning	High	Low	High alignment, low depth integration	Cell alignment on planar substrates	[23,24,158,159]
Electrospinning and rotary jet spinning	High	Low to moderate	Excellent for alignment, limited 3D shaping	Aligned muscle sheet fabrication	[174,178]
Self-assembly	Variable (depends on matrix and conditions)	High	Good biological fidelity, low control over structure	Muscle rings, organoid-type models	[30,81]
Microfluidic devices	High	Moderate	Good for neural-muscle compartmentalization	Co-culture systems, interface modeling	[35,160]

and scaffold, seed cells within the mold, and allow the tissue to grow under stress, which maintained fiber alignment and contractility[243]. This modular approach facilitated the manufacture of biohybrid walkers with multidirectional and bidirectional locomotion under optogenetic control[243]. By combining small modules, this approach avoids the diffusion limit of thick tissue and is versed in flexible organization, like spacing or microfluidic perfusion between modules.

A third approach is based on automated layer-by-layer bioprinting. In these systems, alternating layers of cell-laden bioink and structural or sacrificial material are deposited to build thick, functional muscle tissue. Perfusion tubes further contribute to the survival of the construct, proving that layering permits scale-up in thickness without loss of function. Extrusion bioprinters have also bioprinted gelatin methacryloyl bioinks with muscle cells co-printed with sacrificial Pluronic ink and PEG-based pillar supports[237]. This generated muscle slabs with internal microchannel networks and external tension anchors, uniaxially aligned myofibers, and increased oxygenation across the tissue[237].

Scaling is also crucial in cardiomyocyte-governed systems. This study by Liu et al. demonstrates a significant advancement in scaling up the production speed of engineered cardiac tissues using human embryonic stem cell-derived cardiomyocytes (hESC-CMs) through a rapid light-based 3D bioprinting method known as micro-continuous optical printing (μCOP)[244]. The μCOP system utilizes a digital micromirror device (DMD) to project whole-layer digital patterns simultaneously, allowing for high-speed fabrication of cell-laden hydrogel structures with micrometer resolution. Unlike point-by-point laser-based methods, μCOP enables the parallel printing of complex geometries, greatly increasing throughput. This rapid patterning capability allows the direct encapsulation and alignment of high-density hESC-CMs within GelMA hydrogels, producing functional cardiac tissues in a fraction of the time required by traditional methods[244]. The system's ability to fabricate integrated force measurement scaffolds and enable real-time calcium imaging further underscores its utility for high-throughput drug screening and functional cardiac modeling. These advances highlight the potential of μCOP as a scalable platform for fabricating large volumes of structured, contractile cardiac tissues efficiently and reproducibly[244].

As fabrication speed and scale increase, maintaining tissue quality and functional performance across the entire construct becomes increasingly challenging[245]. In particular, two critical factors must be addressed to ensure successful scaling: cellular alignment and tissue viability[246]. Without proper alignment, muscle cells cannot generate coordinated contraction, while insufficient nutrient delivery in larger constructs compromises cell survival[247]. To tackle these issues, techniques such as multimaterial printing have been developed to embed alignment cues (e.g., microgrooves, fibers, or anchoring frames) alongside porous or vascularized regions that facilitate nutrient diffusion and perfusion. Modular approaches preserve alignment at the small scale and build modules in which each cell is within diffusion range. By surmounting the limitations of the early fabrication techniques, these scalable processes enable the fabrication of larger, tougher, and more durable biohybrid robots[40,248]. They eventually drive the field towards achieving real-world applications wherein macroscale function, strength, and cell-level accuracy coexist in the same device.

5. Conclusion

This review adopts a challenge-focused perspective, organizing biofabrication strategies around the specific limitations they address, such as alignment, signal transmission, and structural integration in muscle cell-powered systems. Muscle-powered biohybrid robots represent a transformative convergence of tissue engineering, biofabrication, and robotics, with growing applications in regenerative medicine and drug screening[120,249]. These systems utilize the contractile behavior of cardiomyocytes, skeletal muscle cells, and iPSC-derived motor neurons to construct dynamic platforms that mimic physiological function and assess pharmacological responses. Advances such as optogenetic control, neuromuscular interfaces, and nanomaterial-enhanced muscle

bundles have improved their mechanical performance and adaptability[40].

These developments support applications in soft robotics for environmental sensing, regenerative scaffolds, and autonomous drug testing, enhancing propulsion efficiency, structural fidelity, and stimulus-responsive behavior[250]. Progress in 3D bioprinting[111,251], micro/nano patterning[155,156], electrospinning and rotary jet spinning[15,174,178], self-assembly[30,193,252], and microfluidics[31,32] has enabled more precise cell alignment and improved structural integration. However, the realization of complex robots, such as those requiring coordinated multi-limb actuation controlled by neural interfaces or brain organoids, remains a major challenge[3].

Further innovations in bioelectronic interfaces, neural-muscle connectivity, and adaptive materials are needed to achieve seamless integration between actuators and control systems. These technologies will help reduce dependence on animal models, accelerate drug development, and enable advanced disease modeling and minimally invasive therapies[253–258]. Muscle-based constructs still face challenges such as vascularization, functional longevity, and scalable production[222,259–261]. Overcoming these barriers will require advances in material science, automated biofabrication, and integration with neural engineering and AI-based control systems. Looking ahead, the next generation of biohybrid robots will benefit from adaptive, self-healing materials, multimodal stimulation strategies, and closed-loop feedback systems. By framing current fabrication methods in the context of the structural and functional challenges they address, this review provides a task-oriented framework to guide future research toward more robust and clinically relevant biohybrid robotic systems.

Acknowledgments

This paper was funded by the National Institutes of Health (R01AR077132) and AHA collaborative award (944227). KG is supported by Marie-Curie post-doctoral fellowship awarded by European Commission (GAP-101109659).

Conflict of interests

All authors declare that they have no conflicts of interest.

ORCID iDs

Marina Colin 0009-0001-9618-4101
Su Ryon Shin 0000-0003-0864-6482

References

[1] Appiah C, Arndt C, Siemsen K, Heitmann A, Staubitz A and Selhuber-Unkel C. 2019. Living materials herald a new era in soft robotics. *Adv. Mater.* **31**, 1807747.
[2] Aydin O, Zhang X T, Nuethong S, Pagan-Diaz G J, Bashir R, Gazzola M and Saif M T A. 2019. Neuromuscular actuation of biohybrid motile bots. *Proc. Natl Acad. Sci. USA* **116**, 19841–19847.
[3] Bawa M and Raman R. 2024. Taking control: steering the future of biohybrid robots. *Sci. Robot.* **9**, eadr9299.
[4] Morita T, Nie M H and Takeuchi S. 2024. Human induced pluripotent stem cell-derived cardiac muscle rings for biohybrid self-beating actuator. *Lab Chip* **24**, 3377–3387.
[5] Ricotti L, Trimmer B, Feinberg A W, Raman R, Parker K K, Bashir R, Sitti M, Martel S, Dario P and Menciassi A. 2017. Biohybrid actuators for robotics: a review of devices actuated by living cells. *Sci. Robot.* **2**, eaaq0495.
[6] Raman R. 2024. Biofabrication of living actuators. *Annu. Rev. Biomed. Eng.* **26**, 223–245.
[7] Yuan Z, Guo Q H, Jin D L, Zhang P F and Yang W G. 2023. Biohybrid soft robots powered by myocyte: current progress and future perspectives. *Micromachines* **14**, 1643.
[8] Criscione J, Rezaei Z, Cantu C M H, Murphy S, Shin S R and Kim D H. 2023. Heart-on-a-chip platforms and biosensor integration for disease modeling and phenotypic drug screening. *Biosens. Bioelectron.* **220**, 114840.
[9] Wade R J and Burdick J A. 2014. Advances in nanofibrous scaffolds for biomedical applications: from electrospinning to self-assembly. *Nano Today* **9**, 722–742.
[10] Filippi M, Yasa O, Kamm R D, Raman R and Katzschmann R K. 2022. Will microfluidics enable functionally integrated biohybrid robots?. *Proc. Natl Acad. Sci. USA* **119**, e2200741119.
[11] Yeo M and Kim G H. 2018. Anisotropically aligned cell-laden nanofibrous bundle fabricated via cell electrospinning to regenerate skeletal muscle tissue. *Small* **14**, 1803491.
[12] Dong M et al. 2020. 3D-printed soft magnetoelectric microswimmers for delivery and differentiation of neuron-like cells. *Adv. Funct. Mater.* **30**, 1910323.
[13] Kajtez J et al. 2020. 3D-printed soft lithography for complex compartmentalized microfluidic neural devices. *Adv. Sci.* **7**, 2001150.
[14] Wang N Y. 2021. *An Investigation on Low-Elastic-Modulus Metallic Orthopedic Implants*. (National University of Singapore, Singapore).
[15] Badrossamay M R, McIlwee H A, Goss J A and Parker K K. 2010. Nanofiber assembly by rotary jet-spinning. *Nano Lett.* **10**, 2257–2261.
[16] Guner M B, Dalgic A D, Tezcaner A, Yilanci S and Keskin D. 2020. A dual-phase scaffold produced by rotary jet spinning and electrospinning for tendon tissue engineering. *Biomed. Mater.* **15**, 065014.
[17] Meneghetti D H et al. 2023. Electrical stimulation therapy and rotary jet-spinning scaffold to treat bone defects. *Anat. Rec.* **306**, 79–91.
[18] Rogalski J J, Bastiaansen C W M and Peijs T. 2018. PA6 nanofibre production: a comparison between rotary jet spinning and electrospinning. *Fibers* **6**, 37.
[19] Vida T A, Motta A C, Santos A R Jr, Cardoso G R C, de Brito C C and de Carvalho Zavaglia C A. 2018. Fibrous PCL/PLLA scaffolds obtained by rotary jet spinning and electrospinning. *Mater. Res.* **20**, 910–916.
[20] Yang Y P et al. 2025. 3D-printed manganese dioxide incorporated scaffold promotes osteogenic-angiogenic coupling for refractory bone defect by remodeling osteo-regenerative microenvironment. *Bioact. Mater.* **44**, 354–370.
[21] Lee S J, Jeong W and Atala A. 2024. 3D bioprinting for engineered tissue constructs and patient-specific models: current progress and prospects in clinical applications. *Adv. Mater.* **36**, 2408032.
[22] Gong D, Sun L L, Li X H, Zhang W Q, Zhang D Y and Cai J. 2023. Micro/nanofabrication, assembly, and actuation based on microorganisms: recent advances and perspectives. *Small Struct.* **4**, 2200356.

[23] Handrea-Dragan I M, Botiz I, Tatar A S and Boca S. 2022. Patterning at the micro/nano-scale: polymeric scaffolds for medical diagnostic and cell-surface interaction applications. *Colloids Surf. B* **218**, 112730.
[24] Qin D, Xia Y N and Whitesides G M. 2010. Soft lithography for micro- and nanoscale patterning. *Nat. Protocols* **5**, 491–502.
[25] Rajabasadi F, Schwarz L, Medina-Sánchez M and Schmidt O G. 2021. 3D and 4D lithography of untethered microrobots. *Prog. Mater. Sci.* **120**, 100808.
[26] Dabbagh S R, Alseed M M, Saadat M, Sitti M and Tasoglu S. 2022. Biomedical applications of magnetic levitation. *Adv. Nanobiomed. Res.* **2**, 2100103.
[27] Zhu S L, Xu L, Zhang Y, Zheng Z Y, Lang Z L, Zhang Q D, Gao J, Ye M and Xu R X. 2024. Magnetically controlled strategies for enhanced tissue vascularization. *Adv. Funct. Mater.* **34**, 2401856.
[28] Kang H, Lee D, Yang Y, Kyo Oh D, Seong J, Kim J, Jeon N, Kang D and Rho J. 2023. Emerging low-cost, large-scale photonic platforms with soft lithography and self-assembly. *Proc. SPIE* **2**, R04.
[29] Lin Z N, Jiang T and Shang J Z. 2022. The emerging technology of biohybrid micro-robots: a review. *Bio-Des. Manuf.* **5**, 107–132.
[30] Vannozzi L, Ricotti L, Cianchetti M, Bearzi C, Gargioli C, Rizzi R, Dario P and Menciassi A. 2015. Self-assembly of polydimethylsiloxane structures from 2D to 3D for biohybrid actuation. *Bioinsp. Biomim.* **10**, 056001.
[31] Li Z W, Seo Y, Aydin O, Elhebeary M, Kamm R D, Kong H and Saif M T A. 2019. Biohybrid valveless pump-bot powered by engineered skeletal muscle. *Proc. Natl Acad. Sci. USA* **116**, 1543–1548.
[32] Mestre R, Fuentes J, Lefaix L, Wang J J, Guix M, Murillo G, Bashir R and Sánchez S. 2023. Improved performance of biohybrid muscle-based bio-bots doped with piezoelectric boron nitride nanotubes. *Adv. Mater. Technol.* **8**, 2200505.
[33] Abulaiti M et al. 2020. Establishment of a heart-on-a-chip microdevice based on human iPS cells for the evaluation of human heart tissue function. *Sci. Rep.* **10**, 19201.
[34] Agrawal G, Aung A and Varghese S. 2017. Skeletal muscle-on-a-chip: an *in vitro* model to evaluate tissue formation and injury. *Lab Chip* **17**, 3447–3461.
[35] Shimizu K, Araki H, Sakata K, Tonomura W, Hashida M and Konishi S. 2015. Microfluidic devices for construction of contractile skeletal muscle microtissues. *J. Biosci. Bioeng.* **119**, 212–216.
[36] Su R T, Wang F J and McAlpine M C. 2023. 3D printed microfluidics: advances in strategies, integration, and applications. *Lab Chip* **23**, 1279–1299.
[37] Zhang F, Qu K Y, Zhou B, Luo Y, Zhu Z, Pan D J, Cui C, Zhu Y, Chen M L and Huang N P. 2021. Design and fabrication of an integrated heart-on-a-chip platform for construction of cardiac tissue from human iPSC-derived cardiomyocytes and in situ evaluation of physiological function. *Biosens. Bioelectron.* **179**, 113080.
[38] Rezaei Z, Wang N Y, De Jesus Alarcon Rodriguez A, Higashi S and Shin S R. 2025. Biosensors in biomedical research: bridging cell and tissue engineering and real-time monitoring. *Curr. Opin. Biomed. Eng.* **34**, 100582.
[39] Hassan S et al. 2024. Injectable self-oxygenating cardioprotective and tissue adhesive silk-based hydrogel for alleviating ischemia after Mi injury. *Small* **20**, 2312261.
[40] Mestre R, Patiño T and Sánchez S. 2021. Biohybrid robotics: from the nanoscale to the macroscale. *WIREs Nanomed. Nanobiotechnol.* **13**, e1703.
[41] Wei X W, Zhuang L J, Li H B, He C J, Wan H, Hu N and Wang P. 2020. Advances in multidimensional cardiac biosensing technologies: from electrophysiology to mechanical motion and contractile force. *Small* **16**, 2005828.
[42] Chen Z Y, Fu F F, Yu Y R, Wang H, Shang Y X and Zhao Y J. 2019. Cardiomyocytes-actuated *Morpho* butterfly wings. *Adv. Mater.* **31**, 1805431.
[43] Chan V, Neal D M, Uzel S G M, Kim H, Bashir R and Asada H H. 2015. Fabrication and characterization of optogenetic, multi-strip cardiac muscles. *Lab Chip* **15**, 2258–2268.
[44] Dipalo M et al. 2021. Intracellular action potential recordings from cardiomyocytes by ultrafast pulsed laser irradiation of fuzzy graphene microelectrodes. *Sci. Adv.* **7**, eabd5175.
[45] Vurro V, Shani K, Ardoña H A M, Zimmerman J F, Sesti V, Lee K Y, Jin Q, Bertarelli C, Parker K K and Lanzani G. 2023. Light-triggered cardiac microphysiological model. *APL Bioeng.* **7**, 026108.
[46] McCain M L, Agarwal A, Nesmith H W, Nesmith A P and Parker K K. 2014. Micromolded gelatin hydrogels for extended culture of engineered cardiac tissues. *Biomaterials* **35**, 5462–5471.
[47] Xu N W. 2024. Float like a butterfly, swim like a biohybrid neuromuscular robot. *Sci. Robot.* **9**, eads4127.
[48] Jeon H, Simon C G Jr and Kim G. 2014. A mini-review: cell response to microscale, nanoscale, and hierarchical patterning of surface structure. *J. Biomed. Mater. Res. B* **102**, 1580–1594.
[49] Tetsuka H, Pirrami L, Wang T, Demarchi D and Shin S R. 2022. Wirelessly powered 3D printed hierarchical biohybrid robots with multiscale mechanical properties. *Adv. Funct. Mater.* **32**, 2202674.
[50] Batalov I, Jallerat Q, Kim S, Bliley J and Feinberg A W. 2021. Engineering aligned human cardiac muscle using developmentally inspired fibronectin micropatterns. *Sci. Rep.* **11**, 11502.
[51] Lee K Y, Park S J, Matthews D G, Kim S L, Marquez C A, Zimmerman J F, Ardoña H A M, Kleber A G, Lauder G V and Parker K K. 2022. An autonomously swimming biohybrid fish designed with human cardiac biophysics. *Science* **375**, 639–647.
[52] Zhang C, Wang J Y, Wang W X, Xi N, Wang Y C and Liu L Q. 2016. Modeling and analysis of bio-syncretic microswimmers for cardiomyocyte-based actuation. *Bioinsp. Biomim.* **11**, 056006.
[53] Tanaka Y and Fujita H. 2015. Fluid driving system for a micropump by differentiating iPS cells into cardiomyocytes on a tent-like structure. *Sens. Actuators B* **210**, 267–272.
[54] Bliley J, Tashman J, Stang M, Coffin B, Shiwarski D, Lee A, Hinton T and Feinberg A. 2022. FRESH 3D bioprinting a contractile heart tube using human stem cell-derived cardiomyocytes. *Biofabrication* **14**, 024106.
[55] Wang J et al. 2022. Acoustic fabrication of living cardiomyocyte-based hybrid biorobots. *ACS Nano* **16**, 10219–10230.
[56] Chan V, Park K, Collens M B, Kong H, Saif T A and Bashir R. 2012. Development of miniaturized walking biological machines. *Sci. Rep.* **2**, 857.
[57] Xu B Z, Han X M, Hu Y W, Luo Y M, Chen C H, Chen Z and Shi P. 2019. A remotely controlled transformable soft robot based on engineered cardiac tissue construct. *Small* **15**, 1900006.
[58] Tetsuka H, Gobbi S, Hatanaka T, Pirrami L and Shin S R. 2024. Wirelessly steerable bioelectronic neuromuscular robots adapting neurocardiac junctions. *Sci. Robot.* **9**, eado0051.
[59] Nawroth J C, Lee H, Feinberg A W, Ripplinger C M, McCain M L, Grosberg A, Dabiri J O and Parker K K. 2012. A tissue-engineered jellyfish with biomimetic propulsion. *Nat. Biotechnol.* **30**, 792–797.
[60] Xi J Z, Schmidt J J and Montemagno C D. 2005. Self-assembled microdevices driven by muscle. *Nat. Mater.* **4**, 180–184.

[61] Feinberg A W, Feigel A, Shevkoplyas S S, Sheehy S, Whitesides G M and Parker K K. 2007. Muscular thin films for building actuators and powering devices. *Science* **317**, 1366–1370.
[62] Park S-J et al. 2016. Phototactic guidance of a tissue-engineered soft-robotic ray. *Science* **353**, 158–162.
[63] Shin S R et al. 2015. Aligned carbon nanotube–based flexible gel substrates for engineering biohybrid tissue actuators. *Adv. Funct. Mater.* **25**, 4486–4495.
[64] Wang R Q, Zhang C, Zhang Y W, Tan W J, Chen W Y and Liu L Q. 2023. Soft underwater swimming robots based on artificial muscle. *Adv. Mater. Technol.* **8**, 2200962.
[65] Tieland M, Trouwborst I and Clark B C. 2018. Skeletal muscle performance and ageing. *J. Cachexia Sarcopenia Muscle* **9**, 3–19.
[66] Huang C L H and Lei M. 2023. Cardiomyocyte electrophysiology and its modulation: current views and future prospects. *Phil. Trans. R. Soc. B* **378**, 20220160.
[67] Gehlert S, Bloch W and Suhr F. 2015. Ca^{2+}-dependent regulations and signaling in skeletal muscle: from electromechanical coupling to adaptation. *Int. J. Mol. Sci.* **16**, 1066–1095.
[68] Hasebe A, Suematsu Y, Takeoka S, Mazzocchi T, Vannozzi L, Ricotti L and Fujie T. 2019. Biohybrid actuators based on skeletal muscle-powered microgrooved ultrathin films consisting of poly(styrene-*block*-butadiene-*block*-styrene). *ACS Biomater. Sci. Eng.* **5**, 5734–5743.
[69] Raman R, Cvetkovic C, Uzel S G M, Platt R J, Sengupta P, Kamm R D and Bashir R. 2016. Optogenetic skeletal muscle-powered adaptive biological machines. *Proc. Natl Acad. Sci. USA* **113**, 3497–3502.
[70] Aydin O, Passaro A P, Elhebeary M, Pagan-Diaz G J, Fan A, Nuethong S, Bashir R, Stice S L and Saif M T A. 2020. Development of 3D neuromuscular bioactuators. *APL Bioeng.* **4**, 016107.
[71] Kim Y et al. 2023. Remote control of muscle-driven miniature robots with battery-free wireless optoelectronics. *Sci. Robot* **8**, eadd1053.
[72] Deshmukh D V, Reichert P, Zvick J, Labouesse C, Künzli V, Dudaryeva O, Bar-Nur O, Tibbitt M W and Dual J. 2022. Continuous production of acoustically patterned cells within hydrogel fibers for musculoskeletal tissue engineering. *Adv. Funct. Mater.* **32**, 2113038.
[73] Wang Z, Lee W J, Koh B T H, Hong M, Wang W, Lim P N, Feng J, Park L S, Kim M and Thian E S. 2018. Functional regeneration of tendons using scaffolds with physical anisotropy engineered via microarchitectural manipulation. *Sci. Adv.* **4**, eaat4537.
[74] Morimoto Y, Onoe H and Takeuchi S. 2018. Biohybrid robot powered by an antagonistic pair of skeletal muscle tissues. *Sci. Robot.* **3**, eaat4440.
[75] Wang Y Z, Uesugi K, Nitta T, Hiratsuka Y and Morishima K. 2024. Contractile and tensile measurement of molecular artificial muscles for biohybrid robotics. *Cyborg. Bionic Syst.* **5**, 0106.
[76] Pagan-Diaz G J et al. 2018. Simulation and fabrication of stronger, larger, and faster walking biohybrid machines. *Adv. Funct. Mater.* **28**, 1804580.
[77] Kinjo R, Morimoto Y, Jo B and Takeuchi S. 2024. Biohybrid bipedal robot powered by skeletal muscle tissue. *Matter* **7**, 948–962.
[78] Cvetkovic C, Raman R, Chan V, Williams B J, Tolish M, Bajaj P, Sakar M S, Asada H H, Saif M T A and Bashir R. 2014. Three-dimensionally printed biological machines powered by skeletal muscle. *Proc. Natl Acad. Sci. USA* **111**, 10125–10130.
[79] Wang J J, Zhang X T, Park J, Park I, Kilicarslan E, Kim Y, Dou Z, Bashir R and Gazzola M. 2021. Computationally assisted design and selection of maneuverable biological walking machines. *Adv. Intell. Syst.* **3**, 2000237.
[80] Li Z W and Saif M T A. 2021. Mechanics of biohybrid valveless pump-bot. *J. Appl. Mech.* **88**, 111004.
[81] Guix M, Mestre R, Patiño T, De Corato M, Fuentes J, Zarpellon G and Sánchez S. 2021. Biohybrid soft robots with self-stimulating skeletons. *Sci. Robot.* **6**, eabe7577.
[82] Xu N W and Dabiri J O. 2020. Low-power microelectronics embedded in live jellyfish enhance propulsion. *Sci. Adv.* **6**, eaaz3194.
[83] Li Z W, Balance W C, Joy M S H, Patel S, Hwang J, Kong H and Saif M T A. 2022. Adaptive biohybrid pumping machine with flow loop feedback. *Biofabrication* **14**, 025009.
[84] Filippi M et al. 2025. Multicellular muscle-tendon bioprinting of mechanically optimized musculoskeletal bioactuators with enhanced force transmission. *Sci. Adv.* **11**, eadv2628.
[85] Yin S K, Yao D R, Song Y, Heng W Z, Ma X T, Han H and Gao W. 2024. Wearable and implantable soft robots. *Chem. Rev.* **124**, 11585–11636.
[86] Gundelach L A, Hüser M A, Beutner D, Ruther P and Bruegmann T. 2020. Towards the clinical translation of optogenetic skeletal muscle stimulation. *Pflügers Arch Eur. J. Physiol.* **472**, 527–545.
[87] Kabumoto K I, Hoshino T, Akiyama Y and Morishima K. 2013. Voluntary movement controlled by the surface EMG signal for tissue-engineered skeletal muscle on a gripping tool. *Tissue Eng. A* **19**, 1695–1703.
[88] Hoshino T and Morishima K. 2010. Muscle-powered cantilever for microtweezers with an artificial micro skeleton and rat primary myotubes. *J. Biomech. Sci. Eng.* **5**, 245–251.
[89] Ren X Z, Morimoto Y and Takeuchi S. 2025. Biohybrid hand actuated by multiple human muscle tissues. *Sci. Robot.* **10**, eadr5512.
[90] Shin M, Ha T, Lim J, An J, Beak G, Choi J H, Melvin A A, Yoon J and Choi J W. 2024. Human motor system-based biohybrid robot-on-a-chip for drug evaluation of neurodegenerative disease. *Adv. Sci.* **11**, 2305371.
[91] Raman R, Cvetkovic C and Bashir R. 2017. A modular approach to the design, fabrication, and characterization of muscle-powered biological machines. *Nat. Protocols* **12**, 519–533.
[92] Wang N Y, Meenashisundaram G K, Kandilya D, Fuh J Y H, Dheen S T and Kumar A S. 2022. A biomechanical evaluation on cubic, octet, and TPMS gyroid Ti6Al4V lattice structures fabricated by selective laser melting and the effects of their debris on human osteoblast-like cells. *Biomater. Adv.* **137**, 212829.
[93] Wang N Y, Meenashisundaram G K, Chang S, Fuh J Y H, Dheen S T and Kumar A S. 2022. A comparative investigation on the mechanical properties and cytotoxicity of Cubic, Octet, and TPMS gyroid structures fabricated by selective laser melting of stainless steel 316L. *J. Mech. Behav. Biomed. Mater.* **129**, 105151.
[94] Wang N Y, Chang S, Li G W, Dheen S T, Kumar A S, Wu W Z, Liu Q P, Zhao J, Ren L Q and Fuh J Y H. 2022. Effects of various processing parameters on mechanical properties and biocompatibility of Fe-based bulk metallic glass processed via selective laser melting at constant energy density. *Chin. J. Mech. Eng. Addit. Manuf. Front.* **1**, 100038.
[95] Meenashisundaram G K, Wang N Y, Maskomani S, Lu S L, Anantharajan S K, Dheen S T, Nai S M L, Fuh J Y H and Wei J. 2020. Fabrication of Ti+Mg composites by three-dimensional printing of porous Ti and subsequent pressureless infiltration of biodegradable Mg. *Mater. Sci. Eng. C* **108**, 110478.
[96] Sun W H, Schaffer S, Dai K, Yao L N, Feinberg A and Webster-Wood V. 2021. 3D printing hydrogel-based soft

and biohybrid actuators: a mini-review on fabrication techniques, applications, and challenges. *Front. Robot. AI* **8**, 673533.

[97] Kumar N, Alathur Ramakrishnan S, Lopez K G, Wang N Y, Vellayappan B A, Hallinan J T P D, Fuh J Y H and Kumar A S. 2023. Novel 3D printable PEEK-HA-Mg_2SiO_4 composite material for spine implants: biocompatibility and imaging compatibility assessments. *Eur. Spine J.* **32**, 2255–2265.

[98] Kumar N, Alathur Ramakrishnan S, Lopez K G, Wang N Y, Madhu S, Vellayappan B A, Tpd Hallinan J, Fuh J Y H and Kumar A S. 2023. Design and 3D printing of novel titanium spine rods with lower flexural modulus and stiffness profile with optimised imaging compatibility. *Eur. Spine J.* **32**, 1953–1965.

[99] Pathak K et al. 2023. 3D printing in biomedicine: advancing personalized care through additive manufacturing. *Explor. Med.* **4**, 1135–1167.

[100] Wang N Y, Dheen S T, Fuh J Y H and Kumar A S. 2021. A review of multi-functional ceramic nanoparticles in 3D printed bone tissue engineering. *Bioprinting* **23**, e00146.

[101] Zhang W X, Zhu Y, Li J, Guo Q Y, Peng J, Liu S C, Yang J H and Wang Y. 2016. Cell-derived extracellular matrix: basic characteristics and current applications in orthopedic tissue engineering. *Tissue Eng. B* **22**, 193–207.

[102] Feng W H, Wang N Y, Weng F, Su J L, Lim P G H, Yan L N and O'Neill G K. 2023. The influence of laser surface remelting on the in vitro cell viability of additively manufactured Ti–6Al–4V plates. *Prog. Addit. Manuf.* **8**, 997–1005.

[103] Feng W H, Wang N Y, Wan Y C, Hui P L G, Yan L N and O'Neill G K 2022. The influence of laser surface remelting (LSR) on the surface morphology and in vitro cell viability of additively manufactured 316L stainless steel bone plate. *In Proceedings of the 9th International Conference of Asian Society for Precision Engineering and Nanotechnology*. (ASPEN, Singapore, Singapore). pp 271–274.

[104] Wang N Y, Maskomani S, Meenashisundaram G K, Fuh J Y H, Dheen S T and Anantharajan S K. 2020. A study of titanium and magnesium particle-induced oxidative stress and toxicity to human osteoblasts. *Mater. Sci. Eng. C* **117**, 111285.

[105] Ashammakhi N et al. 2022. Highlights on advancing frontiers in tissue engineering. *Tissue Eng. B* **28**, 633–664.

[106] Groll J et al. 2016. Biofabrication: reappraising the definition of an evolving field. *Biofabrication* **8**, 013001.

[107] Murphy S V and Atala A. 2014. 3D bioprinting of tissues and organs. *Nat. Biotechnol.* **32**, 773–785.

[108] Zhuang P, An J, Chua C K and Tan L P. 2020. Bioprinting of 3D in vitro skeletal muscle models: a review. *Mater. Des.* **193**, 108794.

[109] Soleimanzadeh H, Rolfe B, Bodaghi M, Jamalabadi M, Zhang X and Zolfagharian A. 2023. Sustainable robots 4D printing. *Adv. Sustain. Syst.* **7**, 2300289.

[110] Prinz V Y and Fritzler K B. 2023. 3D printed biohybrid microsystems. *Adv. Mater. Technol.* **8**, 2101633.

[111] Gul J Z, Sajid M, Rehman M M, Siddiqui G U, Shah I, Kim K H, Lee J W and Choi K H. 2018. 3D printing for soft robotics—a review. *Sci. Technol. Adv. Mater.* **19**, 243–262.

[112] Maines E M, Porwal M K, Ellison C J and Reineke T M. 2021. Sustainable advances in SLA/DLP 3D printing materials and processes. *Green Chem.* **23**, 6863–6897.

[113] Li Y, Mao Q J, Yin J, Wang Y F, Fu J Z and Huang Y. 2021. Theoretical prediction and experimental validation of the digital light processing (DLP) working curve for photocurable materials. *Addit. Manuf.* **37**, 101716.

[114] Morimoto Y, Onoe H and Takeuchi S. 2020. Biohybrid robot with skeletal muscle tissue covered with a collagen structure for moving in air. *APL Bioeng.* **4**, 026101.

[115] Hull S M, Brunel L G and Heilshorn S C. 2022. 3D bioprinting of cell-laden hydrogels for improved biological functionality. *Adv. Mater.* **34**, 2103691.

[116] Esser T U, Anspach A, Muenzebrock K A, Kah D, Schrüfer S, Schenk J, Heinze K G, Schubert D W, Fabry B and Engel F B. 2023. Direct 3D-bioprinting of hiPSC-derived cardiomyocytes to generate functional cardiac tissues. *Adv. Mater.* **35**, 2305911.

[117] Mestre R, Patiño T, Barceló X, Anand S, Pérez-Jiménez A and Sánchez S. 2019. Force modulation and adaptability of 3D-bioprinted biological actuators based on skeletal muscle tissue. *Adv. Mater. Technol.* **4**, 1800631.

[118] Wang D, Wang J Q, Shen Z Q, Jiang C R, Zou J, Dong L, Fang N X and Gu G Y. 2023. Soft actuators and robots enabled by additive manufacturing. *Annu. Rev. Control Robot. Auton. Syst.* **6**, 31–63.

[119] Xie R X et al. 2024. Magnetically driven formation of 3D freestanding soft bioscaffolds. *Sci. Adv.* **10**, eadl1549.

[120] Yu C, Zhu W, Sun B J, Mei D Q, Gou M L and Chen S C. 2018. Modulating physical, chemical, and biological properties in 3D printing for tissue engineering applications. *Appl. Phys. Rev.* **5**, 041107.

[121] Sachyani Keneth E, Kamyshny A, Totaro M, Beccai L and Magdassi S. 2021. 3D printing materials for soft robotics. *Adv. Mater.* **33**, 2003387.

[122] Thai M T, Phan P T, Tran H A, Nguyen C C, Hoang T T, Davies J, Rnjak-Kovacina J, Phan H P, Lovell N H and Do T N. 2023. Advanced soft robotic system for in situ 3D bioprinting and endoscopic surgery. *Adv. Sci.* **10**, 2205656.

[123] Zhang Y S, Haghiashtiani G, Hübscher T, Kelly D J, Lee J M, Lutolf M, Mcalpine M C, Yeong W Y, Zenobi-Wong M and Malda J. 2021. 3D extrusion bioprinting. *Nat. Rev. Meth. Primers* **1**, 75.

[124] Ning L Q and Chen X B. 2017. A brief review of extrusion-based tissue scaffold bio-printing. *Biotechnol. J.* **12**, 1600671.

[125] Schlatter S, Grasso G, Rosset S and Shea H. 2020. Inkjet printing of complex soft machines with densely integrated electrostatic actuators. *Adv. Intell. Syst.* **2**, 2000136.

[126] Li X D, Liu B X, Pei B, Chen J W, Zhou D Z, Peng J Y, Zhang X Z, Jia W and Xu T. 2020. Inkjet bioprinting of biomaterials. *Chem. Rev.* **120**, 10793–10833.

[127] Ng W L and Shkolnikov V. 2024. Jetting-based bioprinting: process, dispense physics, and applications. *Bio-Des. Manuf.* **7**, 771–799.

[128] Kérourédan O, Washio A, Handschin C, Devillard R, Kokabu S, Kitamura C and Tabata Y. 2024. Bioactive gelatin-sheets as novel biopapers to support prevascularization organized by laser-assisted bioprinting for bone tissue engineering. *Biomed. Mater.* **19**, 025038.

[129] Gülcan O, Günaydın K and Tamer A. 2021. The state of the art of material jetting—a critical review. *Polymers* **13**, 2829.

[130] Tee Y L, Tran P, Leary M, Pille P and Brandt M. 2020. 3D Printing of polymer composites with material jetting: mechanical and fractographic analysis. *Addit. Manuf.* **36**, 101558.

[131] Karakurt I, Aydoğdu A, Çıkrıkcı S, Orozco J and Lin L W. 2020. Stereolithography (SLA) 3D printing of ascorbic acid loaded hydrogels: a controlled release study. *Int. J. Pharm.* **584**, 119428.

[132] Chen Q H, Zou B, Wang X F, Zhou X G, Yang G X, Lai Q G and Zhao Y. 2024. SLA-3d printed building and characteristics of GelMA/HAP biomaterials with gradient porous structure. *J. Mech. Behav. Biomed. Mater.* **155**, 106553.

[133] Zorlutuna P, Jeong J H, Kong H and Bashir R. 2011. Stereolithography-based hydrogel microenvironments to examine cellular interactions. *Adv. Funct. Mater.* **21**, 3642–3651.

[134] Jiang Z, Diggle B, Tan M L, Viktorova J, Bennett C W and Connal L A. 2020. Extrusion 3D printing of polymeric materials with advanced properties. *Adv. Sci.* **7**, 2001379.
[135] Cui X L, Li J, Hartanto Y, Durham M, Tang J N, Zhang H, Hooper G, Lim K and Woodfield T. 2020. Advances in extrusion 3D bioprinting: a focus on multicomponent hydrogel-based bioinks. *Adv. Healthcare Mater.* **9**, 1901648.
[136] Mo X W, Ouyang L L, Xiong Z and Zhang T. 2022. Advances in digital light processing of hydrogels. *Biomed. Mater.* **17**, 042002.
[137] Yang M, Chu L, Zhuang Y F, Qi C, Meng S, Liu Z and Kong T T. 2024. Multi-material digital light processing (DLP) bioprinting of heterogeneous hydrogel constructs with perfusable networks. *Adv. Funct. Mater.* **34**, 2316456.
[138] Zanon M, Baruffaldi D, Sangermano M, Pirri C F, Frascella F and Chiappone A. 2021. Visible light-induced crosslinking of unmodified gelatin with PEGDA for DLP-3D printable hydrogels. *Eur. Polym. J.* **160**, 110813.
[139] Mueller E, Poulin I, Bodnaryk W J and Hoare T. 2022. Click chemistry hydrogels for extrusion bioprinting: progress, challenges, and opportunities. *Biomacromolecules* **23**, 619–640.
[140] Xin S J, Deo K A, Dai J, Pandian N K R, Chimene D, Moebius R M, Jain A, Han A R M, Gaharwar A K and Alge D L. 2021. Generalizing hydrogel microparticles into a new class of bioinks for extrusion bioprinting. *Sci. Adv.* **7**, eabk3087.
[141] Negro A, Cherbuin T and Lutolf M P. 2018. 3D inkjet printing of complex, cell-laden hydrogel structures. *Sci. Rep.* **8**, 17099.
[142] Dou C R, Perez V, Qu J, Tsin A, Xu B and Li J Z. 2021. A state-of-the-art review of laser-assisted bioprinting and its future research trends. *Chem. Bio Eng. Rev.* **8**, 517–534.
[143] Guillotin B et al. 2010. Laser assisted bioprinting of engineered tissue with high cell density and microscale organization. *Biomaterials* **31**, 7250–7256.
[144] Hall G N, Fan Y C, Viellerobe B, Iazzolino A, Dimopoulos A, Poiron C, Clapies A, Luyten F P, Guillemot F and Papantoniou I. 2024. Laser-assisted bioprinting of targeted cartilaginous spheroids for high density bottom-up tissue engineering. *Biofabrication* **16**, 045029.
[145] Cabral M, Cheng K and Zhu D H. 2024. Three-dimensional bioprinting of organoids: past, present, and prospective. *Tissue Eng. A* **30**, 314–321.
[146] Yan L N, Soh S L, Wang N Y, Ma Q H, Lu W F, Dheen S T, Kumar A S and Fuh J Y H. 2022. Evaluation and characterization of nitinol stents produced by selective laser melting with various process parameters. *Prog. Addit. Manuf.* **7**, 1141–1153.
[147] Baniasadi H, Abidnejad R, Fazeli M, Lipponen J, Niskanen J, Kontturi E, Seppälä J and Rojas O J. 2024. Innovations in hydrogel-based manufacturing: a comprehensive review of direct ink writing technique for biomedical applications. *Adv. Colloid Interface Sci.* **324**, 103095.
[148] Clegg J R, Wagner A M, Shin S R, Hassan S, Khademhosseini A and Peppas N A. 2019. Modular fabrication of intelligent material-tissue interfaces for bioinspired and biomimetic devices. *Prog. Mater. Sci.* **106**, 100589.
[149] Gao L, Akhtar M U, Yang F, Ahmad S, He J K, Lian Q, Cheng W, Zhang J H and Li D C. 2021. Recent progress in engineering functional biohybrid robots actuated by living cells. *Acta Biomater.* **121**, 29–40.
[150] Harley W S, Li C C, Toombs J, O'Connell C D, Taylor H K, Heath D E and Collins D J. 2021. Advances in biofabrication techniques towards functional bioprinted heterogeneous engineered tissues: a comprehensive review. *Bioprinting* **23**, e00147.
[151] MacDonald E and Wicker R. 2016. Multiprocess 3D printing for increasing component functionality. *Science* **353**, aaf2093.
[152] Lee M, Rizzo R, Surman F and Zenobi-Wong M. 2020. Guiding lights: tissue bioprinting using photoactivated materials. *Chem. Rev.* **120**, 10950–11027.
[153] Aubin H, Nichol J W, Hutson C B, Bae H, Sieminski A L, Cropek D M, Akhyari P and Khademhosseini A. 2010. Directed 3D cell alignment and elongation in microengineered hydrogels. *Biomaterials* **31**, 6941–6951.
[154] Choi H K, Kim C H, Lee S N, Kim T H and Oh B K. 2021. Nano-sized graphene oxide coated nanopillars on microgroove polymer arrays that enhance skeletal muscle cell differentiation. *Nano Converg.* **8**, 40.
[155] Hu C Z, Pané S and Nelson B J. 2018. Soft micro- and nanorobotics. *Annu. Rev. Control Robot. Auton. Syst.* **1**, 53–75.
[156] Chang S T, Paunov V N, Petsev D N and Velev O D. 2007. Remotely powered self-propelling particles and micropumps based on miniature diodes. *Nat. Mater.* **6**, 235–240.
[157] Li Y L, Wang Y, Wan K M, Wu M X, Guo L, Liu X M and Wei G. 2021. On the design, functions, and biomedical applications of high-throughput dielectrophoretic micro-/nanoplatforms: a review. *Nanoscale* **13**, 4330–4358.
[158] Barcelo S and Li Z Y. 2016. Nanoimprint lithography for nanodevice fabrication. *Nano Converg.* **3**, 21.
[159] Tognato R, Armiento A R, Bonfrate V, Levato R, Malda J, Alini M, Eglin D, Giancane G and Serra T. 2019. A stimuli-responsive nanocomposite for 3D anisotropic cell-guidance and magnetic soft robotics. *Adv. Funct. Mater.* **29**, 1804647.
[160] Filippi M, Buchner T, Yasa O, Weirich S and Katzschmann R K. 2022. Microfluidic tissue engineering and bio-actuation. *Adv. Mater.* **34**, 2108427.
[161] Novosel E C, Kleinhans C and Kluger P J. 2011. Vascularization is the key challenge in tissue engineering. *Adv. Drug Deliv. Rev.* **63**, 300–311.
[162] Shao C M, Chi J J, Chen Z Y, Sun L Y, Shang L R, Zhao Y J and Ye F F. 2021. Nano-imprinted anisotropic structural color graphene films for cardiomyocytes dynamic displaying. *Mater. Today* **51**, 117–125.
[163] Yang B, Yang Z H, Zhao Z Y, Hu Y W and Li J P. 2014. The assembly of carbon nanotubes by dielectrophoresis: insights into the dielectrophoretic nanotube–nanotube interactions. *Physica E* **56**, 117–122.
[164] Zhang Y, Duan H W, Li G Q, Peng M Y, Ma X, Li M and Yan S. 2022. Construction of liquid metal-based soft microfluidic sensors via soft lithography. *J. Nanobiotechnol.* **20**, 246.
[165] Zandi Shafagh R, Shen J X, Youhanna S, Guo W J, Lauschke V M, van der Wijngaart W and Haraldsson T. 2020. Facile nanoimprinting of robust high-aspect-ratio nanostructures for human cell biomechanics. *ACS Appl. Bio Mater.* **3**, 8757–8767.
[166] Pu R C, Yang X Y, Mu H R, Xu Z H and He J. 2024. Current status and future application of electrically controlled micro/nanorobots in biomedicine. *Front. Bioeng. Biotechnol.* **12**, 1353660.
[167] Ferreira D A, Rothbauer M, Conde J P, Ertl P, Oliveira C and Granja P L. 2021. A fast alternative to soft lithography for the fabrication of organ-on-a-chip elastomeric-based devices and microactuators. *Adv. Sci.* **8**, 2003273.
[168] Mita H, Mizuno Y, Tanaka H and Fujie T. 2024. UV laser-processed microstructure for building biohybrid actuators with anisotropic movement. *Biofabrication* **16**, 025010.
[169] Mühlberger M, Schwinger W, Gmainer M, Schöftner R, Glinsner T, Hasenfuß C, Hingerl K, Schmidt H and Kley E B. 2007. High precision alignment in multi-layer nanoimprint lithography. *AIP Conf. Proc.* **893**, 1495–1496.

[170] Aghaamoo M, Aghilinejad A, Chen X L and Xu J. 2019. On the design of deterministic dielectrophoresis for continuous separation of circulating tumor cells from peripheral blood cells. *Electrophoresis* **40**, 1486–1493.
[171] Rezaei Z and Mahmoudifard M. 2019. Pivotal role of electrospun nanofibers in microfluidic diagnostic systems–a review. *J. Mater. Chem. B* **7**, 4602–4619.
[172] Rezaei Z, Alemzadeh I and Vossoughi M. 2022. Design and fabrication of an electrochemical-based nanofibrous immunosensor for detection of prostate cancer biomarker, PSMA. *Polym. Adv. Technol.* **33**, 1967–1977.
[173] Odularu A T. 2022. Basic principles of electrospinning, mechanisms, nanofibre production, and anticancer drug delivery. *J. Chem.* **2022**, 9283325.
[174] Bhardwaj N and Kundu S C. 2010. Electrospinning: a fascinating fiber fabrication technique. *Biotechnol. Adv.* **28**, 325–347.
[175] Jun I, Han H S, Edwards J R and Jeon H. 2018. Electrospun fibrous scaffolds for tissue engineering: viewpoints on architecture and fabrication. *Int. J. Mol. Sci.* **19**, 745.
[176] Luraghi A, Peri F and Moroni L. 2021. Electrospinning for drug delivery applications: a review. *J. Control. Release* **334**, 463–484.
[177] Nioradze N, Ciornii D, Kölsch A, Göbel G, Khoshtariya D E, Zouni A and Lisdat F. 2021. Electrospinning for building 3D structured photoactive biohybrid electrodes. *Bioelectrochemistry* **142**, 107945.
[178] Rahmati M, Mills D K, Urbanska A M, Saeb M R, Venugopal J R, Ramakrishna S and Mozafari M. 2021. Electrospinning for tissue engineering applications. *Prog. Mater. Sci.* **117**, 100721.
[179] Si Y F, Shi S and Hu J L. 2023. Applications of electrospinning in human health: from detection, protection, regulation to reconstruction. *Nano Today* **48**, 101723.
[180] Zhao Q L, Du X M and Wang M. 2023. Electrospinning and cell fibers in biomedical applications. *Adv. Biol.* **7**, 2300092.
[181] Zhang Y P, Zhang Z Y, Wang Y T, Su Y C and Chen M L. 2020. 3D myotube guidance on hierarchically organized anisotropic and conductive fibers for skeletal muscle tissue engineering. *Mater. Sci. Eng. C* **116**, 111070.
[182] Beldjilali-Labro M et al. 2022. Multiscale-engineered muscle constructs: PEG hydrogel micro-patterning on an electrospun PCL mat functionalized with gold nanoparticles. *Int. J. Mol. Sci.* **23**, 260.
[183] Wang N Y, Fuh J Y H, Dheen S T and Senthil Kumar A. 2021. Functions and applications of metallic and metallic oxide nanoparticles in orthopedic implants and scaffolds. *J. Biomed. Mater. Res. B* **109**, 160–179.
[184] Wang N Y, Fuh J Y H, Dheen S T and Senthil Kumar A. 2021. Synthesis methods of functionalized nanoparticles: a review. *Bio-Des. Manuf.* **4**, 379–404.
[185] Atıcı B, Ünlü C H and Yanilmaz M. 2022. A review on centrifugally spun fibers and their applications. *Polym. Rev.* **62**, 1–64.
[186] Schätzlein E and Blaeser A. 2022. Recent trends in bioartificial muscle engineering and their applications in cultured meat, biorobotic systems and biohybrid implants. *Commun. Biol.* **5**, 737.
[187] Chang H B et al. 2022. Recreating the heart's helical structure-function relationship with focused rotary jet spinning. *Science* **377**, 180–185.
[188] Chan B P and Leong K W. 2008. Scaffolding in tissue engineering: general approaches and tissue-specific considerations. *Eur. Spine J.* **17**, 467–479.
[189] Uribe-Gomez J, Schönfeld D, Posada-Murcia A, Roland M M, Caspari A, Synytska A, Salehi S, Pretsch T and Ionov L. 2022. Fibrous scaffolds for muscle tissue engineering based on touch-spun poly(ester-urethane) elastomer. *Macromol. Biosci.* **22**, 2100427.
[190] Park D, Lee S J, Choi D K and Park J W. 2023. Therapeutic agent-loaded fibrous scaffolds for biomedical applications. *Pharmaceutics* **15**, 1522.
[191] Dolgin J, Hanumantharao S N, Farias S, Simon C G Jr and Rao S. 2023. Mechanical properties and morphological alterations in fiber-based scaffolds affecting tissue engineering outcomes. *Fibers* **11**, 39.
[192] Quashie D Jr, Benhal P, Chen Z, Wang Z H, Mu X L, Song X X, Jiang T, Zhong Y K, Cheang U K and Ali J. 2022. Magnetic bio-hybrid micro actuators. *Nanoscale* **14**, 4364–4379.
[193] Anil-Inevi M, Delikoyun K, Mese G, Tekin H C and Ozcivici E. 2021. Magnetic levitation assisted biofabrication, culture, and manipulation of 3D cellular structures using a ring magnet based setup. *Biotechnol. Bioeng.* **118**, 4771–4785.
[194] Sarigil O, Anil-Inevi M, Firatligil-Yildirir B, Unal Y C, Yalcin-Ozuysal O, Mese G, Tekin H C and Ozcivici E. 2021. Scaffold-free biofabrication of adipocyte structures with magnetic levitation. *Biotechnol. Bioeng.* **118**, 1127–1140.
[195] Wang Y Z, Nitta T, Hiratsuka Y and Morishima K. 2022. In situ integrated microrobots driven by artificial muscles built from biomolecular motors. *Sci. Robot.* **7**, eaba8212.
[196] Lin D Z, Yang F, Gong D and Li R H. 2023. Bio-inspired magnetic-driven folded diaphragm for biomimetic robot. *Nat. Commun.* **14**, 163.
[197] Kriegman S, Blackiston D, Levin M and Bongard J. 2020. A scalable pipeline for designing reconfigurable organisms. *Proc. Natl Acad. Sci. USA* **117**, 1853–1859.
[198] Uzel S G M, Platt R J, Subramanian V, Pearl T M, Rowlands C J, Chan V, Boyer L A, So P T C and Kamm R D. 2016. Microfluidic device for the formation of optically excitable, three-dimensional, compartmentalized motor units. *Sci. Adv.* **2**, e1501429.
[199] Ma Z C, Fan J H, Wang H S, Chen W D, Yang G Z and Han B. 2023. Microfluidic approaches for microactuators: from fabrication, actuation, to functionalization. *Small* **19**, 2300469.
[200] Grosberg A, Nesmith A P, Goss J A, Brigham M D, McCain M L and Parker K K. 2012. Muscle on a chip: in vitro contractility assays for smooth and striated muscle. *J. Pharmacol. Toxicol. Methods* **65**, 126–135.
[201] Arrigoni C, Petta D, Bersini S, Mironov V, Candrian C and Moretti M. 2019. Engineering complex muscle-tissue interfaces through microfabrication. *Biofabrication* **11**, 032004.
[202] Keating S M et al. 2018. Opportunities and challenges in implementation of multiparameter single cell analysis platforms for clinical translation. *Clin. Transl. Sci.* **11**, 267–276.
[203] Schaefer J A and Tranquillo R T. 2016. Tissue contraction force microscopy for optimization of engineered cardiac tissue. *Tissue Eng. C* **22**, 76–83.
[204] Duc P, Vignes M, Hugon G, Sebban A, Carnac G, Malyshev E, Charlot B and Rage F. 2021. Human neuromuscular junction on micro-structured microfluidic devices implemented with a custom micro electrode array (MEA). *Lab Chip* **21**, 4223–4236.
[205] Wu Y P and Meng Y Q. 2023. Cell manipulation and single cell characterization on microfluidic devices. *TrAC Trends Anal. Chem* **168**, 117301.
[206] Leng Y B et al. 2023. Advances in in vitro models of neuromuscular junction: focusing on organ-on-a-chip, organoids, and biohybrid robotics. *Adv. Mater.* **35**, e2211059.
[207] Rezaei Z, Wang N Y, Yang Y P, Govindaraj K, Velasco J J, Blanco A D M, Bae N H, Lee H and Shin S R. 2025. Enhancing organoid technology with carbon-based nanomaterial biosensors: advancements, challenges, and future directions. *Adv. Drug Deliv. Rev.* **222**, 115592.

[208] Alapan Y, Yasa O, Yigit B, Yasa I C, Erkoc P and Sitti M. 2019. Microrobotics and microorganisms: biohybrid autonomous cellular robots. *Annu. Rev. Control Robot. Auton. Syst.* **2**, 205–230.
[209] Gullo M R, Takeuchi S and Paul O. 2017. Multicellular biohybrid materials: probing the interplay of cells of different types precisely positioned and constrained on 3D wireframe-like microstructures. *Adv. Healthcare Mater.* **6**, 1601053.
[210] Mestre R, Patiño T, Guix M, Barceló X and Sanchez S 2019. Design, optimization and characterization of biohybrid actuators based on 3D-bioprinted skeletal muscle tissue. *In Proceedings of the 8th International Conference on Biomimetic and Biohybrid Systems*. (Springer, Nara, Japan). pp 205–215.
[211] Kim H, Kim M C and Asada H H. 2019. Extracellular matrix remodelling induced by alternating electrical and mechanical stimulations increases the contraction of engineered skeletal muscle tissues. *Sci. Rep.* **9**, 2732.
[212] Volpi M, Paradiso A, Costantini M and Święszkowski W. 2022. Hydrogel-based fiber biofabrication techniques for skeletal muscle tissue engineering. *ACS Biomater. Sci. Eng.* **8**, 379–405.
[213] Wang N Y, Dai Y C, Fuh J Y H, Yen C C and Lu W F. 2023. Applications of triboelectric nanogenerators in bone tissue engineering. *Adv. Mater. Technol.* **8**, 2201310.
[214] Mao M, Han K, Gao J Y, Ren Z S, Zhang Y B, He J K and Li D C. 2025. Engineering highly aligned and densely populated cardiac muscle bundles via fibrin remodeling in 3D-printed anisotropic microfibrous lattices. *Adv. Mater.* **37**, e2419380.
[215] Lin Z N, Jiang T, Yang Y, Hong Y, Gao Y, Xie H and Luo Z R. 2024. Matrigel-fibrinogen-thrombin hydrogels with high bioactivity for the fabrication of self-propelled in vitro muscular tissues. *Appl. Mater. Today* **39**, 102315.
[216] Gao L, Wu W Z, Tong S K, Li D C, Xie X X, Liang T, He J K, Cheng W, Zhang Y and Feng J N. 2023. A muscle-machine hybrid crawler: omnidirectional maneuverability and high load capacity. *Sens. Actuators B* **393**, 134333.
[217] Apsite I, Salehi S and Ionov L. 2022. Materials for smart soft actuator systems. *Chem. Rev.* **122**, 1349–1415.
[218] Loget G and Kuhn A. 2011. Electric field-induced chemical locomotion of conducting objects. *Nat. Commun.* **2**, 535.
[219] Wang B, Shen J, Huang C Y, Ye Z C, He J J, Wu X Y, Guo Z G, Zhang L and Xu T T. 2025. Magnetically driven biohybrid blood hydrogel fibres for personalized intracranial tumour therapy under fluoroscopic tracking. *Nat. Biomed. Eng.* **2025**, 1–15.
[220] Shen J, Wang Y, Yao M, Liu S B, Guo Z G, Zhang L and Wang B. 2025. Long-span delivery of differentiable hybrid robots for restoration of neural connections. *Matter* **8**, 101942.
[221] Seong M et al. 2024. Multifunctional magnetic muscles for soft robotics. *Nat. Commun.* **15**, 7929.
[222] Vedadghavami A, Minooei F, Mohammadi M H, Khetani S, Rezaei Kolahchi A, Mashayekhan S and Sanati-Nezhad A. 2017. Manufacturing of hydrogel biomaterials with controlled mechanical properties for tissue engineering applications. *Acta Biomater.* **62**, 42–63.
[223] Fischer K M, Scott T E, Browe D P, McGaughey T A, Wood C, Wolyniak M J and Freeman J W. 2021. Hydrogels for skeletal muscle regeneration. *Regen. Eng. Transl. Med.* **7**, 353–361.
[224] Liu H R, Liu D, Yang J C, Gao H F and Wu Y C. 2023. Flexible electronics based on organic semiconductors: from patterned assembly to integrated applications. *Small* **19**, 2206938.
[225] Pantula A, Datta B, Shi Y P, Wang M, Liu J Y, Deng S M, Cowan N J, Nguyen T D and Gracias D H. 2022. Untethered unidirectionally crawling gels driven by asymmetry in contact forces. *Sci. Robot.* **7**, eadd2903.
[226] Shin M, Lim J, An J, Yoon J and Choi J W. 2023. Nanomaterial-based biohybrid hydrogel in bioelectronics. *Nano Converg.* **10**, 8.
[227] Yuk H, Lin S T, Ma C, Takaffoli M, Fang N X and Zhao X H. 2017. Hydraulic hydrogel actuators and robots optically and sonically camouflaged in water. *Nat. Commun.* **8**, 14230.
[228] Cao D F, Martinez J G, Hara E S and Jager E W H. 2022. Biohybrid variable-stiffness soft actuators that self-create bone. *Adv. Mater.* **34**, 2107345.
[229] Dou W Q, Zhong G L, Cao J L, Shi Z, Peng B W and Jiang L Z. 2021. Soft robotic manipulators: designs, actuation, stiffness tuning, and sensing. *Adv. Mater. Technol.* **6**, 2100018.
[230] Webster-Wood V A, Guix M, Xu N W, Behkam B, Sato H, Sarkar D, Sanchez S, Shimizu M and Parker K K. 2023. Biohybrid robots: recent progress, challenges, and perspectives. *Bioinsp. Biomim.* **18**, 015001.
[231] Pellicciotta N, Bagal O S, Sosa V C, Frangipane G, Vizsnyiczai G and Leonardo R D. 2023. Light controlled biohybrid microbots. *Adv. Funct. Mater.* **33**, 2214801.
[232] Chansoria P, Narayanan L K, Schuchard K and Shirwaiker R. 2019. Ultrasound-assisted biofabrication and bioprinting of preferentially aligned three-dimensional cellular constructs. *Biofabrication* **11**, 035015.
[233] Hoffman T, Antovski P, Tebon P, Xu C, Ashammakhi N, Ahadian S, Morsut L and Khademhosseini A. 2020. Synthetic biology and tissue engineering: toward fabrication of complex and smart cellular constructs. *Adv. Funct. Mater.* **30**, 1909882.
[234] Nie M H, Shima A, Yamamoto M and Takeuchi S. 2025. Scalable tissue biofabrication via perfusable hollow fiber arrays for cultured meat applications. *Trends Biotechnol.* **43**, 1938–1960.
[235] Maharjan S, Ma C S, Singh B, Kang H, Orive G, Yao J J and Zhang Y S. 2024. Advanced 3D imaging and organoid bioprinting for biomedical research and therapeutic applications. *Adv. Drug Deliv. Rev.* **208**, 115237.
[236] Lee J, Lee H, Jin E J, Ryu D and Kim G H. 2023. 3D bioprinting using a new photo-crosslinking method for muscle tissue restoration. *NPJ Regen. Med.* **8**, 18.
[237] Filippi M, Yasa O, Giachino J, Graf R, Balciunaite A, Stefani L and Katzschmann R K. 2023. Perfusable biohybrid designs for bioprinted skeletal muscle tissue. *Adv. Healthcare Mater.* **12**, 2300151.
[238] D'Arcangelo E and McGuigan A P. 2015. Micropatterning strategies to engineer controlled cell and tissue architecture in vitro. *Biotechniques* **58**, 13–23.
[239] Cheng J X, Yu S Y, Wang R and Ge Q. 2024. Digital light processing based multimaterial 3D printing: challenges, solutions and perspectives. *Int. J. Extrem. Manuf.* **6**, 042006.
[240] Zhou L Y, Fu J Z and He Y. 2020. A review of 3D printing technologies for soft polymer materials. *Adv. Funct. Mater.* **30**, 2000187.
[241] Nam J and Kim M. 2024. Advances in materials and technologies for digital light processing 3D printing. *Nano Converg.* **11**, 45.
[242] Xie R X, Zheng W C, Guan L D, Ai Y J and Liang Q L. 2020. Engineering of hydrogel materials with perfusable microchannels for building vascularized tissues. *Small* **16**, 1902838.
[243] Wang J J, Wang Y J, Kim Y, Yu T Q and Bashir R. 2022. Multi-actuator light-controlled biological robots. *APL Bioeng.* **6**, 036103.
[244] Liu J, He J J, Liu J F, Ma X Y, Chen Q, Lawrence N, Zhu W, Xu Y and Chen S C. 2019. Rapid 3D bioprinting of in vitro cardiac tissue models using human embryonic stem cell-derived cardiomyocytes. *Bioprinting* **13**, e00040.

[245] Jana S, Levengood S K L and Zhang M Q. 2016. Anisotropic materials for skeletal-muscle-tissue engineering. *Adv. Mater.* **28**, 10588–10612.
[246] Bian W N and Bursac N. 2009. Engineered skeletal muscle tissue networks with controllable architecture. *Biomaterials* **30**, 1401–1412.
[247] Jafari A, Behjat E, Malektaj H and Mobini F. 2023. Alignment behavior of nerve, vascular, muscle, and intestine cells in two- and three-dimensional strategies. *WIREs Mech. Dis.* **15**, e1620.
[248] Won P, Ko S H, Majidi C, Feinberg A W and Webster-Wood V A. 2020. Biohybrid actuators for soft robotics: challenges in scaling up. *Actuators* **9**, 96.
[249] Palagi S and Fischer P. 2018. Bioinspired microrobots. *Nat. Rev. Mater.* **3**, 113–124.
[250] Fu F F, Shang L R, Chen Z Y, Yu Y R and Zhao Y J. 2018. Bioinspired living structural color hydrogels. *Sci. Robot.* **3**, eaar8580.
[251] Bliley J M, Stang M A, Behre A and Feinberg A W. 2024. Advances in 3D bioprinted cardiac tissue using stem cell-derived cardiomyocytes. *Stem Cells Transl. Med.* **13**, 425–435.
[252] Lyu C X, Zhang C Q, Tang D F and Zhao P. 2024. Magnetic levitation in medicine and bioengineering. *In Magnetic Levitation: Innovation of Density-Based Applications* (ed P Zhao) (Springer, Singapore) pp 163–179.
[253] Mazzolai B and Laschi C. 2020. A vision for future bioinspired and biohybrid robots. *Sci. Robot* **5**, eaba6893.
[254] Luo Z Q, Weiss D E, Liu Q Y and Tian B Z. 2018. Biomimetic approaches toward smart bio-hybrid systems. *Nano Res.* **11**, 3009–3030.
[255] Lussi J, Mattmann M, Sevim S, Grigis F, De Marco C, Chautems C, Pané S, Puigmartí-luis J, Boehler Q and Nelson B J. 2021. A submillimeter continuous variable stiffness catheter for compliance control. *Adv. Sci.* **8**, 2101290.
[256] Phillips J W, Prominski A and Tian B Z. 2022. Recent advances in materials and applications for bioelectronic and biorobotic systems. *VIEW* **3**, 20200157.
[257] Ranzani T, Cianchetti M, Gerboni G, Falco I D and Menciassi A. 2016. A soft modular manipulator for minimally invasive surgery: design and characterization of a single module. *IEEE Trans. Robot.* **32**, 187–200.
[258] Wang Z B, Xu Z J, Zhu B, Zhang Y, Lin J W, Wu Y G and Wu D Z. 2022. Design, fabrication and application of magnetically actuated micro/nanorobots: a review. *Nanotechnology* **33**, 152001.
[259] Biewener A A, Bomphrey R J, Daley M A and Ijspeert A J. 2022. Stability and manoeuvrability in animal movement: lessons from biology, modelling and robotics. *Proc. R. Soc. B* **289**, 20212492.
[260] Zhang C, Zhang Y W, Wang W X, Xi N and Liu L Q. 2022. A manta ray-inspired biosyncretic robot with stable controllability by dynamic electric stimulation. *Cyborg. Bionic Syst.* **2022**, 9891380.
[261] Nguyen P Q, Courchesne N M D, Duraj-Thatte A, Praveschotinunt P and Joshi N S. 2018. Engineered living materials: prospects and challenges for using biological systems to direct the assembly of smart materials. *Adv. Mater.* **30**, 1704847.